Role of PAX2 in maintaining the differentiation of oviductal epithelium and inhibiting the transition to a stem cell state

KHOLOUD ALWOSAIBAI

A Thesis submitted to the Faculty of Graduate and Postdoctoral Studies in partial fulfillment of the requirements for a doctoral degree in Cellular and Molecular Medicine.

Department of Cellular and Molecular Medicine
Faculty of Medicine
University of Ottawa

DEDICATION

To my kids for their patience and love

ABSTRACT

Several studies have proposed the fallopian tube epithelium as a site of origin of ovarian cancer. The discovery of precursor lesions in the fallopian tube in patients at risk for ovarian cancer supports a probable origin for high-grade serous ovarian carcinoma in this tissue. While the fallopian tube epithelium consists of three distinct cell types, the paired box protein 2 (PAX2) positive cells and potentially the CD44 positive stem-like cells are most relevant to ovarian cancer. Loss of PAX2 expression in the fallopian tube cells is considered to be an early event in epithelial transformation, but the specific role of PAX2 in this transition is unknown.

The aim of this study was to define the role of PAX2 in oviductal epithelial cells (OVE) cells and in mouse ovarian surface epithelial cells (MOSE), and to understand its contribution to the formation of serous precursor lesions in the fallopian tubes. Herein, we studied the OVE response to transforming growth factor β (TGFβ, a cytokine found in follicular fluid) and provide evidence of its potential involvement in the regulation of stem cell-like behaviors that may contribute to formation of cancer-initiating cells. Treatment of primary cultures of OVE cells with TGFβ at concentrations found in ovulatory follicular fluid induced an epithelial-mesenchymal transition (EMT) with expected changes in proliferation, cell morphology and expression of SNAIL, Vimentin and E-cadherin. EMT was also associated with decreased expression of PAX2 and an increase in the fraction of cells expressing CD44. *Pax2* knockdown in OVE cells and overexpression in ovarian epithelial cells confirmed that PAX2 inhibits CD44 expression and regulates the degree of epithelial differentiation of OVE cells. These results suggest

that the loss of PAX2 seen in serous tubal intraepithelial carcinomas (STIC) leads to a shift to a more mesenchymal phenotype associated with stem-like features. *Pax2* overexpression in MOSE cells also induced the formation of vascular channels both *in vitro* and *in vivo*, which indicate a possible contribution of PAX2 to ovarian cancer progression by increasing the vascular channels to supply nutrients to the tumor cells.

Furthermore, since loss of PAX2 in STIC was found associated with *P53* and *BRCA1* mutations, OVE cells with mutations of the tumor suppressor genes *Trp53* and *Brca1* were studied. We found that loss of *Trp53* with or without loss of *Brca1* increased cell proliferation and colony formation *in vitro*. In addition, loss of *Trp53* induced OVE cells to undergo EMT and induced the expression of stem cell–associated genes. We therefore suggest a potential contribution of stem cells in initiating the precursor lesions in the fallopian tubes in combination with tumor suppressor gene mutation.

TABLE OF CONTENTS

DEDICATION ..... **II**

ABSTRACT ..... **II**

TABLE OF CONTENTS ..... **V**

LIST OF FIGURES ..... **VIII**

LIST OF TABLES ..... **X**

LIST OF ABBREVIATIONS ..... **XI**

ACKNOWLEDGMENTS ..... **XV**

Chapter 1- Introduction **1**
1.1 Ovarian Cancer **1**
1.1.1 Types of epithelial ovarian cancer 1
1.1.2 Origin of epithelial ovarian cancer 2
1.2 Fallopian tube as a source of serous ovarian carcinoma **8**
1.2.1 Fallopian tube location 8
1.2.2 Fallopian tube cells 11
1.3 Tubal Intraepithelial Carcinoma **14**
1.4 PAX2 in the fallopian tube and ovarian cancer **17**
1.5 Tumor suppressor genes and ovarian cancer **18**
1.5.1 BRCA1 and ovarian cancer 18
1.5.2 P53 and ovarian cancer 22
1.6 Physiological risk factors for ovarian cancer **23**
1.6.1 Ovulation 23
1.6.2 Transforming growth factor beta (TGFβ) 25
1.7 Epithelial -Mesenchymal Transition (EMT) **29**
1.8 Stem cells in the reproductive tract **33**
1.8.1 CD44 structure and functions 36
1.8.2 Stem cell antigen-1 (SCA-1) 39
1.9 Angiogenesis and PAX2. ..... **39**

Rationale and Hypothesis **43**
Specific aims **43**

Chapter 2 – Materials and Methods **45**
2.1 Experimental animals **45**
2.2 Superovulation of mice **45**
2.3 Cell lines and cell culture **46**
2.4 Modulation of gene expression **47**
2.4.1 Lentiviral vectors 47
2.4.2 PAX2 overexpression and knockdown 48
2.4.3 Adenovirus infection to inactivate tumor suppressors 48
2.4.4 Detection of recombination using PCR 49
2.5 Proliferation assay **50**
2.6 Migration assay **50**

2.7 Sphere formation assay 51
2.8 Colony formation assay in soft agar 51
2.9 Label retaining assay 52
2.10 Gene expression analysis 52
2.11 3D culture in matrigel 53
2.12 Protein analyses 55
2.12.1 Western blot analysis 55
2.12.2 Immunofluorescence 55
2.12.3 Immunohistochemistry (IHC) 56
2.12.4 Flow Cytometry for CD44 and SCA-1 Expression 57
2.12.5 Periodic Acid-Schiff (PAS) staining 58
2.13 Statistical analyses 58

Chapter 3: Results (Part 1) 59
TGFβ induces the epithelial-to-mesenchymal transition associated with stem cell characteristics in OVE cells. 59
3.1 OVE cell characterization 59
3.2 OVE cells possess stem cell characteristics 61
3.3 OVE cells express stem cell proteins on the cell surface 65
3.4 TGFB induces EMT in OVE cells 69
3.5 TGFβ enhances stem cell characteristics 74
3.6 TGFβ decreases PAX2 expression 77

Chapter 4: Results (Part II). 80
PAX2 negatively regulates stemness in OVE cells and OSE cells. 80
4.1 PAX2 negatively regulates CD44 in OVE cells. 80
4.2 PAX2 negatively regulates CD44 and stemness in mouse OSE cells 86
4.3 PAX2 enhances cell differentiation in OVE cells to form luminal structures 91

Chapter 5: Results (Part III) 95
PAX2 induces vasculogenic mimicry in OSE cells and ovarian cancer 95
5.1.1 PAX2 induces vascular channels *in vitro* in MOSE cells 95
5.1.2 PAX2 enhances vascular channel formation *in vivo* in a tumor formed by an ovarian cancer cell line 101

Chapter 6: Results (Part IV) 101
Consequences of loss of *Trp53* alone or in combination with *Brca1* in oviductal epithelial cells 101
6.1 Isolation and characterization of OVE cells from mice with conditional expression of *Trp53* and/or *Brca1* 101
6.2 Conditional inactivation of *Trp53, Brca1* and *Trp53/Brca1*. 109
6.3 Analysis of OVE cells after loss of *Brca1* or/and *Trp53* 111
6.4 Loss of *Trp53* alone or in combination with *Brca1* induced OVE cells to undergo epithelial-mesenchymal transition. 114
6.5 Loss of *Trp53* enhances sphere-forming capacity and expression of the stem cell markers CD44 and SCA-1 117
6.6 Loss of *Trp53* decreases PAX2 expression and enhances SCA-1 positive population associated with colony formation. 118

Chapter 7- Discussion 122
Fallopian tube epithelial cell morphology 123
Stem-like cells in the OVE clonal cell lines 124
Follicular fluid, TGFβ and their impact on fallopian tube epithelial cells 127
PAX2 maintains epithelial differentiation of OVE cells and inhibits stemness 129
Effects of *Trp53* and *Brca1* mutation on OVE cell activity 134
Does PAX2 play a role in vasculogenic mimicry? 137
Conclusions 142
References 143

LIST OF FIGURES

Figure 1-1: The hypothesized implantation process of fallopian tube epithelial cells from the distal end of the fallopian tube (fimbriae) to the ovary..... 7
Figure 1-2: Female reproductive system anatomy. 10
Figure 1-3: Human fallopian tube cytology. 13
Figure 1-4: Model of the development of high-grade serous ovarian cancer..... 16
Figure 1-5: A schematic presentation of BRCA1 gene and encoded proteins including the functional domains..... 21
Figure 1-6: CD44 gene and structure. 38
Figure 3-1: Oviductal epithelial cell line characterization. 60
Figure 3-2: OVE cells have the ability to form spheres when grown in suspension..... 63
Figure 3-3: OVE cells retain PKH26 labeling..... 64
Figure 3-4: OVE cells expressing CD44 and SCA-1 can form spheres when plated in the suspensions. 67
Figure 3-5: Immunohistochemistry shows CD44 expression in the mouse ovary and oviduct. 68
Figure 3-6: OVE cells respond to TGFβ. 70
Figure 3-7: TGFβ increases characteristics of EMT in OVE cells..... 72
Figure 3-8: E-cadherin expression in the oviduct of superovulated mice 73
Figure 3-9: TGFβ induces sphere formation capacity in OVE cells. 75
Figure 3-10: TGFβ increases the expression of stem cell associated genes in OVE cells.76
Figure 3-11: TGFβ decreases Pax2 in OVE cells. 79
Figure 4-1: CD44 expression is highly expressed in PAX-null OVE cells..... 81
Figure 4-2: CD44 and PAX2 expression in mouse oviducts..... 83
Figure 4-3: Loss of PAX2 enhanced stem cell characteristics in OVE cells. 85
Figure 4-4: Pax2 decreases sphere-forming capacity in MOSE cells. 87
Figure 4-5: PAX2 down-regulates CD44 expression..... 89
Figure 4-6: PAX2 suppressed expression of stem cell markers. 90
Figure 4-7: Pax2 induces cell differentiation in the 3D culture, enabling OVE to form luminal structures..... 93
Figure 4-8: PAX2 positively regulates OVE differentiation. 94
Figure 5-1: PAX2 induced the formation of vascular-like channels in 3D culture..... 98
Figure 5-2: M1102-PAX2 cells formed vascular-like channels. 99
Figure 5-3: PAX2 induced vascular-like channel formation in RM cells in 3D culture. 100
Figure 5-4: Immunohistochemistry for CD31 and PAS staining of the tumors formed by RM cells and RM cells with forced expression of PAX2..... 103
Figure 5-5: Double staining for PAS and CD31 in RM-PAX2 and RM-WPI tumors. 104
Figure 5-6: PAX2 is expressed in the cells that line the vascular channels. 105
Figure 6-1: OVE clonal cells have different cell morphology and gene expression.... 108
Figure 6-2: Conditional inactivation of *Trp53* and Brca1 in OVE cells. 110
Figure 6-3: Microphotograph of OVE clonal cells with conditional inactivation of *Trp53* and/or *Brca1* shows differences in cell morphology with loss of *Brca1*. 112

Figure 6-4: Loss of *Trp53* alone or in combination with *Brca1* increases cell proliferation and colony formation. 113
Figure 6-5: Loss of *Trp53* alone or in combination with *Brca1* induced OVE cells to undergo epithelial -mesenchymal transition. 115
Figure 6-6: Migration assay of OVE cells after loss of *Trp53* and /or *Brca1* 116
Figure 6-7: Sphere formation assays of OVE cells after inactivation of *Trp53* and/or *Brca1*. 119
Figure 6-8: qPCR analysis of stem cell markers for OVE cells with inactivation of *Brca1*, *Trp53* and *Trp53/Brca1*. 120
Figure 6- 9: Inactivation of *Trp53* increased SCA-1+ population and decreased PAX2 expression. 121
Figure 7-1: An illustration presents proposed events occurring in the precursor lesion within the fallopian tube. 133
Figure 7-2: Summary of the findings in this thesis showing the effects of TGFβ, PAX2, and *Trp53* and *Brca1* mutations in OVE cells or MOSE cells. 141

LIST OF TABLES

Table 1: List of primers and probes used for qPCR analysis..... 54
Table 2: Summary of OVE clonal cells characteristics 140

LIST OF ABBREVIATIONS

3D	Three-dimensional
AdCre	Ad5CMVCre recombinant adenovirus
AdGFP	Ad5CMVeGFP recombinant adenovirus
ALDH1	Aldehyde dehydrogenase
ANOVA	Analysis of variance
APC	Allophycocyanin
bp	Base pair
Brca1	Breast cancer 1, early onset
BRCT	BRCA1 C Terminus
BRDU	Bromodeoxyuridine
C-KIT	Tyrosine protein kinase
C-myc	Avian myelocytomatosis virus oncogene cellular homolog
CD133	Cluster of differentiation 133
CD147	Cluster of differentiation 147
CD24	Cluster of differentiation 24
CD31	Cluster of differentiation 31
CD34	Cluster of differentiation 34
CD44	Cluster of differentiation 44
cDNA	Complementary deoxyribonucleic acid
CK-19	Cytokeratin-19
CK8	Cytokeratin 8
COX-2	Cyclooxygenase-2
CTNNB1	Catenin-Beta 1
D-MEM	Dulbecco's Modified Eagle Medium
DAPI	4',6-diamidino-2-phenylindole
Dicer	Ribonuclease type III
DNA:	Deoxyribonucleic acid

EGF	Epidermal growth factor
eGFP	Enhanced green fluorescent protein
EGFR	Epidermal growth factor receptor
EMT	Epithelial-to-mesenchymal transition
ERK1/2	Extracellular signal-regulated kinase
FBS	Fetal bovine serum
FOXJ1	Forkhead box J1
FSH	Follicle-stimulating hormone
FITC	Fluorescein isothiocyanate
GAPDH	Glyceraldehyde 3-phosphate dehydrogenase
HA	Hyaluronic acid
HCG	Human chorionic gonadotropin
HGSC	High-grade serous cancer
HRP	Horseradish peroxidase
IDT	Integrated DNA technology
IHC	Immunohistochemistry
IL-6	Interleukin-6
ITSS	Insulin-Transferrin-Sodium-Selenite Solution
K-RAS	Kirsten rat sarcoma virus
KDa	Kilodalton
Ki67	Cellular marker for proliferation
LGR5	Leucine-rich repeat-containing G-protein coupled receptor 5
LGSC	Low-grade serous cancer
LMP	Low melting point
LOH	Loss of heterozygosity
loxP	Locus of X-over P1
LTBP-1	Latent TGFβ binding protein-1
MCF7	Human breast adenocarcinoma cell line
MET	Mesenchymal-epithelial transition
MMP	Matrix metalloproteinase

MOSE	Mouse ovarian surface epithelium
MSH2	DNA mismatch repair-2
NANOG	Homeobox protein
OV90	Ovarian cancer cell line
OVCAR8	Ovarian cancer cell line
OVE	Oviductal epithelial cells
OVGP1	Oviduct-specific glycoprotein
P53	Tumor suppressor protein 53
PARP	Poly [ADP-ribose] polymerase
PAS	Periodic acid-schiff
PAX2	Paired box gene 2
PAX8	Paired box gene 8
PBS	Phosphate buffer saline
PCR	Polymerase chain reaction
PGE2	Prostaglandin E2
PI3K	Phosphoinositide 3 kinase
PKH26	Red fluorescent cell linker
Ppia	peptidylprolylisomerase A (cyclophilin A)
PTEN	Phosphatase and tensin homolog
Ptgs-2	Prostaglandin-endoperoxide synthase 2
Q-PCR	Quantitative polymerase chain reaction
RAD51	Protein that assists in repair of DNA double strand breaks
RB	Retinoblastoma
RNA	Ribonucleic acid
RM	Mouse ovarian surface epithelial cells transformed by K-Ras and c-Myc
SARA	SMAD anchor for receptor activation
SCA-1	Stem cell sntigen-1
SCOUT	Secretory cell outgrowth
SDF-1	Stromal cell-derived factor-1
SDS-PAGE	Sodium dedocyl sulfate-polyacrylamide gel electrophoresis

SEE-FIM	Sectioning and Extensively Examining the FIMbria
shRNA	short hairpin RNA
SKOV3	Ovarian cancer cell line
SLUG	Snail family zinc finger 2
SMAD	Small body size (SMA) and mothers against decapentaplegic
SNAIL	Snail homolog 1 (Drosophila)
STIC	Serous tubal intraepithelial carcinoma
TAE	Tris-acetate-EDTA
TGFβ	Transforming growth factor beta
TIC	Tubal intraepithelial carcinoma
TNFα	Tumor necrosis factor alpha
VEGF	Vascular endothelial growth factor
VM	Vasculogenic mimicry
α-MEM	Minimum Essential Medium Alpha
γ-H2AX	DNA marker of double strand breaks
µg	microgram
µl	microliter
µm	micrometer
µM	micromolar

ACKNOWLEDGMENTS

First and foremost I would like to send my thanks to my supervisor, Dr. Barbara Vanderhyden, who always has provided guidance and direction. You helped me to be a better person and better scientist.

Many thanks to my thesis advisory committee, Drs. Tsang, Baltz and McBurney, who always challenged me and constantly provided countless pieces of advice.

I have been fortunate to work with some wonderful people, some of whom have become life-long friends. I'd like to thank my lab advisors, Olga Collins and Elizabeth Macdonald for their expertise, and willingness to teach. Special and sincere thanks to Dr. Kenneth Garson: You were always there to answer my questions and have taught me so much; thanks for endless patience.

Thanks to my friend and lab mate, Ensaf Alhujaily, who is a great friend. I miss your warm heart! Thanks to Dr. Josée Coulombe for listening to me and giving me advice all the way through my PhD! Your cheerful spirit and beautiful smile will be always in my memory.

Finally, a special thanks to all my cheerleaders, especially my parents and my husband, who without hesitation were always there to offer support, encouragement and prayers. To my kids, who handled a busy mother very well, you are the best thing to have happened to me in this life!

Chapter 1- Introduction

1.1 Ovarian Cancer

1.1.1 Types of epithelial ovarian cancer

Epithelial ovarian cancer is the most prevalent type of ovarian cancer. Based on pathological and molecular analysis, epithelial ovarian cancer has been broadly classified into two types (Kurman et al., 2010). Type I tumors include low-grade serous carcinoma (LGSC), low-grade endometrioid carcinomas, clear cell, mucinous carcinomas, and Brenner tumors. Type I tumors involve poorly aggressive and low proliferative cells that present several mutations including *KRAS*, *BRAF*, *PIK3CA*, *CTNNB1* and *PTEN* but are not associated with prevalent *TP53* mutations. Type II tumors include high-grade serous carcinomas (HGSC), high-grade endometrioid carcinomas, carcinosarcomas, and undifferentiated carcinomas. Type II tumors comprise invasive cells that are genetically unstable and frequently present with *TP53* mutations (Ahmed et al., 2010).

The most common subtype of epithelial ovarian cancer is serous adenocarcinoma. Approximately 70% of ovarian cancers are diagnosed as ovarian serous carcinoma, either low-grade or high-grade (McCluggage et al., 2011), with LGSC being less prevalent. It has been proposed that LGSC originates in a stepwise process from ovarian inclusion cysts to generate a cystadenoma which can progress to a serous borderline tumor. Some borderline tumors may progress to invasive LGSC (Kurman et al., 2010). Histologically, LGSC consists of well differentiated cells (McCluggage et

al., 2011) that can display as an invasive or non-invasive micropapillary serous phenotype (Yemelyanova et al., 2008).

In contrast, HGSC, the most common subtype of epithelial ovarian cancer, forms papillary tumors with poorly differentiated and highly proliferative cells (McCluggage, 2011). Most HGSC cases are diagnosed in an advanced stage with pelvic lesions and ascites. Histologically, HGSC tumors are composed of aggressive and invasive cells as a result of harboring *TP53* mutations (Kuhn et al., 2012). Since serous ovarian cancer represents the vast majority of epithelial ovarian cancer, understanding the cell of origin and risk factors for this type of cancer is essential.

1.1.2 Origin of epithelial ovarian cancer

The origin of ovarian cancer is still a matter of debate. Researchers are investigating several types of cells and looking for factors from the reproductive tract that could contribute to the initiation of epithelial ovarian cancers, with the goal to identify mechanisms to inhibit this process for cancer prevention. For more than 30 years, scientists focused on the poorly differentiated ovarian surface epithelial cells (OSE) with the widely accepted theory that the OSE gives rise to all epithelial ovarian cancers histotypes (Scully et al, 1995). It was proposed that ovarian cancer originated from OSE cells that had migrated into the ovarian stroma, likely during ovulation, and formed inclusion cysts that could become transformed. The epithelial cells lining the inclusion cysts were capable of differentiating and were shown to gain expression of numerous proteins associated with ovarian cancer, including CA125 (Duffy et al., 2005). It was

hypothesized that, depending on the path of differentiation, the epithelial cells could develop into the different subtypes of epithelial ovarian cancer including serous, endometrioid, clear, mucinous and transitional cell. This was supported by evidence that mouse OSE cells could be transformed by various *Hox* genes into cancers with different histologies similar to those present in human ovarian cancers (Ko et al., 2010).

It has been found, however, that the markers of serous ovarian carcinoma most closely match those expressed by the secretory cells of the fallopian tube, suggesting another possible origin. The molecular analysis of HGSC revealed a common set of gene expressions that is shared with the fallopian tube (Kessler et al., 2013). PAX2 and PAX8 are two proteins normally expressed in the fallopian tube and in some HGSC, but generally not in the OSE cells on the surface of the ovary (Tong et al., 2007), although evidence for PAX8 expression in human OSE has recently been reported (Adler et al., 2015). Moreover, lesions identified in the fallopian tube carry identical mutations in *TP53* found in co-existing HGSC tumors. Precursor lesions have been detected in the distal end of the fallopian tubes in patients carrying germline *BRCA1* or *BRCA2* mutations (Callahan et al., 2007). These precursor lesions in the fallopian tube include stratified and atypical epithelial cells which have been defined as serous tubal intraepithelial carcinoma (Cass et al., 2014). Thus, the current recommendation for women with *BRCA1* and *BRCA2* mutations is bilateral salpingo-oophorectomy (removal of both ovaries and fallopian tubes) to reduce the risk of developing ovarian cancer (Eisen et al., 2000; Kauff et al., 2002).

It has been proposed that the close association between the ovary and fallopian tube in the female reproductive system may increase the possibility of cancerous fallopian tube cells exfoliating and implanting on the surface of the ovary. Furthermore, exfoliated epithelial cells from the fallopian tube to the surface of the ovary may also invaginate into the ovary to form inclusion cysts that could develop as ovarian cancers (Kurman, 2013; Figure 1-1). This theory has received extensive support and led to investigations into mechanisms that might allow or promote the migration of epithelial cells to the surface of the ovary.

Several animal studies have provided evidence that fallopian tube lesions can initiate ovarian cancer and the fallopian tube epithelium is therefore considered a potential cell of origin for serous carcinomas. One study demonstrated that double knockout of *Dicer* and *Pten* in the oviducts of mice resulted in lesions in the distal end of oviduct. These lesions spread and metastasized to the ovary and developed ovarian cancer. The removal of fallopian tubes prevented tumor formation, which supports the hypothesis of the fallopian tube origin of ovarian cancer (Kim et al., 2012). The primary limitation of this model is that it appeared that the lesions first appeared in the stromal compartment of the fallopian tube, not the epithelium. A recent study in which *Trp53* mutation has been added to the *Dicer* and *Pten* mutations revealed that these mice developed HGSC in the fallopian tubes and the ovary. However, when the oviducts were removed, the deficient mice could still develop HGSC in the ovaries and metastasis to the peritoneal cavity (Kim et al., 2015), adding strength to the hypothesis that HGSC can arise from both the ovary and the fallopian tube. It could be argued that, since the fallopian tubes were removed from the

mice at two months of age, the oviductal epithelial cells might have had an opportunity before then to migrate from the fimbria and implant on the surface of the ovary.

Recent findings from mouse models that incorporate hereditary risk also implicate the fallopian tube as an origin for HGSC. It has been reported that oviductal secretory cells with *Brca1*, *Trp53* and *Pten* mutations developed fallopian tube lesions that metastasized to the ovaries and to the peritoneal cavity to form HGSC in mice (Perets et al., 2013).

Although most studies investigating the fallopian tube as an origin for ovarian cancer attribute its contribution to HGSC, other studies have found that fallopian tubes may also initiate LGSC, endometrioid and clear cell cancers (Kurman et al., 2010). Investigators have shown that ovarian LGSC may originate in inclusion cysts, however such cysts have epithelial cells that resemble fallopian tube cells (Li et al., 2011). Therefore, it has been suggested that cells lining the inclusion cyst may have originated from the fallopian tube. In fact, a study on 178 patients with cystadenoma, borderline tumors and serous tumors provide convincing evidence that LGSC might originate from inclusion cysts derived from either tubal or OSE cells. Twenty-two % of the ovarian inclusion cysts were positive for calretinin staining similar to OSE cells and 78% of the inclusion cysts were positive for PAX8 and tubulin, similar to fallopian tube cells (Li et al., 2011).

Several recent studies support the view that the inclusion cysts are made of either OSE invaginations from the surface of the ovary or tubal epithelial cells invaginating from the ovarian surface after migrating from the fimbriae and implanting on the surface of the ovary (Erickson et al., 2013; Zhang et al., 2015). It has been suggested that inclusion cysts formed by the tubal cells develop into HGSC which represent the vast

majority of serous cancers, whereas the inclusion cysts formed by OSE cells develop into LGSC (Auersperg et al., 2001).

Because of its recent implication in the origins of HGSC, the cellular origin of the inclusion cyst is now hotly debated. It was widely accepted that the inclusion cysts are formed by the invagination of OSE cells and these inclusion cysts develop LGSC in a step-wise fashion by undergoing "Mullerian metaplasia" in which OSE cells expressing Mullerian cell markers (tubulin and PAX8). Alternatively the PAX8-expressing fallopian tube epithelial cells migrated to the ovary and formed the inclusion cysts. The use of PAX8 as a marker of fallopian tube epithelium has itself become controversial, with the recent publication of evidence that PAX8 can be detected in OSE cells (Adler et al., 2015).

To complicate things further, it has been proposed that the inclusion cyst may be formed by the invagination of implanted cells consisting of both types of tubal cells: ciliated and secretory. During the malignant transformation of the inclusion cyst, it is hypothesized that the secretory cells rapidly proliferate and the number of the secretory cells expands, whereas the ciliated cells stop proliferating and the number starts to diminish in a step-wise process. This idea is supported by a study showing a reduced number of ciliated cells expressing tubulin during malignant transformation. The percentage of the ciliated cells was 30% in inclusion cysts, 10% in cystadenomas, 5% in borderline tumors and fully absent in both types of serous epithelial ovarian cancer, LGSC and HGSC (Li et al., 2011). What is needed is additional cell-specific markers and/or better model systems that can be used to study the process of inclusion cyst formation.

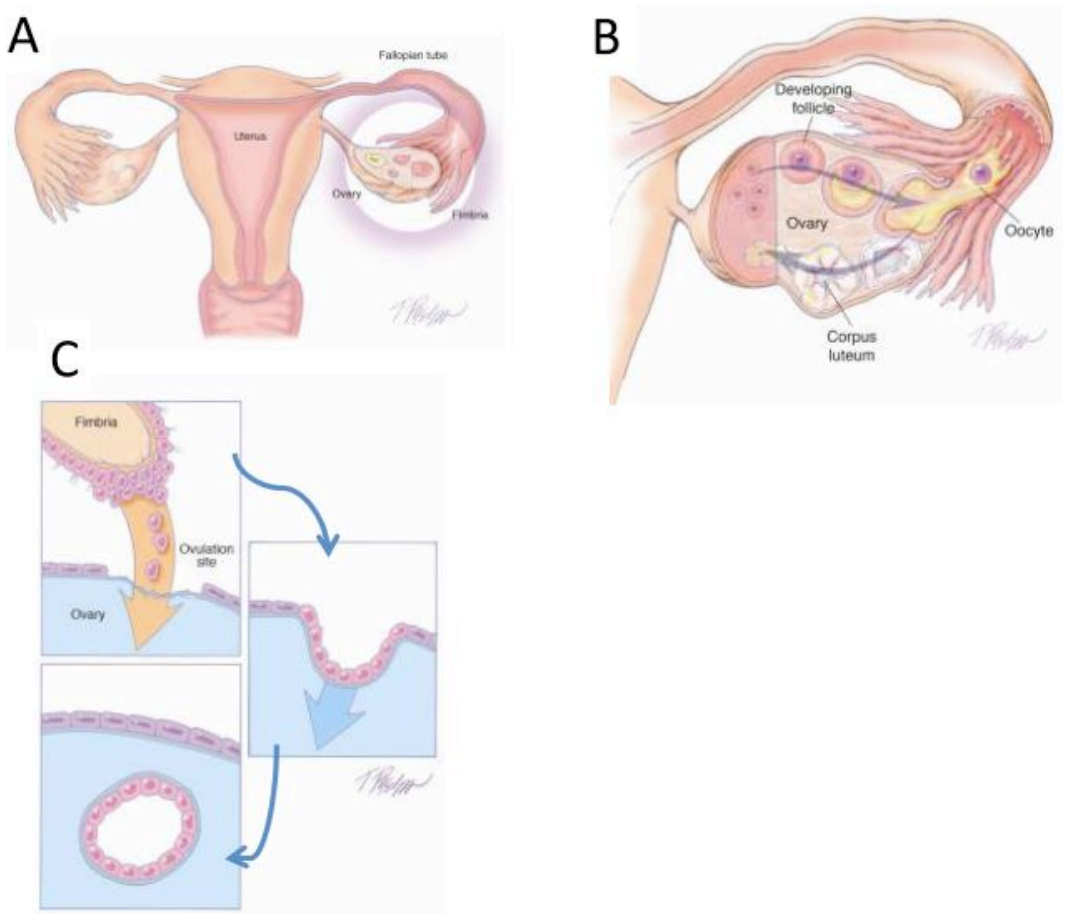

Figure 1-1: The hypothesized implantation process of fallopian tube epithelial cells from the distal end of the fallopian tube (fimbriae) to the ovary.

A and B: The anatomy of the female reproductive system shows the close association of the fimbriae to the ovary at the time of the ovulation. C: The fallopian tube sheds cells from a fimbrial projection and the cells implant on the ovulation site of the ovary, resulting in invagination and the formation of an inclusion cyst (Taken from Kurman, 2013, with permission).

1.2 Fallopian tube as a source of serous ovarian carcinoma

Fallopian tubes, also known as oviducts or uterine tubes form the upper part of the female genital tract and are longitudinal structures that connect the uterus with the ovaries to carry the ovulated ova every month (Brussow et al., 2008). The fallopian tubes have several distinct sections. The distal end of the fallopian tube includes finger-like projections called fimbriae that surround portions of the ovary to catch the oocyte at ovulation. The papillary configurations of the fimbria connect to the next portion of the fallopian tube, known as the infundibulum. The infundibulum leads to the ampulla, where fertilization mostly occurs. The next portion, called the isthmus, is the narrowest part of the fallopian tube and leads to the portion opening to the uterus known as the interstitium in human and uterotubal junction in mice (Figure 1-2).

The fallopian tubes are thought to be a source of early ovarian cancer for many reasons, including their proximity to the ovary, the type of cells that line the fallopian tubes, gene mutations, and exposure to assorted physiological risk factors such as ovulation.

1.2.1 Fallopian tube location

Fallopian tubes are located adjacent to and merge with the ovarian surface in a region called the "junctional zone". Since there are no clear margins separating the fallopian tube epithelial cells from the OSE cells in the junctional zone, this region represents a transitional zone (Auersperg et al., 2011).

It has been hypothesized that epithelial cells in the junctional zone cells are prone to neoplastic transformation (Rabban et al., 2011). Consistent with that hypothesis, the

junctional zone is enriched with label-retaining cells that express stem/progenitor cell markers such as ALDH, LGR5 and CD133 (Flesken-Nikitin et al., 2013). Further, the junctional zone cells have transformation potential when the tumor suppressor genes *TP53* and *Rb1* are inactivated, suggesting that the stem/progenitor cells in the junctional zone may be cells of origin of HGSC (Flesken-Nikitin et al., 2013). Whether this is true remains a controversial issue, but some studies have suggested that the junctional zone cells are fimbrial precursor cells since they acquire expression of the fallopian cell marker PAX8 (Auersperg et al., 2011).

The fimbrial ends of the fallopian tubes are lined with epithelial cells that are exposed to the peritoneal cavity. The connection site between the tubal cells in the fimbriae and the mesothelial cells lining the peritoneal cavity is known as the fallopian tube-peritoneal junction. It has been proposed that the tube-peritoneal junction increases the possibility of the fallopian tube shedding cells into the peritoneal cavity during ovarian carcinoma metastasis (Seidman et al., 2011).

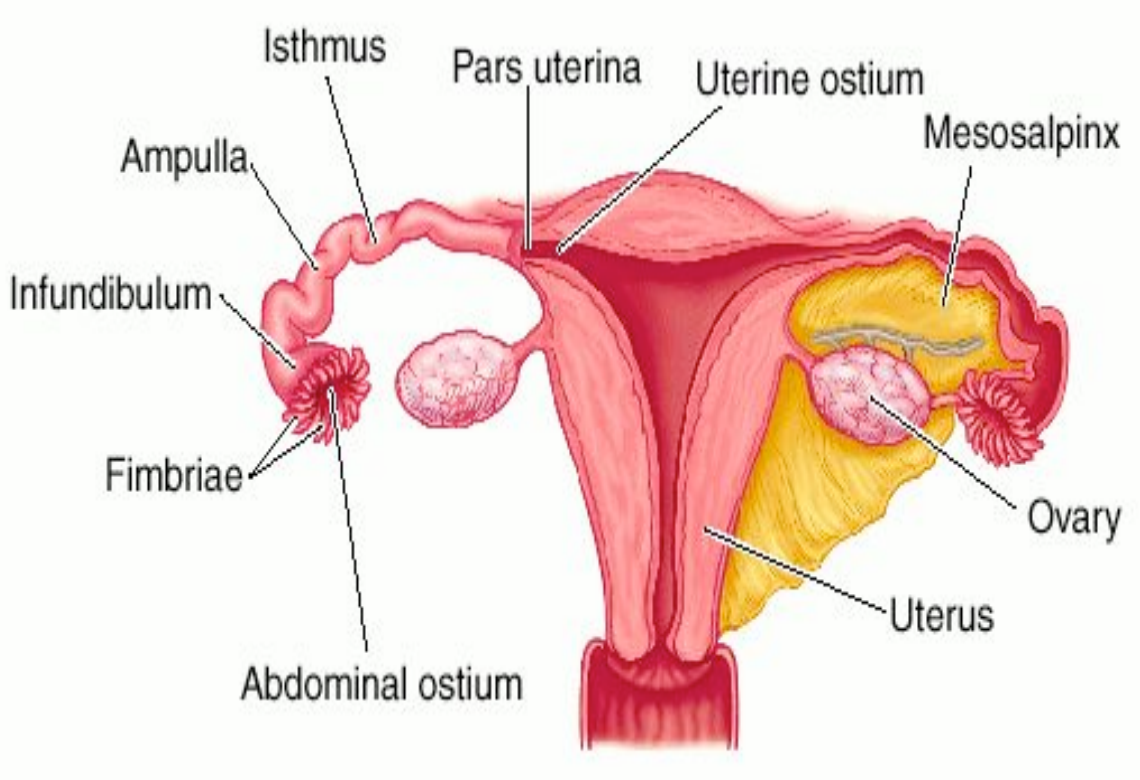

Figure 1-2: Female reproductive system anatomy.
A female reproductive system shows fallopian tubes close to the ovary and consists of different tubal segments (*http://medical-dictionary.thefreedictionary.com/tube, downloaded on November 13, 2015*).

1.2.2 Fallopian tube cells

Fallopian tubes are embryologically derived from the Mullerian duct, whereas OSE cells are derived from the coelomic epithelium (Lengyel et al., 2010) and the idea that the cells of origin of ovarian epithelial tumors arise in cells derived from the Mullerian duct is now highly supported by several studies as reviewed by Dubeau et al. (1999). The fallopian tube mucosa is lined with four types of cells: secretory epithelial cells, ciliated cells, intercalary and basal cells (Bogaert et al.,1978) (Figure 1-3). The majority of the tubal cells are secretory cells, which represent 60% of the fallopian tube cells and produce tubular fluid to promote the fertilization process. These cells arise in the isthmus more than other fallopian tube sites (Yamanouchi et al., 2010). The secretory cells are commonly distinguished from ciliated cells by the expression of PAX8 and OVGP1 (Endsley et al., 2015). Interestingly, one study reported that each secretory cell possesses a single primary cilium extending from the apical surface and visible when the cells are imaged by electronic microscopy (Hagiwara et al., 2008). Progesterone and estrogen regulate the secretory activity of these cells (Chen et al., 2013).

Secretory cells have been identified in HGSC, suggesting that the secretory cell types are more likely to transform to initiate ovarian cancer (Zhang et al., 2015). A recent study reported that secretory cells expressing PAX8 from mouse oviducts lacking *Trp53*, *Brca1* and *Pten* developed HGSC (Perets et al., 2013). Although it has been reported that secretory cells may differentiate into ciliated cells (Comer et al., 1998), frequent passages of murine oviductal cells exhibit loss of ciliated cells and outgrowth of the secretory cells (Endsley et al., 2015). Furthermore, highly passaged

mouse secretory cells can spontaneously transform and form tumors when the cells are xenografted into female nude mice (Endsley et al., 2015). These studies suggest that the secretory cells are the cells that may develop into spontaneous ovarian cancer associated with aging.

Ciliated cells represent 25% of fallopian tube cells and estrogen enhances the production of cilia on these cells (Comer et al., 1998). Scientists identify ciliated cells by their expression of acetylated beta tubulin (Comer et al., 1998) or FOXJ (Okada et al., 2004). Although the ratio of ciliated cells to secretory cells varies depending on the region of the fallopian tube and the phase of the menstrual cycle, ciliated cells are mostly concentrated in the fimbriae to facilitate the movement of the oocyte forward to the uterus (Crow et al., 1994).

Intercalary cells, which represent less than 10% of fallopian tube cells, are also known as peg cells (Bogaert at al.,1978). Intercalary cells are located between ciliated cells and it is believed that these cells are inactive secretory cells that secrete nutrients into the fallopian tube fluid in response to estrogen (Lauschová, 2003).

The remaining cells are small rounded cells located in the basement membrane of the mucosal layer and are known as basal cells, intraepithelial lymphocytes or “indifferent” cells. Their function has yet to be determined. Some studies report only three types of fallopian tube cells and propose that basal cells are progenitor cells with stem cell characteristics located in the basement membrane (Paik et al. 2012; Auersperg 2013). Paik et al. (2012) have suggested that basal cells are the potential cells of origin for ovarian cancer. In fact, the definitive identity and function of the fallopian tube cells, particularly intercalary and basal cells remains incomplete.

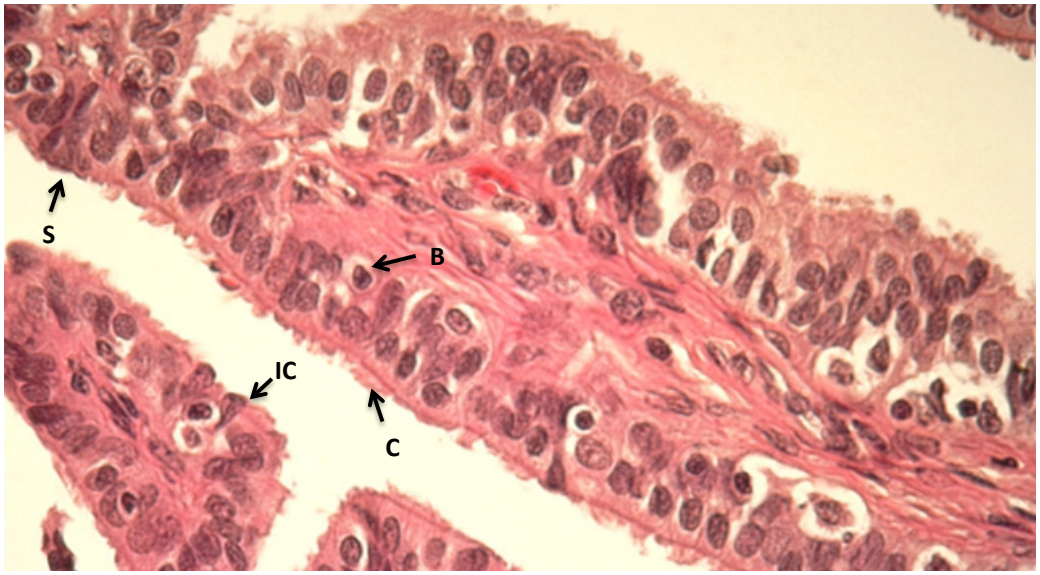

Figure 1-3: Human fallopian tube cytology.
Human fallopian tube shows different types of epithelial cells lining the mucosa layer: ciliated cell (C), Secretory cells (s), Intercalary cells (IC) and Basal cells (B). (*http://medpics.ucsd.edu, downloaded on November 13, 2015)*

1.3 Tubal Intraepithelial Carcinoma

Tubal intraepithelial carcinoma (TIC) is an abnormal growth of the cells in the distal end of the fallopian tube that is adjacent to the ovary (Medeiros et al., 2006). The abnormal growth in the fimbriae has been discovered in patients with ovarian cancer and in patients with high risk of developing ovarian cancer such as BRCA1 carriers. TICs have been found to be frequently associated with serous cancer, predominantly HGSC (Perets et al., 2013). Therefore the lesion is now termed serous tubal intraepithelial carcinoma (STIC) and is proposed to be a precursor lesion for ovarian carcinoma (Chen et al. 2010; Li et al., 2014). Although the tubal lesions in the prophylactically-removed fallopian tube have been described using different terms, such as TIC, STIC or high-grade tubal intraepithelial neoplasm (reviewed in Zeppernick et al., 2015), all agree that these lesions are predominantly located in the fimbria and are considered precursor lesions that may initiate the ovarian cancer.

STIC cells acquire several characteristics that help to distinguish them from normal fallopian tube cells, including the lack of polarity, cell disorganization and a rapid mitotic index for non-ciliated cells (Kurman, 2013). They have been found in 10-15% of patients carrying a germ line *BRCA1* mutation and who are at risk of developing ovarian cancer (Cass et al., 2014). Further, 50-60% of sporadic ovarian cancers have associated STICs in the fallopian tubes (Kurman et al. 2011).

Crum et al. (2007) proposed a model to explain the tumor progression from normal cells to invasive carcinoma (Figure 1-4). They suggested that precursor lesions in the fallopian tube could be identified initially as secretory cell outgrowths (SCOUT) in which 10 or more non-ciliated cells in a row have lost paired box protein 2 (PAX2) expression

in the distal end of the fallopian tube (Chen et al., 2010). Only 25% of total detected SCOUTs presented P53 staining, but almost all SCOUTs with abnormal P53 display loss of PAX2 in the fimbria. Since almost all SCOUTs are associated with loss of PAX2 and not all of them presented *TP53* mutation, it is likely that loss of PAX2 is an early event in developing STIC (Chen et al., 2010).

Consistently, a positive relationship between the number of secretory cells and age in high-risk populations has been demonstrated (Li et al., 2013), suggesting that determining the ratio of secretory cells to ciliated cells may be a sensitive biomarker to predict early serous carcinogenesis (Li et al., 2013).

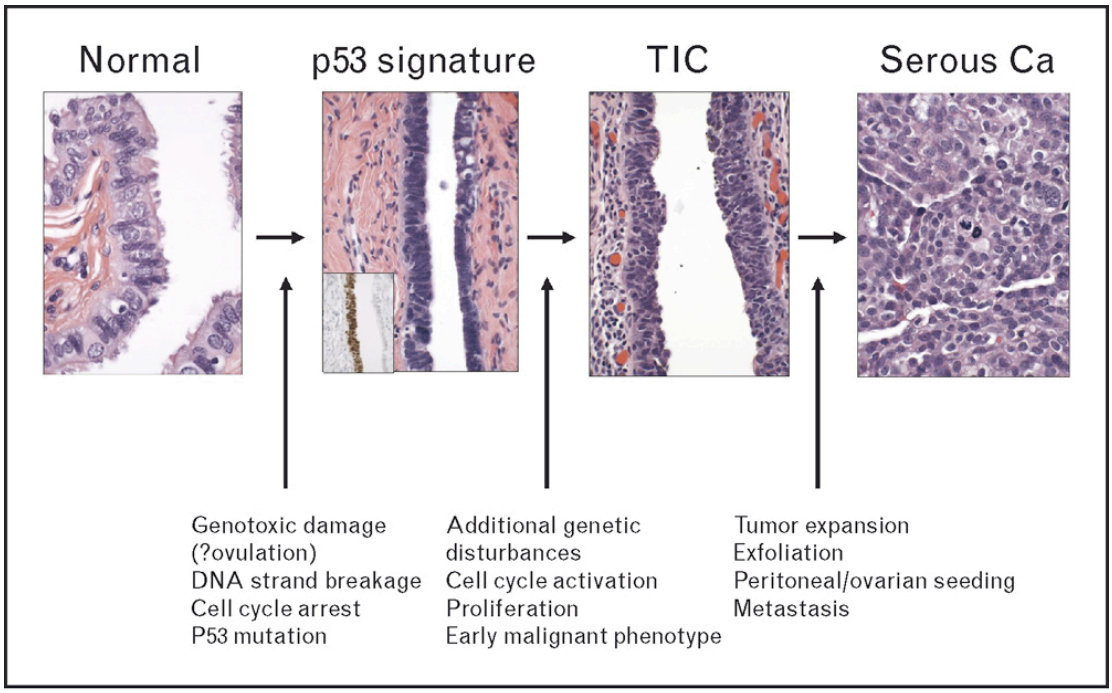

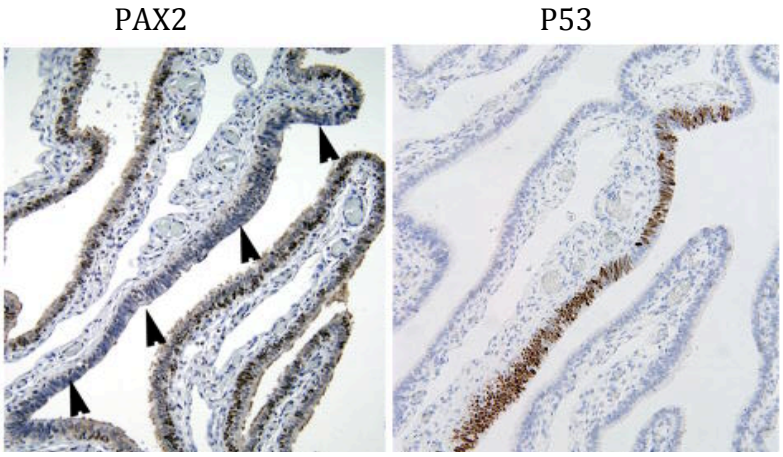

Figure 1-4: Model of the development of high-grade serous ovarian cancer.
Upper panel is a model of STIC development showing the P53 signature in fallopian tube cells that is thought to induce cell proliferation (step 1). *BRCA1* mutation influences the likelihood of transition from enhanced cell proliferation to tubal intraepithelial carcinoma (TIC, Step 2). The metastasized TIC cells expand the tumor to the ovarian surface or peritoneum to develop serous carcinoma (step 3) (Taken from Crum et al., 2007, with permission). The lower panel shows a STIC presenting loss of PAX2 (black arrows) in the left picture and P53 signature in the right picture (Taken from Chen et al., 2010, with permission).

1.4 PAX2 in the fallopian tube and ovarian cancer

PAX2 is a transcription factor that plays an important role during embryogenesis and development (Torres et al., 1995). It is required for fallopian tube and kidney formation and protects cells from apoptosis (Torres et al., 1995). *PAX2* mutations cause developmental abnormalities in the kidney and the oviduct. *Pax2*-null mice lack kidneys and the entire genital tract after birth (Torres et al., 1995). Interestingly, heterozygous mutation of *Pax2* affects kidney formation, whereas the uterus and oviduct are affected only with homozygous mutation (Eccles et al., 2002). *PAX8* is another *PAX* gene closely related to *PAX2* that is normally expressed by fallopian tube epithelial cells. PAX2 and PAX8 proteins have combined function for fallopian tube formation and maintenance (Kobayashi et al., 2003).

In adult tissues, PAX2 protein is expressed in normal oviductal epithelial cells (OVE) and some ovarian cancer cells but it is not expressed in normal OSE (Chen et al., 2010). A recent study reported that PAX2 is expressed in 100% of serous ovarian carcinoma cases (Wang et al., 2015); however this is not supported by previous studies reporting that as low as 9% of these cancers express PAX2 (Tung et al., 2009). These discordant observations emphasize the need to better understand the role of PAX2 in tubal epithelium and the cause and biological consequences of the loss of PAX2 expression that is seen in SCOUT and STIC. These might help to define its potential role in the initiation of ovarian carcinomas.

Despite the important role of PAX2 in fallopian tube development, no study has yet reported its transcriptional targets (Bose et al., 2009; Jiang et al., 2014). However, it has been proposed that the crucial role of PAX2 in morphogenesis requires complementary

actions to manipulate the pluripotency state of stem cells during organogenesis (Blake et al., 2014; Chi et al., 2002). Therefore, a better understanding of the role of PAX2 in fallopian tubes and ovarian cancer includes the need to identify the transcriptional targets of PAX2 that may inhibit cell proliferation and STIC lesion formation.

1.5 Tumor suppressor genes and ovarian cancer

Type II ovarian cancer, including HGSC, is genetically unstable and exhibits frequent mutation in the tumor suppressor gene *TP53.* Mutation of another tumor suppressor gene, *BRCA1,* has also been associated with ovarian high-grade carcinoma and it has been suggested that this subtype arises from the fallopian tube STIC. Although *TP53* and *BRCA1* genes are well known tumor suppressor genes, the actual effects of *TP53* and *BRCA1* mutations in enhancing the development of ovarian cancer that initiates from STIC are poorly understood.

1.5.1 BRCA1 and ovarian cancer

Breast cancer type1 (*BRCA1*) inactivation can be hereditary or sporadic. Germline mutations are an established risk factor for breast and ovarian cancer (Hilton et al., 2002). Both familial and sporadic breast and ovarian cancer risk is increased by women's age (Antoniou et al., 2003). *BRCA1* mutation in women reaching 60 years confers a breast cancer risk of 54% and an ovarian cancer risk of 30% of *BRCA1* mutation carriers (Easton et al., 1995). Current evidence suggests that *BRCA1* mutation carriers are more likely to develop ovarian cancer initiated in fallopian tube precursor lesions. Patients with *BRCA1* mutations were found to develop lesions in the fallopian tubes (Folkins et al., 2008), but not in the OSE layer of cells (Barakat et al., 2000). Malignant tubal lesions

have been discovered at the time of prophylactic surgery for 5.7 % of women carrying *BRCA1/2* mutations (Callahan et al., 2007). Therefore, risk-reducing salpingo-oophorectomy is highly recommended for women carrying a *BRCA1* mutation.

BRCA1 is expressed normally in breast cells and other tissues in the body. It is involved in the DNA repair process for both double-strand break and single-strand break repair. For example, in normal cells exposed to radiation and DNA-damaging drugs, BRCA1 interacts with RAD51 to repair the double-strand break (Junran et al., 2005). BRCA1 is also involved in DNA mismatch repair that results from a single-strand break in which BRCA1 binds with DNA mismatch repair proteins such MSH2, MSH6 and PARP to repair the DNA damage (Gudmundsdottir et al., 2006). Absent or defective BRCA1 proteins resulting from *BRCA1* mutations are not able to repair DNA damage, increasing the accumulation of gene mutations, which leads to increased cell proliferation and cell tumorigenicity. Hereditary ovarian, fallopian tube and peritoneal carcinoma are also associated with mutations in other tumor suppressor genes, including *BRCA2, TP53, RAD5, RAD51, BARD and MSH6* (Walsh et al., 2011).

Germline mutations that result in hereditary ovarian cancer represent up to 20% of ovarian cancers. However, 5-10% of sporadic ovarian cancers have been associated with impaired BRCA1 function as a result of somatic *BRCA1* mutation, hypermethylation, loss of heterozygosity or haploinsufficiency (Weberpals et al., 2008; Burgess et al., 2014). Mutations in *BRCA1* have been found in three different domains of the *BRCA1* gene, including the ring domain, BRCT domain and central domain (Figure 1-5). The ring domain is responsible for E3-ubiquitin ligase activity. The BRCT domain binds directly to damaged DNA double strands for DNA repair activity. However, the most frequent

BRCA1 mutations occur in the central domain within exons 11-13, which have a significant role in tumor suppression. The BRCA1 protein encoded by these exons contains binding sites for several cellular regulatory proteins including Retinoblastoma (RB), C-Myc, RAD50 and RAD51. BRCA1 binds the phosphorylated form of RB to induce cell cycle arrest. Deletion of the *BRCA1* segment containing the RB binding site eliminates the effect of BRCA1 in cell growth suppression (Aprelikova et al., 1999). In addition, BRCA1 binds to C-Myc to decrease transcription and transformation, whereas segments encoded by exon 11 bind RAD50 and RAD51 as part of the DNA damage response. BRCA1 exons 11-13 also encode a nuclear localization signal, and the deletion of these exons prevents localization of BRCA1 to the nucleus, where DNA repair is needed (Clark et al., 2012).

In a mouse model, oviductal secretory cells with combined mutations in *Brca1*, *Trp53* and *Pten* lead to the development of invasive HGSC. Interestingly, a *Trp53/Pten* null mouse model developed only STIC in the fallopian tubes with no invasive tumors, suggesting that *Brca1* mutation has a role in inducing tumor progression and metastasis (Perets et al., 2013).

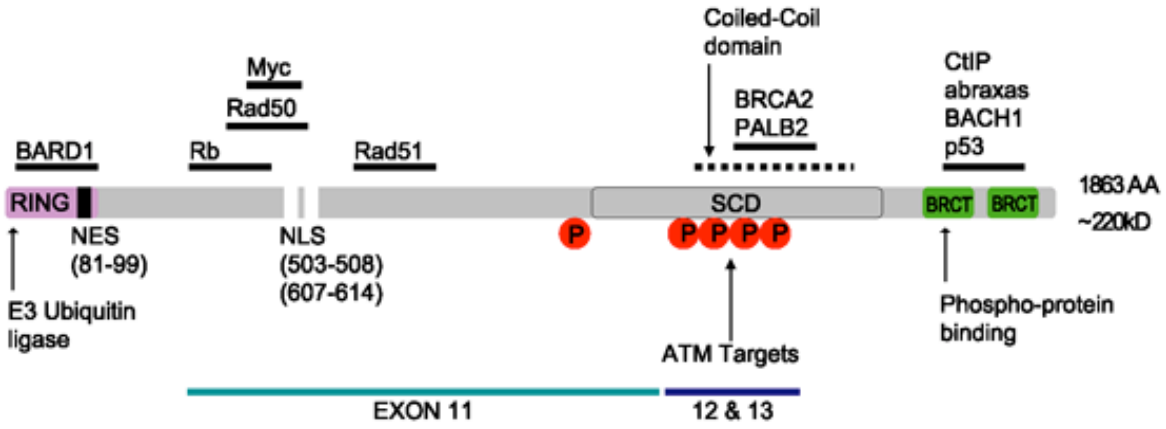

Figure 1-5: A schematic presentation of the *BRCA1* gene and encoded proteins including the functional domains.
Mutations on *BRCA1* commonly exist in three domains including the ring domain (RING), BRCT domain and central domain encoded by exon 11, which presents the most frequent *BRCA1* mutations (Taken from Clark et al., 2012, with permission).

1.5.2 P53 and ovarian cancer

The examination of the fallopian tubes removed from predisposed patients (women with a family history of cancer) resulted in the observation of neoplastic lesions in 50% of the patients (Piek et al., 2001). As a result of this and other studies indicating a tubal site as an origin for ovarian cancer, removal of the fimbria from patients at risk of ovarian cancer has been highly recommended (Kauff et al., 2002). The removed fimbria are extensively investigated with a method known as Sectioning and Extensively Examining the FIMbria (SEE-FIM), where malignant lesions can be detected through the serially sectioned fimbria (Medeiros et al., 2006). The prevalence of P53 expression was investigated to determine if the fallopian tube lesions are associated with tumor suppressor mutation, and non-ciliated cells in the fimbria were found to exhibit a robust P53 expression. Thereafter, P53 immunoreactivity in the fallopian tube, called the "P53 signature" (Lee et al., 2007), has been confirmed to correlate with *TP53* mutation in STICs and HGSC. Strong and diffuse P53 staining associates with missense *TP53* mutations and was present in 61% of STICs, whereas the absence of P53 staining correlates with null mutation and was observed in 39% of STICs (Kuhn et al., 2012).

The P53 signature has been associated with DNA damage by investigating its co-localization with γ-H2AX. Further, Ki67 has been detected in the proliferative non-ciliated cells in the fimbria that acquire the P53 signature (Lee et al., 2007). Unexpectedly, in 75 samples from *BRCA1* mutation carriers, the P53 signature was identified in 29 cases in the fimbria and only one case in OSE cells and none in inclusion cysts (Folkins et al., 2008). However, *in vitro* experiments on OSE cells isolated from *BRCA1* mutation carriers reported low expression of P53 in predisposed cases compared

to control non-predisposed cases (women without a family history of cancer) (Piek et al,. 2006).

Subsequently, P53 signatures have been associated with Ki67 staining and used to identify fimbriated precursor lesions (Leonhardt et al., 2011). Several studies have reported P53 signatures in STICs, which contain transformed fallopian tube cells (Leonhardt et al., 2011). Secretory cell expansion and P53 signature were also detected in normal fallopian tubes from *BRCA* mutation carriers (Medeiros et al., 2006), indicating that there are physiological factors that may induce DNA damage in the fallopian tubes. The incidence of STIC has been examined in cases diagnosed as peritoneal serous (Horn et al., 2013), mucinous, endometrioid, clear cell carcinomas, and malignant Brenner tumors, but found only associated with serous carcinoma (Munakata et al., 2015).

Finally, 82% of STIC samples that have been identified by P53 signature present decreased telomere length (DNA sequence protecting the chromosomes) compared to both adjacent normal tube and to HGSC. The authors have suggested that telomere shortening in STIC is a result of oxidative stress that is associated with ovulation which leads to cellular damage, and that HGSC may arise from those STICs (Kuhn et al., 2010).

1.6 Physiological risk factors for ovarian cancer

1.6.1 Ovulation

Ovulation is the process of releasing a mature oocyte from the ovary to be fertilized in the fallopian tube and implant in the uterine endometrium (Brussow et al., 2008). During the ovulation process, the dominant follicle containing the full-grown oocyte is

ruptured, creating a wound on the surface of the ovary to release the oocyte and the follicular contents (Yang-Hartwich et al., 2014). Frequent ovulation associated with aging and early puberty has been determined to be a risk factor for ovarian cancer. In contrast, pregnancy and the use of contraceptive pills are protective factors that reduce the risk of ovarian cancer (Auersperg et al., 2008).

Fathalla reported in 1971 his hypothesis that stimulating the OSE with frequent ovulations increases the risk of ovarian cancer (Fathalla et al., 1971). Subsequent evidence has supported this hypothesis by assessing the OSE response to factors associated with ovulation. It has been reported that OSE cells proliferate significantly more in response to the hormones associated with ovulation in a mouse model (Burdette et al., 2006). Ovulation also induces an inflammatory response in OSE cells as well as DNA damage and oxidative stress, possibly contributing to OSE cell transformation (Murdoch et al., 2001).

Since the fimbriae of the fallopian tubes are close to the ovary, King et al. (20110) have hypothesized that ovulation may impact on the fallopian tubes as well. Ovulation increases the inflammatory response and DNA damage seen in the oviduct 12 and 16 hours after injection of mice with human chorionic gonadotropin (to induce ovulation) compared to the control with injection of PBS alone (Hennessy et al., 2009). Macrophage infiltration was observed in the oviducts from ovulated mice, indicating an inflammatory response. Furthermore, DNA damage was identified in the ovulated mice by detecting histone protein phospho-γH2A.X that was released upon formation of double stranded DNA breaks. Notably, proliferation of the fallopian tube epithelial cells didn't increase

after ovulation, suggesting either no effect on proliferation, or that later time points after ovulation are needed (Hennessy et al., 2009).

Fallopian tube fimbriae and ampulla from *BRCA1/BRCA2* mutation carriers were investigated for their proliferation index during the menstrual cycle. The study showed a significant increase in cell proliferation in the fallopian tubes in the follicular phase of the menstrual cycle, potentially indicating the impact of ovulation in enhancing proliferation and lesion formation (George et al., 2012). Morphological changes in tubal epithelial cells have also been noted during the menstrual cycle. During the follicular phase (pre-ovulation), the fallopian tube cells become more stratified and the cells revert back to a single layer of epithelial cells after ovulation (Crow et al., 1994).

Ovulation may also influence migration of the epithelial cells from the fallopian tube to implant on the surface of the ovary, as has been shown for cancer cell migration from the oviduct to the ovary in superovulated mice. The cytokines released during ovulation such as granulosa cell-secreted SDF-1, may attract the cancer cells to migrate and it has been suggested that the migrated cells enter through the ovulatory wound and then form a tumor in the ovary (Yang-Hartwich et al., 2014).

Beside SDF-1, the follicular fluid contains many cytokines, chemokines and growth factors including EGF, IL-6, TNFα, TGFβ1 and TGFβ2. Any of these pro-inflammatory cytokines alone or in combination may promote favourable conditions for the initiation of ovarian cancer (Yang-Hartwich et al., 2014).

1.6.2 Transforming growth factor beta (TGFβ)

TGFβ and TGFβ receptors have been detected on the ovarian surface cells in normal

human ovaries and in ovarian tumor cells (Nilsson et al., 2001). TGFβ has a number of known functions, including the ability to induce the pro-inflamotory response at the ovulation site (Jabbour et al., 2009). Ovarian follicular fluid in the human (Fried et al, 1998) and bovine (Nilsson et al. 2001) contains TGFβ that is released at the time of ovulation. Zhao and coworkers have found that fallopian tube epithelial cells express TGFβ as well (Zhao et al. 1994).

TGFβ proteins belong to the TGFβ superfamily and include three isoforms; TGF-β1, TGF-β2 and TGF-β3. All three isoforms have similar effects but they have different cell targets. Different cell types in the body express TGFβ in a large latent complex binding the extracellular matrix (Miyazono et al., 1991). Proteases cleave the latent TGFβ1 complex to release the TGFβ cytokine from the extracellular matrix and active TGFβ is then able to bind its receptor on the cell surface. TGFβ cleavage and activation is a response to specific signals such as cell growth, wound repair and inflammation (Annes et al., 2003). Active TGFβ ligands on the cell membrane bind to type II TGFβ receptors (TGFBRII). TGFBRII dimers recruit TGFβ receptor type I (TGFBRI) dimers to form hetero-tetrameric dimers with the ligand. TGFBRII phosphorylates TGFBRI and activates the binding to SMAD2/3 through the SMAD anchor for receptor activation (SARA). Phosphorylated SMAD2/3 binds SMAD4 in the cytoplasm and forms a complex that enters the nucleus. The complex binds the promoter of genes involved in many cell functions including apoptosis, cell cycle arrest and immunosuppression (Heldin et al., 2012). While this conical TGF-β pathway requires SMAD signaling, a

non-canonical SMAD-independent signaling pathway involves activation of MAP kinase signaling and phosphorylation of ERK1/2 (Vaidya et al., 2015).

In the ovary, TGFβ is expressed by granulosa and theca cells and plays various functions during the menstrual cycle. TGFβ likely has a significant role in follicular development and selection of the dominant follicle (Field et al., 2014) and induces the expression of FSH receptors on granulosa cells. TGFβ also interacts with VEGF to promote angiogenesis during follicular development (Kuo et al., 2011), suggesting that it may also synergize with VEGF to form a new microvessel network at the ovulation rupture site during extracellular matrix remodeling.

Importantly, TGFβ plays critical roles in ovulation and fertilization. Knockout of *SMAD4* (the canonical TGFβ signaling pathway) in ovarian granulosa cells causes defects in luteinization and disrupts ovulation, resulting in premature ovarian failure (Yu et al., 2013; Pangas et al., 2006). In human, TGFβ induces the expression of cyclooxygenase-2 (COX-2) and the derived protein prostaglandin E2 (PGE2) in granulosa cells (Fang et al., 2014). COX2 and PGE2 play very important roles in ovulation; mice lacking COX2 are infertile due to failure of ovulation (Lim et al., 1997).

Although TGFβ is known to have tumor-suppressing activity and decreases cell proliferation in normal epithelial cells, TGFβ proteins play multiple roles in cancerous cells (Akhurst et al., 2001). TGFβ can act as tumor suppressor and induce cell apoptosis in benign tumor cells (Havrilesky et al., 1995). However, it increases tumor progression, cell migration and invasion in malignant tumors, which leads to tumor metastasis (Rodriguez et al., 2001; Basu et al., 2015). Latent TGFβ binding protein-1 (LTBP-1) is

extensively expressed in serous and mucinous ovarian carcinoma compared to normal OSE cells, suggesting that LTBP-1 may interfere with TGFβ protein distribution in ovarian cancer cells (Higashi et al., 2001).

Several mechanisms have been considered that may implicate TGFβ in the transformation process. Estrogen replacement therapy is a known risk factor for ovarian cancer (Rodriguez et al., 2001a), and it has been shown that estrogen can regulate TGFβ expression and signaling in bovine stromal cells (Nilsson et al., 2002). *In vivo* and *in vitro*, bovine follicles displayed a significant negative relationship between follicular TGFβ and estradiol concentration, raising the possibility that increased estrogen may inhibit TGFβ and its proliferation suppressive effects (Ouellette et al., 2005).

Furthermore, gene mutations of TGFβ-signaling molecules such as TGFβ receptors genes (Biswas et al., 2004) and *SMAD* genes (Ungefroren et al., 2011) may abrogate the inhibitory effect of TGFβ and result in TGFβ-associated disease and cancer (Zhu et al. 1998). Similarly, other cross-talk signaling pathways, such as RAS may interfere with TGFβ signaling, as it has been shown that TGFβ loses its inhibitory effects if mutant RAS is expressed in TGFβ-sensitive intestinal cells (Filmus et al., 1992).

TGFβ treatment decreases OSE cell proliferation *in vitro* (Berchuck et al., 1992). Along with other wound repair signals, TGFβ is known as an essential pro-inflammatory cytokine for wound repair (Kasuya et al., 2014). Since ovulation creates a wound on the surface of the ovary, it is likely that TGFβ/SMAD signaling contributes to and/or responds to the inflammation signals to repair the wound through as yet unknown mechanisms. OSE cells appear to undergo an epithelial to mesenchymal transition (EMT)

at the time of ovulation (Gamwell et al., 2012), possibly to induce cell motility to facilitate wound closure. TGFβ is a well-established inducer of EMT in many tissues (Xu et al., 2009). In addition to facilitating cell migration, it has been reported that epithelial cells undergoing EMT increase characteristics similar to stem cells (Mallini et al., 2014). Consequently, it has been hypothesized that TGFβ production and EMT induction in the OSE cells every menstrual cycle may induce stem cell proliferation which could contribute to ovarian cancer (Gamwell et al., 2012).

Although TGFβ has been detected in the fallopian tube (Srivastava et al., 1996), no study has yet investigated the effects of TGFβ on fallopian tube cells. Therefore, and because of the strong evidence supporting the fallopian tube origin of ovarian cancer, we focused in this study on the effects of TGFβ on fallopian tube epithelial cells.

1.7 Epithelial -Mesenchymal Transition (EMT)

Cells commonly respond to tissue wounding by activating EMT to refurbish the tissue. In the ovary, ovulatory rupture activates OSE cells to acquire more mesenchymal characteristics to regenerate the cell layer (Auersperg et al. 2001; Hay et al; 1995). While there is no evidence that OVE cells undergo EMT, and the fallopian tube cells have not been characterized for this transition during ovulation, the possibility that ovulation may also impact the OVE cells has been demonstrated by King and coworkers. They have shown increasing DNA damage in OVE in response to the ovulation-associated inflammatory reaction (King et al., 2011).

EMT is a normal process first described in tissues during development, embryogenesis and in wound healing, but it also occurs in some cancerous tissues (Hay et

al., 1995) where it may enhance tumor progression and metastasis. Epithelial cells converted to mesenchymal cells fail to keep their unique epithelial characteristics. The cells lose cell-to-cell contact and cell polarity, and acquire a fibroblast-like shape.

Epithelial cells are connected to each other through cell junctions, including tight junction molecules, adherens junctions, desmosomes and hemi-desmosomes (Shin et al., 2006). The extent of cell junctions depends on the type of tissue and cell functions in this tissue. Tight junctions are located close to the apical surface of the cells and protect the cells from paracellular diffusion (i.e occludin, claudins). Below the tight junctions, are the adherens junctions, which bind the juxtaposed cells through calcium-dependent channels (i.e. calcium-dependent cell-cell adhesion molecules; E-cadherin). Desmosomes are located close to the basolateral surface and are similar to adherens junctions in structure (i.e desmosolin). Desmosomes strengthen the tissue stability by linking the extended intermediate filaments to the plasma membrane, whereas hemi-desmosomes provide the attachment to the extracellular matrix.

Healthy epithelial cells are polarized, quiescent and non-traveling. Cell polarity maintains the cells' integrity and functionality through a specific distribution of proteins, lipids and organelles within the cells and cell membranes (Tervonen et al., 2011). Loss of polarization is an initial hallmark for cells undergoing EMT and for cancer cells (Ellenbroek et al., 2012). Cell polarity is regulated by epithelial cell junction molecules, which restrict the intracellular protein diffusion across epithelial cells. Protein complexes in the tight junctions maintain the apico-basal polarity by determining the apical and basolateral domain. Tight junctions regulate cell signaling transduction and, consequently, gene expression in the nucleus which regulates cell proliferation and

differentiation (Shin et al., 2006). Loss of polarity and reduced intracellular junction molecules in cells undergoing EMT results in disorganization of cell shape and alignment, which induces cell migration, invasion and tumor progression. Migratory cells undergoing EMT may be converted to invasive cells, where the extracellular matrix proteins are degraded, allowing cells to escape from the epithelial structure to invade the adjacent tissue (Xu et al., 2009). Loss of desmosomal desmocollin and E-cadherin can result in reduced polarity of mammary epithelial cells (Shin et al., 2006).

The alterations in gene expression of cells undergoing EMT induce additional mesenchymal features, including the spindle shaped morphology, cell migration and invasion. Loss of E-cadherin expression and a switch to N-cadherin is a fundamental indicator of cells undergoing EMT (Gheldof et al., 2013). E-cadherin suppression is regulated by the zinc-finger transcription family including SNAIL, SLUG, ZEB1, ZEB2 and TWIST (Yang et al., 2005). SNAIL has been widely investigated as an E-cadherin suppressor and EMT inducer (Elloul et al., 2006; van Roy et al., 2008), and SNAIL overexpression was found in primary and metastatic ovarian cancer and associated with loss of E-cadherin expression (Mirantes et al., 2013).

Various growth factors have been reported to induce EMT in ovarian cancer such as TGFβ, fibroblast growth factor, hepatic growth factor and platelet derived growth factor (Campo et al., 2015). Very recently, Interlukin-6 has been reported to induce EMT in ovarian cancer cell lines, enhancing cell migration and invasion (So et al., 2015). Among these growth factors, TGFβ is the most well-established as an inducer of EMT in many cell types of epithelial cells.

In OSE cells, TGFβ treatment has different effects since OSE cells are poorly differentiated and possess both epithelial and mesenchymal morphologies (Davidson et al., 2012). This concept is based on the co-expression of both epithelial markers (CK8) and mesenchymal markers (vimentin, N-cadherin and lack of E-cadherin) (Auersperg et al., 2001). Although the observation of EMT in these cells is challenging, *in vitro* experiments have shown that TGFβ treatment induces partial EMT processes in human OSE cells (Yihong Zhu, et al., 2010), and can induce EMT by increasing Snail expression and decreasing E-cadherin in mouse OSE cells (Gamwell et al., 2012). This EMT in mouse OSE cells was associated with increased stem cell characteristics, similar to what has been reported in mammary epithelial cells (Welm et al., 2002). It remains to be determined whether oviductal epithelial cells respond in the same way.

Early neoplasia in epithelial cells for several tissues, excluding ovarian carcinoma, is often associated with loss of E-cadherin expression and EMT. Based on cytological investigations, primary ovarian tumors lacked mesenchymal cells and were composed of differentiated epithelial cells. Thus, it has been suggested that OSE cell transformation is unique, needing cells to undergo mesenchymal-epithelial transition (MET) to induce ovarian cancer (Yihong Zhu et al., 2010). Nevertheless, Snail up-regulation and E-cadherin suppression have been found in high-grade ovarian cancers, and the knockdown of SNAIL increased E-cadherin expression (Wang et al., 2015), perhaps suggesting a role in cancer progression, rather than initiation.

1.8 Stem cells in the reproductive tract

Identifying the type of cells that are responsible for initiating tumor growth and metastasis has been the main objective for many studies, and more recent evidence suggests that stem cells may become cancer-initiating cells (Kai et al., 2010; Navarro-Alvarez et al., 2010; Welte et al, 2010). Quiescent stem cells have been recognized in numerous epithelial tissues, including mammary, ovarian, prostate, and colon cells (Tosoni et al., 2012; Flesken-Nikitin et al., 2013; Guo et al., 2012; Barker et al., 2007). Somatic stem cells in these tissues are activated when tissue repair is needed to promote homeostasis of the tissue. Active stem cells have a unique ability to self-renew and differentiate to maintain tissue homeostasis. Stem cell proliferation and differentiation can be stimulated by several factors and cytokines. In the reproductive system, TGFβ has been shown to enhance sphere formation in suspension culture (an assay evaluating self-renewal capacity) of adult stem cells isolated from ovary (Gamwell et al., 2012; Ng et al. 2014; Flesken-Nikitin et al. 2013).

Stem cell conversion into cancer stem cells might be a consequence of the EMT process. Stem cell markers and morphology have been identified in both normal and cancer cells undergoing EMT (Yang and Weinberg, 2008). In human mammary carcinomas, cells express EMT markers and stem cell markers at the same time (Mallini et al., 2014). Cancer stem cells expressing ALDH1 have been identified in a cervical cancer cell line and these cells simultaneously exhibited EMT properties (Lin et al., 2015).

Some studies have shown that stem-like cells acquire self–renewing properties and

lose their control of proliferation in neoplastic tissues (Barbieri et al., 2012; O'Brien et al., 2010). Tumor–initiating cells that are CD44+/CD24- were isolated from human epithelial mammary cells and characterized as stem cells (Al-Hajj et al., 2003). Cancer stem cells have been isolated from most solid tumors (Bomken et al., 2010) and are defined primarily by their cancer-initiating potential.

In the ovary, there is mounting evidence for resident progenitor cells in the OSE layer that display stem cell characteristics. Progenitor cells expressing LY6a (SCA-1) have been identified in mouse OSE cells (Gamwell et al., 2012). Cells expressing the surface protein LGR5, a stem cell marker in the small intestine and colon (Barker et al., 2007), have been identified in the layer of OSE cells and the ovarian hilum (the connection between the ovary and the ovarian medulla) (Ng et al., 2014).

Cancer stem cells have been identified and isolated from ovarian cancers arising from epithelial cells (Pan and Huang, 2008), although there is limited evidence as yet that they share markers with OSE progenitor cells. In ovarian cancers, cancer stem cells have been identified with high expression of CD133, CD24 (Burgos-Ojeda et al., 2015; Gao et al., 2010) and c-Kit (Huang et al., 2014; Garson et al., 2015). It has been reported that 51% of patients with epithelilial ovarian carcinoma highly expressed CD44 compared to normal ovary which has few cells that are CD44 postive (Sillanpaa et al., 2003)

Cancer stem cells with high expression of aldehyde dehydrogenase 1 (ALDH1) have been isolated from serous and clear cell ovarian carcinomas. ALDH1+ cells were sphere forming, invasive and tumorigenic (Kuroda et al., 2013). The observation of ALDH1+ cells in both normal mouse and human OSE (Auersperg et al., 2013), as well as the evidence that label retaining OSE cells expressing LGR5, ALDH1 and CD133 may have

transformation potential in mice (Flesken-Nikitin et al,. 2013), provide increasing evidence for normal stem/progenitor cells as potential cells of origin for cancer-initiating cells.

Few studies have reported stem cell populations in fallopian tubes. A label-retaining assay using BrdU has identified slow dividing cells in the distal end of the mouse oviduct (Snegovskikh et al., 2014). When the slow dividing cells were labeled with GFP and sorted by Fluorescence-activated cell sorting (FACS), they were able to self-renew and form spheres and differentiate into glandular structures expressing Mullerian surface proteins (Wang et al., 2012).

Recent studies attempting to identify and isolate stem cells from fallopian tubes have reported putative stem cells located on the basement membrane of the human fallopian tube epithelium. These cells are undifferentiated, possess self-renewal capacity, are CD44 positive, and do not express markers of either secretory or ciliated cells (Paik et al., 2012). Analysis of STIC revealed another stem cell marker, ALDH1, located in cells on the basement membrane and overexpressed in all STIC cells, suggesting that STICs may originate from basal cells that possess stem cell-like activity (Ning et al., 2014).

Finally, since P53 and BRCA1 control cell proliferation by inducing DNA repair or apoptosis to eliminate cells with damaged DNA, their contributions in controlling the proliferation disorder of stem cells is possible. *Trp53* deletion in the mammary gland increased stem cell number and self-renewal potential (Cicalese et al., 2009; Tao et al., 2011) in both basal and luminal mammary epithelial cells (Chiche et al., 2013). *Trp53* deletion in the mammary gland from a transgenic mouse model resulted in an increase of symmetric divisions, which led to expansion of the stem cell population that favored the

tumor formation (Cicalese et al., 2009). In addition, *Trp53* inactivation increased hematopoietic stem cells expressing SCA-1 and c-Kit and bone marrow transplantation with defective P53 resulted in recipient mortality (TeKippe et al., 2003). Likewise, *BRCA1* mutation has been reported to be associated with enriched mammary stem cell populations expressing ALDH1 (Liu et al., 2008).

1.8.1 CD44 structure and functions

CD44 is a surface protein on some types of epithelial cells and stem cells. The normal function of CD44 is important for cell repair, inflammatory response and regulation of cell migration. The N-terminus of CD44 binds hyaluronic acid (HA) and results in increased cell proliferation and migration. Existence of CD44-HA complexes has been associated with multidrug resistance in breast and ovarian cancer (Negi et al., 2012).

CD44 glycoproteins are 85-230 KD, encoded by a single gene that includes 20 exons located on chromosome 11 in human and on chromosome 2 in mice. The CD44 protein is composed of five main domains: an extracellular domain encoded by exons 1-5, a variable domain encoded by alternatively splicing exons 6-15, a membrane proximal region encoded by exons 16 and 17, a transmembrane domain encoded by exon 18, and a cytoplasmic domain encoded by exons 19 and 20 (Figure 5) (Naor et al., 1997). The 10 variable region exons generate multiple variant isoforms (designated CD44v) such as the CD44v8-10 isoform (130 KD) which is mainly expressed on epithelial cells, and CD44v3-10 (230 KD) which is expressed in keratinocytes. The standard form of CD44 (CD44s) is 85-95 KD and includes the extracellular domain, membrane proximal region,

transmembrane domain and cytoplasmic tail and is expressed mostly on cells of lymphohematopoietic origin (Zoller et al., 2011).

Tumor-initiating cells that are CD44+ have been isolated from human mammary carcinoma (Barbieri et al., 2012) and colon cancer (Du et al., 2008), and have been characterized as cancer stem cells. CD44 positive cells have also been identified in different types of ovarian carcinoma (Sillanpaa et al., 2003). In serous ovarian cancer, effusion mesothelial cells in the ascites and abdominal fluid from benign tumors presented abundant CD44s expression (96%), whereas neoplastic cells in effusions from malignant tumors presented high levels of CD44V3-10 (86%) (Afify et al., 2007). Pan CD44 analysis in different types of ovarian cancers revealed higher levels in metastatic and recurrent ovarian samples compared to primary ovarian tumors. Moreover, the ovarian cancer cell lines SKOV3 and OV90 display high levels of expression of CD44 and low expression of CD24 and these cells exhibit increased cancer invasion, migration, and colony formation compared to other cell phenotypes (Meng et al., 2012). *CD44* knockdown in the ovarian cancer cell line OVCAR8 decreased sphere formation capacity, migration and invasion activity (Gao et al., 2015).

As there is only a single study of CD44+ cells in human fallopian tube (Paik et al., 2012), it will be useful to understand CD44 expression and function in the fallopian tube and to begin to determine its possible association with ovarian cancer.

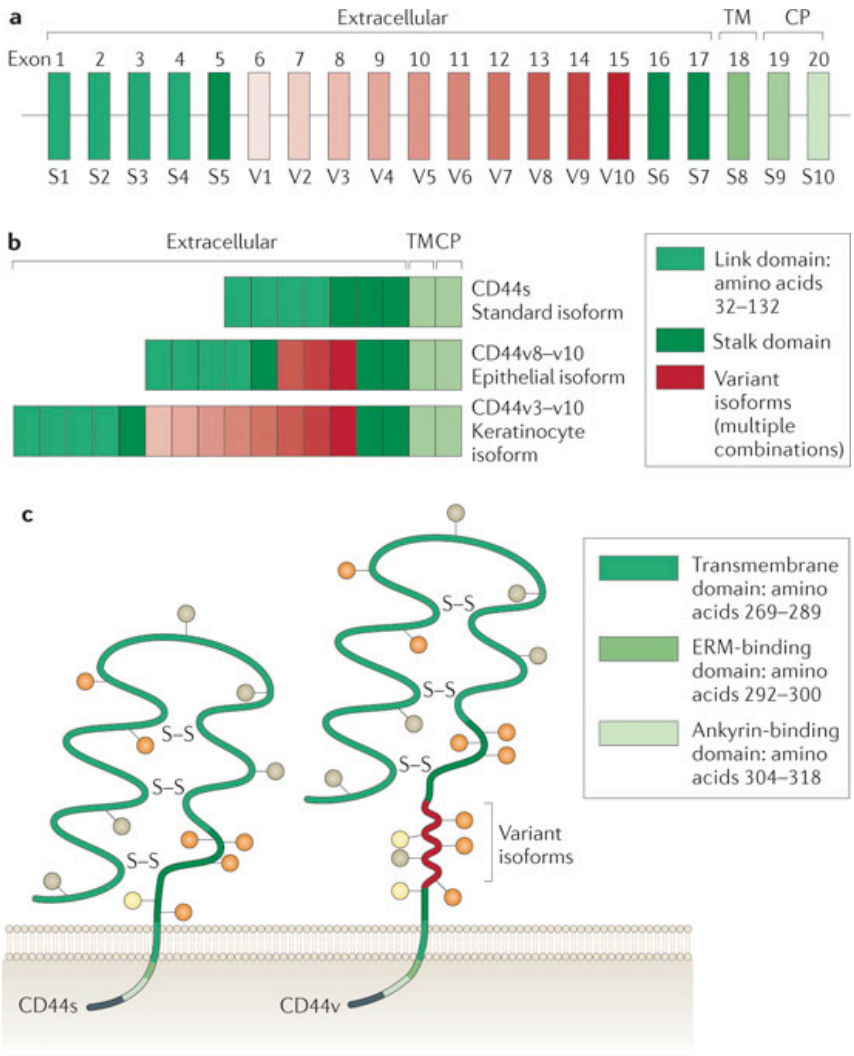

Figure 1-6: CD44 gene and structure.
a) The CD44 gene consists of 20 exons. The green exons are constant and the red exons are variants. b) Example of alternative splicing. c) The CD44 protein showing different domains (Taken from Zoller et al., 2011, with permission).

1.8.2 Stem cell antigen-1 (SCA-1)

Stem cell antigen Sca-1 or LY6A/E is a surface protein first identified in mouse hematopoietic cells (van de Rijn et al., 1989). In our laboratory, SCA-1+ cells isolated from mouse ovarian surface epithelial cells were able to form spheres and the expression of SCA-1 was highly up-regulated in response to the follicular growth factors TGFβ and LIF (Gamwell et al., 2012). However, SCA-1 expression has never been investigated in mouse oviducts.

SCA-1 protein plays an essential role in hematopoietic stem cell differentiation (Matsuura et al., 2004) and tissue remodeling (Wang et al., 2006). SCA-1 has been identified in normal mouse tissues such as skeletal muscle (Asakura et al., 2002), myocardial cells (Wang et al., 2006), and mammary cells (Welm et al., 2002), and has been used to isolate stem cells from lung cancer (Bertoncello et al., 2011). Burger and coworkers have reported that SCA-1+ cells isolated from proximal prostatic duct are more highly proliferative when they have been injected under the mouse renal capsule compared with SCA-1- cells (Burger et al., 2005). Furthermore, TGFβ regulates the growth of the stem cell population isolated from the proximal region of the prostate duct by inhibiting proliferation and stimulating differentiation (Salm et al., 2012).

1.9 Angiogenesis and PAX2

Angiogenesis is required to expand the blood supply needed for tumor growth. Anti-angiogenesis molecules have been used widely to inhibit neovascularization, but the

results have been unsatisfactory in invasive and aggressive cancers (Helfrich et al., 2010; Piao et al., 2013). The growth of tumors even in the presence of anti-angiogenesis molecules indicates that tumor cells may have other ways to be supplied with blood. Anti-angiogenesis therapies, such as anti-VEGF antibodies, target only endothelial cell proliferation, whereas cancerous cells may proliferate and form *de novo* vascular channels connected to the endothelial-lined vasculature.

In 1999, Maniotis et al. observed aggressive melanoma cells forming a blood vessel-like pattern in 3D culture, and when the cells were injected into mice they formed tumors that contained vessel-like structures. This formation of vessel-like structures is known as vasculogenic mimicry (VM). Interestingly, red blood cells have been detected inside the vessels while the cells lining these vessels are negative for the endothelial markers CD31 and CD34. The tumor cells are organized in a pattern that is supported by remodeling extracellular matrix, as determined by periodic acid-schiff (PAS) staining to label the carbohydrates in the remodeling extracellular matrix.

In more recent studies, CD31-/PAS+ vessels formed by tumor cells have been used in several studies to demonstrate VM *in vitro* and *in vivo* (Itzhaki et al., 2013; Dong et al., 2014; Luo et al., 2014) and some attempts have been made to determine the molecular mechanism of VM formation (Qiao et al., 2015). In aggressive breast cancer cells, cyclooxygenase-2 (COX2) can induce VM formation in three-dimensional culture, and knockdown of COX2 decreased VM formation (Basu et al., 2006). The ovarian cancer cell line SKOV3 has been reported to form VM *in vitro* and targeting CD147 in these cells caused a significant down-regulation in VM formation (Millimaggi et al., 2009). CD147 protein has been reported to be an inducer of extracellular matrix

metalloproteinase (MMP). However, MMP overexpression has been linked previously with VM incidence in an ovarian cancer cell line by contributing to extracellular matrix remodeling (Sood et al., 2001).

Ovarian carcinomas are associated with several up-regulated and down-regulated genes. PAX2 has been reported to be up-regulated in some types of ovarian cancer including HGSC (Song et al., 2013). The role of PAX2 in inducing tumor progression in ovarian cancer is not well studied; however, PAX2 plays a very important role during embryogenesis and urogenital tract development (Eccles et al., 2002). While the specific role of PAX2 in the development of the reproductive tract has not been defined, it has been suggested that PAX2 may induce cell elongation during the formation of the oviduct. In the kidney, PAX2 plays an important role in the development of the collecting duct, and has been reported to induce branching morphogenesis (Narlis et al., 2007; Mansouri et al., 1996). PAX2 mutant mice have decreased ability to form branched collecting ducts compared with PAX2 wild type mice (Mansouri et al., 1996). How this might relate to the role of PAX2 in the development of ovarian cancer is unknown, but it is intriguing to speculate that the ability of PAX2 to induce branching during embryogenesis may be re-visited in the adult with potential involvement in the induction of branching associated with VM in cancer cells.

Ovarian cancer cell lines have been reported to form VM in matrigel and in xenografted mice (Sood et al., 2001). The vascular channels formed by these cell lines (SKOV3 and OVCAR3) in matrigel were matrix-enriched and generally endothelial marker independent, but positive for pan-cytokeratin. Interestingly, blood cells were detected inside the vascular channels formed *in vivo*. Some ovarian cancer cell lines

expressed endothelial markers *de novo*, suggesting that cancer cells may differentiate into endothelial cells to induce angiogenesis. The SKOV3 cell line had the ability to form VM in 3D culture and weakly expressed the endothelial marker CD31 on the cell surface both in monolayer culture and in the VM formed by the cells in tumors (Su et al., 2008).

Rationale and Hypothesis

The debate about the origin of ovarian cancer has yielded increasing evidence suggesting that fallopian tube lesions can initiate ovarian cancer. The morphological and gene expression changes associated with the early formation of tubal lesions are now being revealed. STICs arising in fallopian tube cell outgrowths frequently have loss of PAX2 expression and show expansion of CD44 positive cells, but the cause and consequences of these changes are as yet unknown. The overall aim of this study was to define the role of PAX2 in OVE cells and its response to TGFβ, a factor present in follicular fluid, characterizing specifically its potential involvement in the regulation of stem cell-like behaviors that may contribute to the formation of cancer-initiating cells in the fallopian tubes. Since PAX2 is important for epithelial cell differentiation in the reproductive tract, we hypothesized that exposure of OVE cells to TGFβ at concentrations found in ovulatory follicular fluid would induce the cells to undergo EMT, suppress *Pax2* expression, and increase the fraction of cells with CD44 expression. In addition to loss of PAX2, we hypothesized that mutations in two key tumor suppressor genes, *Brca1* and *Trp53* would enhance cell proliferation, capacity for colony formation and stem cell characteristics that could increase OVE cell susceptibility to tumor formation.

Specific aims

Aim 1: To characterize the stem cell subpopulation in OVE cells

Aim 2: To determine the effects of TGFβ on OVE cell proliferation, viability,

migration and sphere formation

Aim 3: To establish the role of PAX2 in modulating stem cell characteristics in OVE cells

Aim 4: To investigate the role of PAX2 in oviductal epithelial cell differentiation and ovarian cancer promotion

Aim 5: To determine the effects of loss of *Brca1* and/or *Trp53* on OVE stem cell characteristics and susceptibility to transformation.

Chapter 2: Materials and Methods

2.1 Experimental animals

Twenty-five day old female FVB/N mice (Jackson Laboratory, Bar Harbor, ME) were housed with free access to food and water. All experiments with mice were performed in accordance with the Canadian Council on Animal Care's *Guidelines for the Care and Use of Animals* under a protocol approved by the University of Ottawa's Animal Care Committee. *Brca1*$^{fl/fl}$ [FVB;129-Brca1^{tm2Brn}], *Trp53*$^{fl/fl}$ [FVB;129-Trp53^{tm1Brn}] and *Trp53*$^{fl/fl}$/*Brca1*$^{fl/fl}$ mice were obtained from the Mouse Models of Human Cancers Consortium Mouse Repository (National Cancer Institute, Rockville, MD, USA). Oviductal cells were isolated from euthanized FVB/N mice, *Trp53*$^{fl/fl}$ (designated P53-flox), *Brca1*$^{fl/fl}$ (designated BRCA1-flox) and *Trp53*$^{fl/fl}$/*Brca1*$^{fl/fl}$ (designated P53/BRCA1-flox). In addition, severe combined immunodeficient (SCID) mice obtained from The Jackson Laboratory were used for determining the tumorigenicity of experimental cells as described (Al-Hujaily et al., 2015). Animals that developed tumors were euthanized when they reached a humane endpoint. The tumors were collected, fixed in 10% buffered formalin and paraffin embedded for histological analysis.

2.2 Superovulation of mice

Female mice at 25 days of age were superovulated by injection of 5 IU of pregnant mare's serum gonadotropin (PMSG; Invervet) and 48 hours later, injected with 5 IU of human chorionic gonadotropin (hCG; Sigma). This hormone regimen induces ovulation at about 12 hours after hCG injection. The female mice were sacrificed before ovulation

or one hour and two hours after ovulation and oviducts with the ovaries were collected.

2.3 Cell lines and cell culture

Four clonal OVE cell lines (OVE4, OVE14A, OVE16 and OVE22) were established for this study. Oviducts from 25-day old female FVB/N mice were isolated, washed with phosphate-buffered saline (PBS), cut into fragments and minced on tissue culture plates. Tissue fragments were incubated in 0.25% trypsin (Invitrogen, Carlsbad, CA) at 37Cº and 5% CO_2 for 30 minutes to dissociate the OVE cells. Small tissue fragments with dissociated cells were cultured in OVE medium which consisted of minimal essential media (MEM; GE Healthcare, Little Chalfont, UK) supplemented with 4% fetal bovine serum (PAA Laboratories), 0.01 nM estradiol (Sigma-Aldrich, St. Louis, MO), 5 U/ml of penicillin and streptomycin solution (Penstrep; Sigma-Aldrich), 0.1 µg/ml of gentamicin (Invitrogen), 0.02 µg/ml of epidermal growth factor (EGF; R&D Systems, Minneapolis, MN) and 1 µg/ml of insulin-transferrin-sodium-selenite supplement (ITSS; Roche, Basel, Swizerland) for two weeks or until the cells attached and spread out. The small fragments were washed off and only attached cells were collected by trypsinization, diluted and plated as single cells. Subsequent colonies were isolated and grown to establish independent lines. The epithelial nature of the resulting cells was verified by analyzing E-cadherin and CK19 expression by qPCR. A similar process was used to generate primary cultures of OVE cells isolated from *Trp53*$^{fl/fl}$, *BRCA1*$^{fl/fl}$ and *Trp53*$^{fl/fl}$/*BRCA1*$^{fl/fl}$ mice. Where indicated, OVE cells were treated with 10 ng/ml human TGFβ1 (R&D Systems) for up to 20 days.

M1102 cells are primary cultures of mouse OSE cells and were maintained in MOSE media as described previously (Al-Hujaily et al., 2015). In this study, a murine ovarian cancer cell line was used (RM cells) which was derived from immortalized mouse OSE cells transduced with retrovirus constructs expressing *K-Ras* ($KRAS^{G12D}$) and *Myc* (Al-Hujaily et al., 2015). Human embryonic kidney 293T cells (ATCC, Manassas, VA) were used to prepare the lentiviral vectors and the cells were maintained in Dulbecco's modified Eagle medium (Life Technologies Inc., Burlington, ON) supplemented with 10% fetal bovine serum (PAA Laboratories, Pasching, Austria).

2.4 Modulation of gene expression

2.4.1 Lentiviral vectors

The murine *Pax2* cDNA, corresponding to the pax2-b variant, was cloned from murine oviducts and inserted into pWPI (Addgene plasmid #12254) to generate the lentivirus expression vector (WPI-Pax2-IRES-eGFP) as described previously (Al-Hujaily et al., 2015). For shRNA-mediated knockdown, lentiviral vectors Tet-pLKO-neo and Tet-pLKO-puro were used to generate the PAX2 specific knockdown vectors pLKO-17 and pLKO19 using the *Pax2* target sequences CCCAAAGTGGTGGACAAGATT and CAGGCATCAGAGCACATCAAA, respectively. Tet-pLKO-neo (Addgene plasmid 21916) and Tet-pLKO-puro (Addgene plasmid 21915) were gifts from Dmitri Wiederschain (Wiederschain et al., 2009). Lentiviral vectors were prepared by co-transfection of vector plasmids (described above), with packaging plasmid pCMVR8.74 (Addgene plasmid #22036) and the ecotropic envelope expression plasmid, pCAG-Eco (Addgene plasmid 35617) into 293T cells as described previously (Kutner et al., 2009).

Plasmids pWPI and pCMVR8.74 were gifts from Didier Trono and plasmid pCAG-Eco was a gift from Arthur Nienhuis and Patrick Salmon.

2.4.2 PAX2 overexpression and knockdown

M1102 cells were infected with either the control lentiviral vector, WPI, or WPI-Pax2-IRES-eGFP to generate cell lines M1102-WPI and M1102-PAX2, respectively, as described in Al-Hujaily et al. (2015). As an additional control, the *Pax2* expression cassette was deleted from M1102-PAX2 cells following Cre-mediated recombination between *loxP* sites resident in both the 5' and 3' LTRs of the integrated WPI-Pax2-IRES-eGFP provirus. Cre recombinase was delivered by the transient infection of M1102-*Pax2* cells with adenovirus expressing Cre recombinase (AdCre; Vector Development Laboratory, Houston, Texas) (Al-Hujaily et al., 2015). For PAX2 knockdown, OVE4 and OVE16 cells were infected with lentiviral vectors (pLKO17, pLKO19) expressing doxycycline-inducible shRNAs targeting murine *Pax2*. Cells infected with a control lentivirus (Tet-pLKO-puro) were used as a negative control. G418 and puromycin were used to select cells with stable incorporation of the *Pax2* or control knockdown vectors.

2.4.3 Adenovirus infection to inactivate tumor suppressors

OVE cells isolated from $Trp53^{fl/fl}$, $Brca1^{fl/fl}$ and $Trp53^{fl/fl}/Brca1^{fl/fl}$ were infected in serum-free medium with 2000 pfu/cell AdCre or adenovirus expressing GFP (AdGFP). The infected cells were incubated at 37°C in serum-free medium and after one hour, serum was added to 10%. Six hours later, the medium containing the adenovirus was removed and the cells were washed three times with PBS and fresh OVE medium was

added. The infected cells were washed with PBS every 12 hours for three days and fresh media was added in each wash.

2.4.4 Detection of recombination using PCR

OVE cells infected with AdCre and AdGFP were incubated until they recovered after 2-3 cell passages, and were then dissociated with trypsin and genomic DNA was extracted using the Extract-N-Amp Tissue PCR kit (Sigma) following the manufacturer's protocol. Recombination of the *Trp53* floxed region was detected by amplification of a 612 bp band using primers for *Trp53* intron 1 forward; (5' CAC-AAA-AAA-CAG-GTT-AAA-CCC-AG 3') and *Trp53* intron 10 reverse; (5' GAA GAC AGA AAA GGG GAG GG 3'). Unrecombined alleles were detected by amplification of a 370 bp band using the primers for *Trp53* intron 1 forward; (5' CAC-AAA-AAA-CAG-GTT-AAA-CCC-AG 3') and *Trp53* intron1 reverse; (5' AGC ACA TAG GAG GCA GAG AC 3'). The deletion of floxed exons 5-13 of *Brca1* was detected by amplification of a 600 bp band using primers for *Brca1* intron 4 forward (5' TAT CAC CAC TGA ATC TCT ACC G 3') and *Brca1* intron 13 reverse (5' TCC ATA GCA TCT CCT TCT AAA C 3'). The unrecombined allele was detected by amplification of a 592 bp band using primers for *Brca1* intron 4 forward (5' TAT CAC CAC TGA ATC TCT ACC G 3') and *Brca1* intron 4 reverse (5' GAC CTC AAA CTC TGA GAT CCA C 3'). The PCR amplification was done in 10 µl volumes consisting of 1 µg of genomic DNA, 1X REDExtract-N-Amp^{TM} (Sigma) and 1 nmole of forward and reverse primers. PCR conditions were initial denature at 94ºC for 3 minutes, then 30 cycles of 94ºC for 30 sec, 56ºC for 30 sec, and 72ºC for 60 sec, followed by 72ºC for 10 minutes. The PCR products were separated on a 1% agarose gel with Tris-

acetate-EDTA buffer.

2.5 Proliferation assay

The proliferation assay was done to measure the effect of TGFβ treatment on OVE cells by plating $1x10^4$ OVE cells in 10 cm dishes in OVE medium. TGFβ (10 ng/ml) was added at the time of cell plating and the medium with TGFβ was replaced every three days. TGFβ-treated and control (untreated) cells were trypsinized after 7 days of TGFβ treatment and cells were counted using a Vi-CELL XR Cell Viability Analyzer (Beckman Coulter, Inc). To measure the effect of inactivation of *Trp53* and/or *Brca1*, the recombined and unrecombined cells were plated at a density of $5x10^3$ cell/ml in 24-well plates. Triplicate samples of each group of cells were trypsinized every day and counted using a Vi-CELL XR Cell Viability Analyzer.

2.6 Migration assay

Capacity for cell migration was assessed using the scratch-wound healing assay to measure the effect of TGFβ treatment and the effect of *Trp53* and/or *BRCA1* mutations. Pipet tips were used to create a 'wound' in a confluent cell culture. Any detached cells were washed off with PBS and fresh OVE medium was added. To assess the effect of TGFβ treatment, OVE cells were pre-treated with and without 10 ng/ml TGFβ for three days before the migration assay and after creating the scratch. The cells were incubated at 37Cº and images were taken at 0 and 24 hours for TGFβ treatment, and at 0 and 6 or 18 hours for *Trp53* and/or *BRCA1* mutations. Migratory cells moved towards the wound and the gap closure analysis was done using ImageJ software (NIH Image).

2.7 Sphere formation assay

OVE and OSE (M1102) cells were trypsinized and single cells were passed through a 40-µm cell strainer. Single cells (5,000) were cultured in suspension in low attachment plates for two weeks in stem cell medium, consisting of DMEM/F12 media (Sigma-Aldrich) containing 0.3% FBS, B27 supplement 50X (0.02 mg/ml; Life Technologies, USA), 0.2 µg/ml of EGF, 0.4 µg/ml of mouse fibroblast growth factor (FGF; R&D Systems), 4 µg/ml of heparin, 10 U/ml Penstrep and 0.2 µg/ml of gentamicin. The ability of OVE and OSE cells to form spheres was assessed by measuring sphere diameters and counting the spheres with diameters more than 60 µm. The percentage of cells that formed spheres was determined and the average diameter of the spheres was measured using ImageJ software (NIH Image).

2.8 Colony formation assay in soft agar

Recombined and unrecombined OVE cells and the breast cancer cell line MCF7 (positive control) were dissociated from adherent culture and single cells were collected after passing the cells through a 40-µm cell strainer (Becton-Dickinson). The 24-well culture plates were prepared with 500 µl of a base layer of agar consisting of 2% ultra-pure low melting point agarose (Life Technologies) and 2X DMEM medium in a ratio of 1:1. The agar layer was solidified at 4°C for 15 minutes and warmed to 37°C for 15 minutes before adding the top layer of 500 µl of an equal volume-mixture of 1% agarose and 2X DMEM medium containing the single cell suspension ($1X10^5$ cell/ml). The cells were then incubated at 37°C for 4-6 weeks and colonies were visualized using the EVOS XL imaging system and counted (Life Technologies Inc., Burlington, ON).

2.9 Label retaining assay

Single cell suspensions of OVE cells were prepared as described above. Cells (10^7) were washed with PBS, collected by centrifugation for 5 minutes at room temperature and resuspended in 5 ml PBS. PKH26 Red Fluorescent (Sigma) was prepared by diluting the stock (1 mM) in PBS (1:5,000) and 5 ml of this working PKH26 solution was added to the 5 mL cell suspension. After 5 minutes of incubation at room temperature, the reaction was terminated by adding OVE medium and pelleting the cells. Fresh stem cell medium was added and the cells were plated in low attachment plates in suspension and incubated for two weeks to allow formation of spheres. The spheres were collected and mechanically dissociated by pipetting repeatedly (around 200 times) with a 1 ml pipette. The medium was replaced with fresh stem cell medium and the cells were replated in suspension and incubated for a further two weeks (Tosoni et al., 2012). The PKH26-labeled spheres were visualized by fluorescent microscopy (Axioskop 2 MOT plus, Zeiss) using the Axiovision software, or single cell suspensions derived from the spheres were analyzed by flow cytometry (Beckman Coulter, Coulter Epics XL).

2.10 Gene expression analysis

Gene expression in OVE cells was analyzed by quantitative polymerase chain reaction (qPCR). RNA was extracted using RNeasy Mini Kits (Qiagen, Valencia, CA) following the manufacturer's instructions and cDNA was made using a Reverse Transcription kit (Qiagen). Gene amplification was determined by qPCR using either Fast SYBR Green Master Mix (Invitrogen) for primers or *iTaq* universal probes supermix (Bio-Rad, Hercules, CA) for probes. The real-time thermal cycler program was 95 Cº for

10 minutes, followed by 40 cycles of 95 Cº for 10 sec and 60 Cº for 30 sec. Primer pairs and probes are listed in Table 1. The gene expression levels were analyzed relative to the endogenous control *Ppia* (Invitrogen) for primers and *TBP* (Integrated DNA Technologies, Coralville, IA) for the probes.

2.11 3D culture in matrigel

Chamber slides (8 wells; Thermo Fisher) were covered with 60 µl of cold growth factor-reduced matrigel (Trevigen, Gaithersburg, MD) and incubated at 37Cº for 30 minutes to polymerize the matrigel. OVE or M1102 cells were mixed with assay media (MEGM™ Mammary Epithelial Cell Growth Medium supplemented with 1 ng/ml EGF and 0.5 ng/ml of insulin, hydrocortisone, cholera toxin and gentamicin (all from Ionza, Basel, Switzerland) and 5% fetal bovine serum. Cells were plated on top of the matrigel as described previously (Debnath et al., 2003), covered with assay media containing 4% matrigel, and incubated at 37^{o}C for 14 days. RM cells were similarly plated, however serum-free DMEM medium was used in place of the MEGM medium described above and chamber slides were incubated at 37^{o}C for only 48 hours. OVE luminal structures formed in the matrigel were imaged and counted after 14 days. M1102 and RM tubular structures were imaged two days after plating the cells and the branches of the tubular structures were counted.

Table 1: List of primers and probes used for qPCR analysis

Gene	Sequence	Source
Cdh1	Forward [F], 5'-ATCCTCGCCCTGCTGATT-3'; reverse [R], 5'-ACCACCGTTCTCCTCCGTA-3'	Invitrogen
Vim	Forward [F], 5'-CGCCAGGCCAAGCAGGAGTC-3'; reverse [R], 5'- CGCTCCAGGGACTCGTTAGTGC-3'	Invitrogen
Snai1	Forward [F], 5'- GTCTGCACGACCTGTGGAA-3'; reverse [R], 5'- CAGGAGAATGGCTTCTCACC-3'	Invitrogen
Pax2	Forward [F], 5'-GGCATCTGCGATAATGACACA-3'; reverse [R], 5'-GTGGAAAGGCTGCTGAACTT-3'	Invitrogen
Pax8	Forward [F], 5'-GCAGCTATGCCTCTGCTA-3'; reverse [R], 5'-GCTGTAGGCATTGCCAGAAT-3'	Invitrogen
Ppia	Forward [F], 5'- AGGGTGGTGACTTTACACGC-3'; reverse [R], 5'- GATGCCAGGACCTGTATGCT-3'	Invitrogen
Sca-1	5'-/56-FAM/ATCTTTGCT/ZEN/TACCCATCTGCCCTCC/3IABkFQ/-3'	IDT
CD44	5'-/56-FAM/TCTTCTGCC/ZEN/CACACCTTCTCCTACT/3IABkFQ/-3'	IDT
Aldh1	5'-/56-FAM/AGTTAACCC/ZEN/ACACCACCCCAGC/3IABkFQ/-3'	IDT
Lgr5	5'-/56-FAM/AGCTACCCG/ZEN/CCAGTCTCCTACAT/3IABkFQ/-3'	IDT
CD133	5'-/ /56-FAM/CCG ATG CCA /ZEN/TCC AGG TCT GAG AA/3IABkFQ/-3'	IDT
OcT3/4	ID # Mm03053917_g1	IDT
Pax2	5'-/56-FAM/TCCCCTGTT/ZEN/CTGATTTGATGTGCTCTG/3IABkFQ//-3'	IDT
Trp53	5'-/56-FAM/CCCCTGTCA/ZEN/TCTTTTGTCCCTTCTCA/3IABkFQ//-3'	IDT
Foxj1	5'-/56-FAM/AGAATTCCA/ZEN/TCCGCCACAACCTGT//3IABkFQ//-3'	IDT
Brca1	5'-/56-FAM/TATACTTCA/ZEN/TGGTCGCCCGCTGC/5'-/56-FAM/	IDT
Ovgp1	NM_007696.2	IDT
TBP	5'-/56-FAM/ACTTGACCT/ZEN/AAAGACCATTGCACTTCGT/3IABkFQ/-3'	IDT

2.12 Protein analyses

2.12.1 Western blot analysis

Cellular proteins were recovered from cell cultures using the M-PER mammalian protein extraction reagent (Thermo Fisher, Waltham, MA). Cell proteins were separated by SDS-PAGE and transferred to nitrocellulose, then probed with the following antibodies: anti-mouse PAX2 (1:20,000, Santa Cruz Biotechnology, Dallas, Texas) and anti-rabbit CD44 (1:500), anti-rabbit E-cadherin (1:10,000), anti-rabbit vimentin (1:10,000), anti-rabbit Snail (1:10,000), anti-rabbit cytokeratin 19, anti-rabbit OVGP (1:1,000) (all from Abcam, Cambridge, UK), and anti-rabbit BRCA1 (1:200, Santa Cruz). For loading controls, mouse anti-GAPDH or mouse anti-β-actin (1:50,000) were used. β-actin expression could be used as a loading control because TGFβ treatment does not change the expression of cytoskeletal actin, although it induces actin reorganization (Boland et al., 1996). Anti-rabbit (1:10,000, Abcam) or anti-mouse (1:10,000, Sigma-Aldrich) horseradish peroxidase-conjugated antibodies were used as secondary antibodies. Immunoreactive proteins were detected using chemiluminescence (Clarity Western ECL Substrate; Bio Rad) and the blots were imaged using FluorChem FC2 (Alpha Innotech).

2.12.2 Immunofluorescence

Immunofluorescence was performed on cells grown on coverslips and in matrigel. The cells were fixed with 4% paraformaldehyde (Sigma-Aldrich) for 20 minutes and permeabilized with 0.5% Triton X-100 for 30 minutes for cells grown on coverslips or

0.2% Triton X-100 for 10 minutes for cells grown in matrigel. After blocking in 5% goat serum, cells were probed with each antibody as follows: anti-mouse PAX2 (1:500, Santa Cruz), anti-mouse PAX8 (1:200, Santa Cruz), anti-rabbit E-cadherin (1:200, Abcam) and anti-rat CD44 (1:200, Abcam). Alexa Fluor goat anti-mouse IgG (1:1000), goat anti-rabbit IgG (1:500) and goat anti-rat (1:500; all from Molecular Probes, Carlsbad, CA) were used as secondary antibodies. The cells on coverslips were then mounted on microscope slides and the cells in the matrigel slides were mounted with cover slips using Vectashield hard set mounting medium with DAPI (Vector Laboratories, Burlingame, CA). The immunofluorescence images were visualized and analyzed using an inverted fluorescence microscope (Axioskop 2 MOT plus, Zeiss) and Axiovision software.

2.12.3 Immunohistochemistry (IHC)

Tissues or tumors were excised from euthanized mice and fixed in formalin overnight, then transferred to 70% ethanol. The tissue was paraffin-embedded, cut in 4 μm sections, de-paraffinized and rehydrated in graded ethanol. For antigen retrieval, the tissues were heated in a microwave in antigen unmasking solution (Vector Laboratories). For regular IHC, tissue sections were blocked with DAKO protein block, serum-free (Dako, Burlington, ON) for 1 hour and then incubated overnight at 4Cº with anti-rat CD44 (1:400, Abcam), anti-rabbit CD31 antibody (1:100, Abcam) or 1 hour at room temperature for anti-rabbit PAX2 (1:1000). After washing in PBS, the sections were incubated with ImmPRESS anti-rat secondary antibody (Vector Laboratories) or with Dako Envision system-HRP labeled polymer anti-rabbit antibodies (Dako) for 30

minutes. The immunoreactivity was imaged using the Aperio ScanScope system and the data were analyzed using ImageScope software (Aperio).

For the fluorescent IHC, the tissue sections were blocked with 10% normal goat serum for 1 hour and incubated first with anti-rat CD44 (1:200, Abcam) for 20 hours, then with anti-rabbit PAX2 for 2 hours (1:1,000, Santa Cruz). After washing in PBS, the sections were incubated for 1 hour with double secondary antibodies: Alexa fluor goat anti-rat (1:500) and goat anti-rabbit (1:1,000). To reduce the background after washing in PBS, the tissue sections were incubated with 5 mM copper sulphate for 1 hour, then with 0.1 % Sudan Black diluted in 70% ethanol for 10 minutes. After washing in PBS, the tissue sections were mounted on coverslips using DAPI mounting media (Vector Laboratories) and analyzed by fluorescent microscopy (Axioskop 2 MOT plus, Zeiss) using the Axiovision software.

2.12.4 Flow Cytometry for CD44 and SCA-1 Expression

OVE cells were dissociated using non-enzymatic stripper (MULTICELL Cell Stripper) and the cells passed through a 40-µm cell strainer. Single cells ($2x10^7$) were incubated with antibodies to human/mouse CD44 conjugated to APC (1:5000; eBioscience, San Diego, CA) or antibody to mouse SCA-1-FITC (1:11, Miltenyi Biotec, Germany) for 15 minutes at 4Cº. Unbound antibody was removed with washing buffer and the fraction of cells with surface protein labeled with CD44 or SCA-1 antibodies was determined using a MoFlo cell sorter (Dako Cytomation).

2.12.5 Periodic Acid-Schiff (PAS) staining

The vascular channels formed by MOSE cells in matrigel in 8 well chamber slides (Section 2.11) were washed carefully with PBS. The cells were fixed with 2% paraformaldehyde for 15 minutes and then washed with PBS three times. PAS staining was done using the Periodic Acid-Schiff kit (Sigma) following the manufacturer's protocol. Periodic acid (250 μl/well) was added to the cells, incubated at room temperature for 5 minutes, and then washed with PBS 3-5 times for 5 minutes each wash. Schiff stain (250 μl/well) was then added, the cells were incubated at room temperature for 15 minutes and then washed 3 times for 5 minutes each wash. All washing steps were with 500 μl/well of PBS using a pipet to drip the solution carefully on top of the matrigel.

2.13 Statistical analyses

Statistical analyses were performed using GraphPad Prism software (GraphPad, La Jolla, CA). A Student t-test (two groups) or an ANOVA with a Tukey post-test (multiple groups) were used to determine statistical significance ($P < 0.05$). Error bars represent the standard error of the mean.

Chapter 3: Results (Part I)

TGFβ induces the epithelial-to-mesenchymal transition associated with stem cell characteristics in OVE cells.

3.1 OVE cell characterization

OVE cells were isolated from mouse oviducts and clonally grown into four independent cell lines. OVE clones have different morphologies and the expression of epithelial and OVE markers are varied and associated with their morphology. OVE4 clonal cells are mostly epithelial and express the epithelial markers E-cadherin and CK19, and the OVE markers PAX2, PAX8 and OVGP (Figure 3-1). OVE22 and OVE16 are two clones having mixed morphologies of epithelial and mesenchymal cells and expressing both epithelial and OVE markers. The OVE14A clone has epithelial morphology and expresses epithelial markers (E-cadherin and CK19), but they have little to no expression of PAX2, PAX8 and OVGP. Notably, PAX2 levels in the more mesenchymal clones (OVE22 and OVE16) are lower than in the most epithelial clone, OVE4 (Figure 3-1).

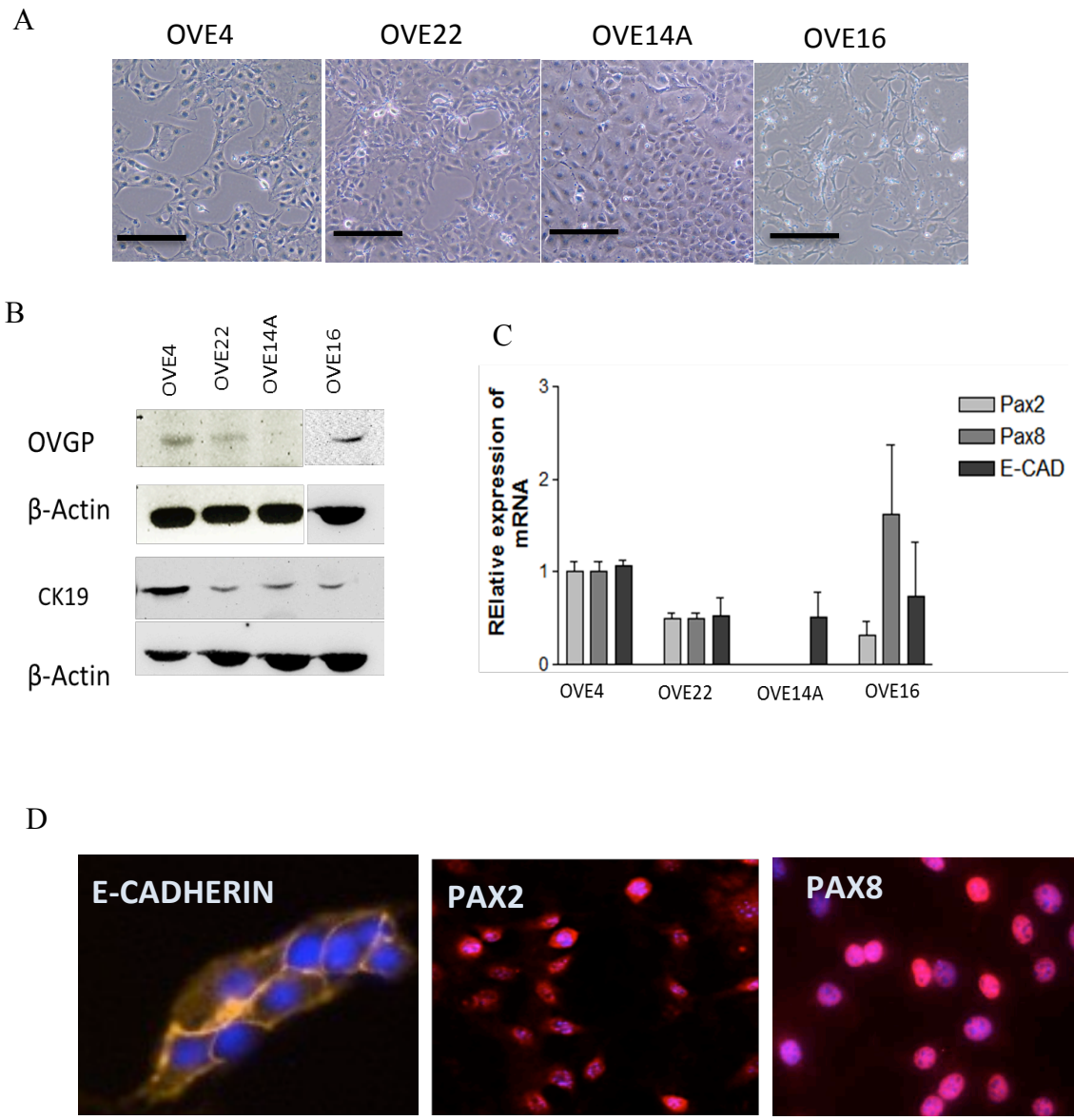

Figure 3-1: Oviductal epithelial cell line characterization.
(A) OVE clonal cell morphology. (B) Western blots show that all OVE cells express the epithelial marker (CK19) and all but OVE14 express the secretory cell marker (OVGP). (C) OVE4, OVE22 and OVE16 cells express all OVE markers (E-cadherin, PAX2 and PAX8), whereas OVE14A cells express only E-cadherin mRNA by qPCR. (D) Immunofluorescence on OVE4 cells shows the expression of E-cadherin, PAX2 and PAX8.

3.2 OVE cells possess stem cell characteristics

One of the fundamental goals of this project was to determine if OVE cells include a subpopulation cells that have stem-like cell characteristics, including self-renewal, label retention, ability to differentiate and express stem cell markers. A unique characteristic of stem cells is the ability to divide asymmetrically to generate one daughter cell and one stem cell that inherits all stem cell characteristics. Plating the cells in stem cell media in suspension allows stem cells to divide and self-renew for long periods. To determine if any of the OVE cell lines possess stem cell characteristics, sphere formation assays were performed in low attachment plates with stem cell media containing the self-renewal enhancer (B27) for two weeks. All four OVE cell lines contained cells that could form spheres, albeit at different proportions, indicating that OVE cells have a subpopulation that demonstrates stem cell characteristic (Figure 3-2).

Stem cells are quiescent cells that have a low mitotic rate. Less frequently dividing cells are able to keep a label in the DNA for long periods, whereas normally replicating cells gradually lose the label during each mitotic cell division. Therefore, label-retention is widely used to identify quiescent cells in tissues. It has been reported that the murine oviduct contains cells that retain 5-bromo-2-deoxyuridine (BrdU), and they are located at the basal layer under the tubal villi (Snegovskikh et al., 2014). To confirm that there is a label-retaining population within the isolated OVE cells, cells were stained with PKH26 dye, a red fluorescent cell linker stain that has been used effectively to label human umbilical stem cells (Shao-Fang et al., 2011) and to purify human and mammary epithelial cells *in vitro* (Tosoni et al., 2012). OVE cells were labeled successfully with

PKH26 dye and the labeled cells formed spheres in suspension with stem cell media (Figure 3-3). After 4 weeks of plating the cells with two passages, the number of OVE cells that retained PKH26 dye was decreased, but a few labeled cells (1.6%) retained the dye. The decreasing number of cells labeled with PKH26 confirm the dye disappearance in proliferating cells, and the few that retain the dye are likely slowly proliferating stem/progenitor cells (Figure 3-3).

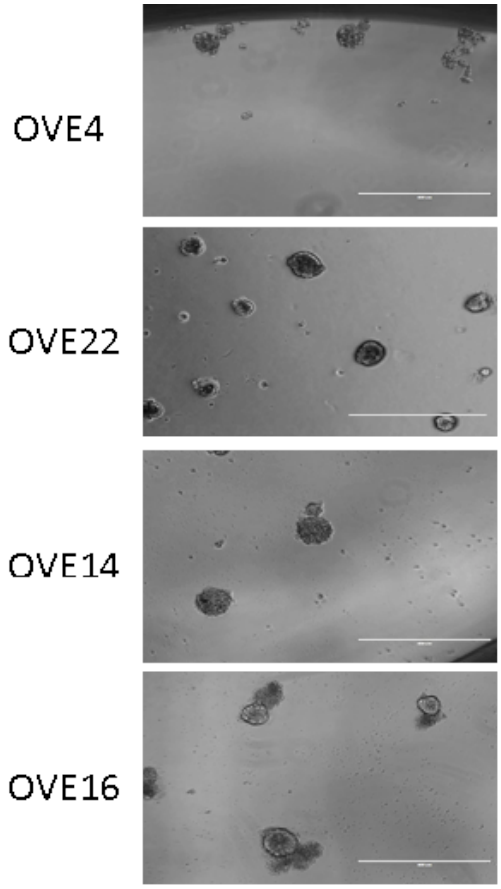

Figure 3-2: OVE cells have the ability to form spheres when grown in suspension. The scale bar represents 400 μm.

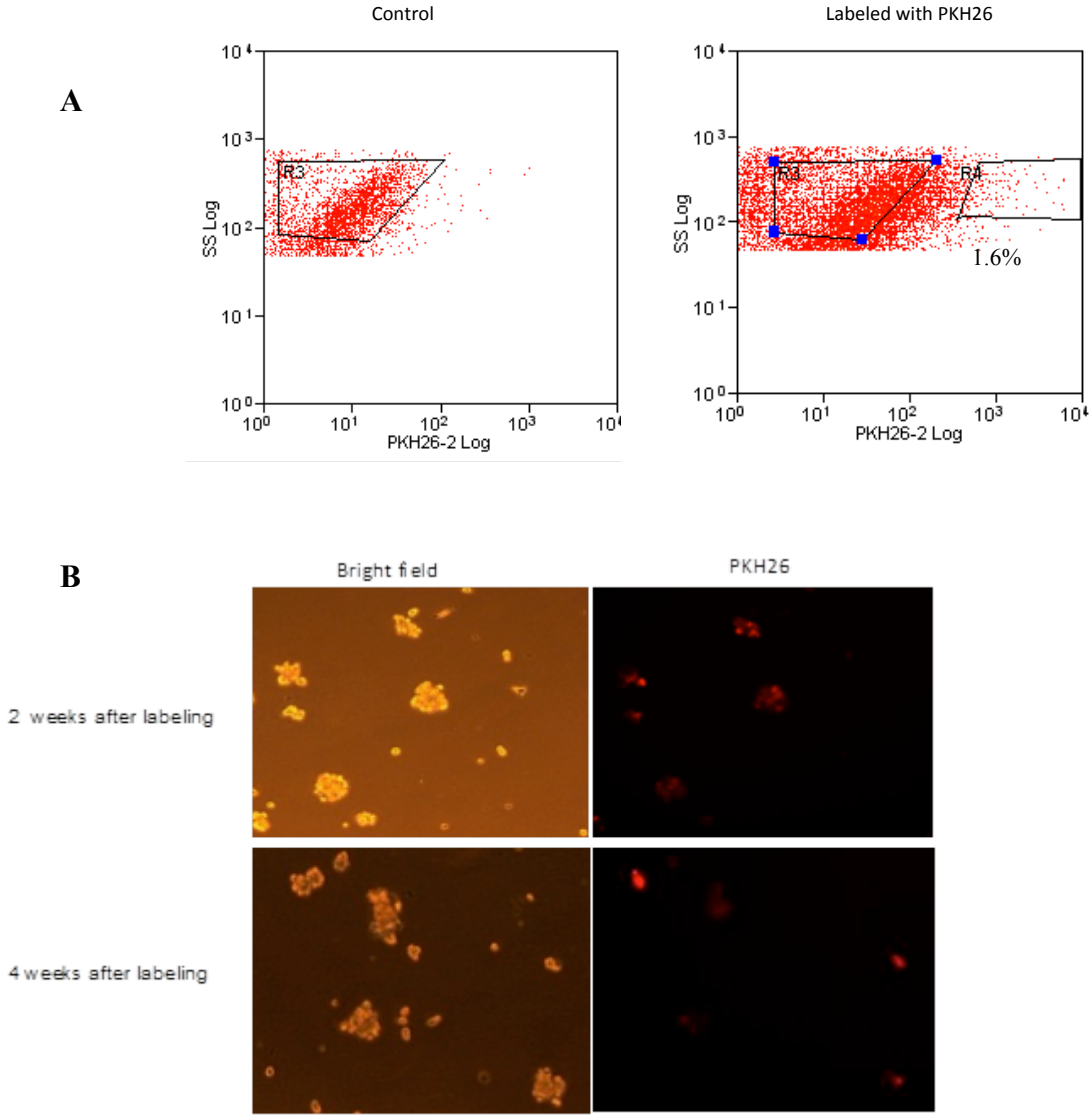

Figure 3-3: OVE cells retain PKH26 labeling

A) OVE cells labeled with PKH26 in culture and analyzed by flow cytometery after 30 days showed that few OVE cells retained the dye for that period. B) OVE cells labeled with PKH26 and plated in suspension to test the ability to form spheres in 2 weeks. The number of labeled cells is decreased by 4 weeks after labeling, indicating that only few cells within the spheres are stem/progenitor cells and able to retain the dye.

3.3 OVE cells express stem cell proteins on the cell surface

Several cell surface proteins have been identified as stem cell markers, although there is notable variability among stem cells from different tissues. We investigated the expression of the most common stem cell genes, including *Oct3/4, CD44, Sca-1, CD133, Lgr5,* and *Aldh* using qPCR. Levels of mRNA encoding for *CD44* and *Sca-1* were most clearly detectable, and so these two were chosen for further investigation.

SCA-1 and CD44 proteins have been reported in several studies to be expressed on the surface of several cell types, including the normal OSE cells which express SCA-1 (Gamwell et al., 2012) and cancerous tissue such as breast cancer cells that express elevated levels of CD44 (Olsson et al., 2011). To confirm that these two genes represent stem cell characteristics in mouse OVE cells, cells expressing CD44 and SCA-1 were isolated using FACS. Flow cytometric analyses showed that all four clonal OVE cells have fractions of cells that can be labeled with CD44 and SCA-1 antibodies on the surface of the cells. The positive and negative populations for both CD44 and SCA-1 were sorted using FACS and plated in suspension to investigate the sphere formation capacity. The CD44-positive cells formed more spheres than the CD44-negative cells in two OVE clones, OVE4 and OVE16 (Figure 3-4B) indicating that CD44 enriches for OVE cells that have self-renewal capacity. Although CD44 protein has numerous isoforms (standard form and variant forms) and the literature generally presents the standard form of CD44 as a stem cell marker (Dang et al., 2015), no mouse antibody can bind only the standard form of CD44. For that reason, when preparing the OVE cells for

FACS we used trypsin, as previously reported (Biddle et al., 2013), to preferentially degrade the variant forms while retaining the standard form.

Both SCA-1-positive and SCA-1-negative cells formed spheres in suspension with stem cell media (Figure 3-4A), however, the proportion of cells forming spheres was very low (Figure 3-4C). The two possible reasons for not getting significant sphere formation by SCA-1-positive cells are either the negative population may have some SCA-1+ cells or perhaps not all stem cells in OVE cells are SCA-1+. It has also been reported that the sphere formation assay might not be an effective method to recognize stem cells *in vitro* for some tissues (Wu et al., 2014).

To confirm our finding that CD44 is expressed in cells from the oviduct, immunohistochemistry was performed to localize the expression of CD44 in the oviduct and ovary. CD44 staining was strong in the distal end of oviductal tubes (fimbria) and a few cells in the rest of oviductal tubes. The expression of CD44 was mostly localized to the basement membrane. Only a few epithelial cells expressing CD44 were found on the surface of the ovary (Figure 3-5).

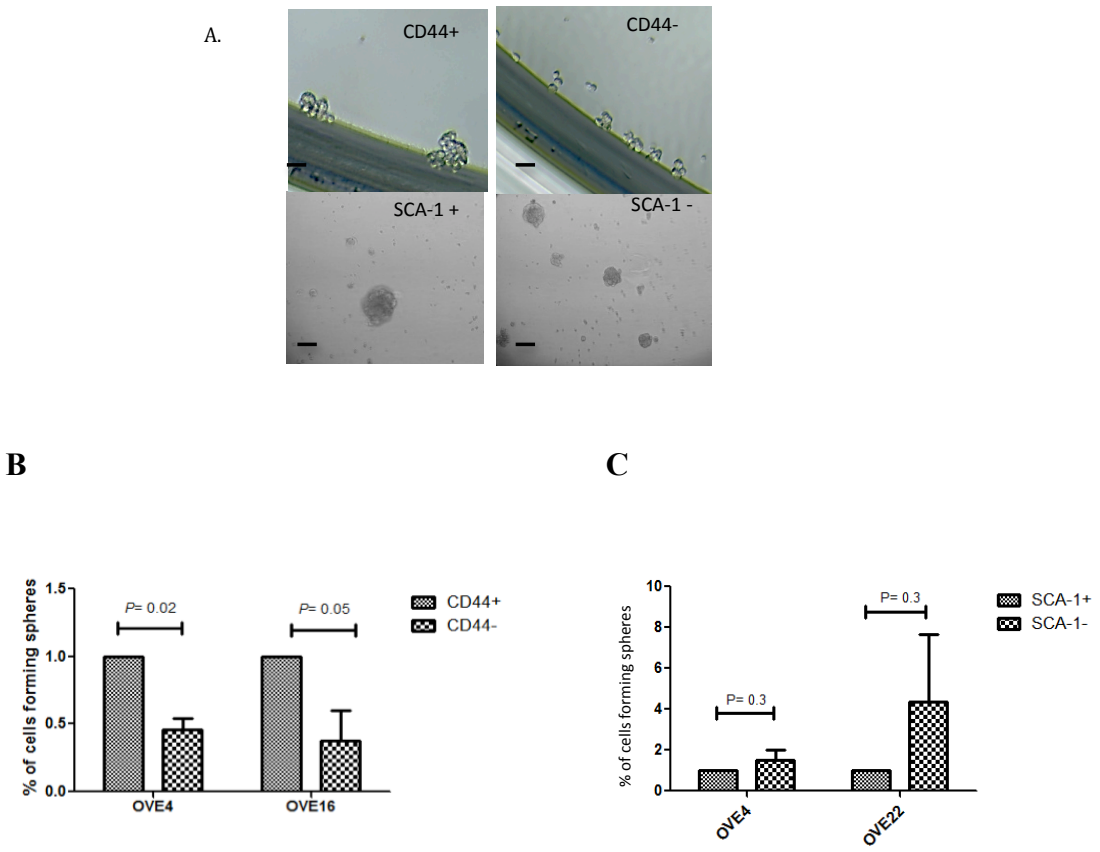

Figure 3-4: OVE cells expressing CD44 and SCA-1 can form spheres when plated in suspension

(A) CD44+ and CD44- OVE cells as well as SCA-1+ and SCA-1- cells plated in suspension were able to form spheres. The scale bar represents 100 µm. B) Quantification of spheres formed by CD44+ and CD44- OVE4 and OVE16 cells, n=3. (C) Quantification of spheres formed by SCA1+ and SCA1- OVE4 and OVE22 cells, n=3. Analyses were performed for all experiments using t-test analysis.

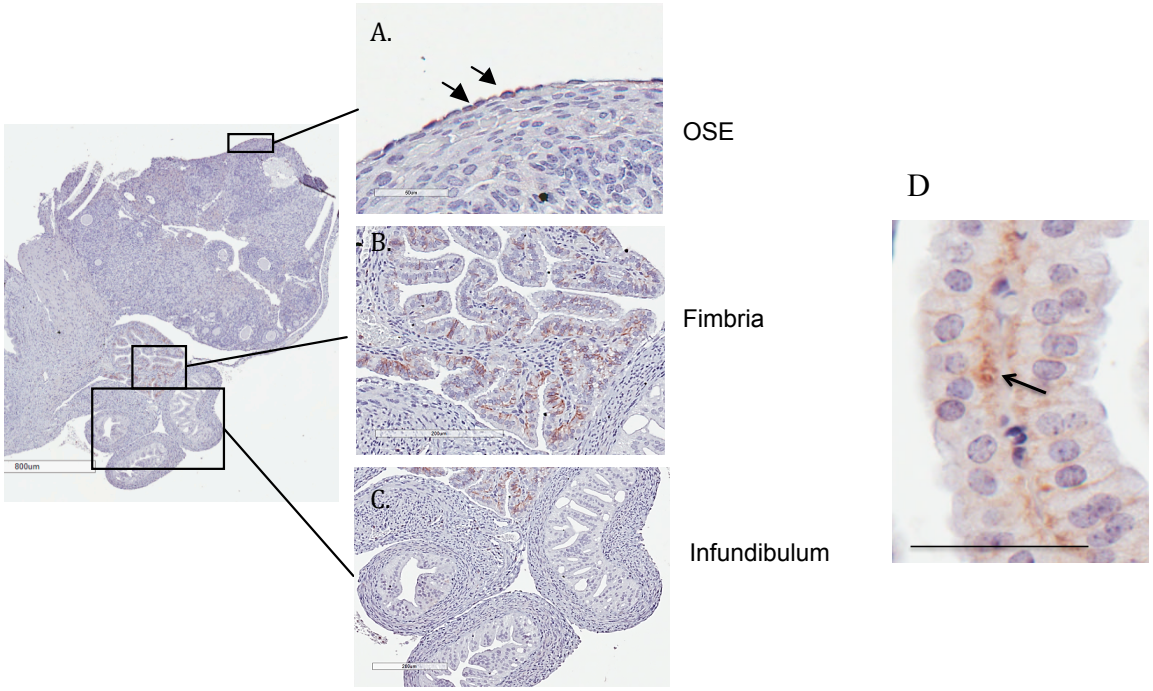

Figure 3-5: Immunohistochemistry shows CD44 expression in the mouse ovary and oviduct.
A) CD44 is expressed in only a few mouse OSE cells in the ovary. Scale bar is 50 µm. B) The distal end of the oviduct (fimbria) has robust expression of CD44 on cells located on the basement membrane. Scale bar is 200 µm. C) The infundibulum of the oviduct is mostly negative for CD44. Scale bar is 200 µm. D) Magnification of the fimbria displays CD44+ cells located on the basement membrane. Scale bar is 50 µm.

3.4 TGFβ induces EMT in OVE cells

Follicular fluid released at ovulation contains TGFβ (Fried et al., 1998) and its expression has also been found in human fallopian tubes (Zhao et al., 1994). The impact of ovulation on OVE cells has been reported by King and coworkers, who have shown increased DNA damage in OVE cells in response to ovulation-associated inflammation (King et al., 2011). To begin to assess the possible impact of ovulatory factors on OVE cells, we treated OVE cells with 10 ng/ml TGFβ (based on a preliminary dose response experiment) and the changes in cell behavior and gene expression were investigated. TGFβ significantly decreased cell proliferation in all four OVE clonal cell lines (Figure 3-6A,B), suppressing the number of cells up to 85% after 7 days of treatment, with no apparent effect on cell viability (Figure 3-6B).

TGFβ signaling has been reported to play an important role in wound repair of the ovarian surface cells after ovulation (Kasuya et al., 2014). Considering its effects on cells on ovarian cell surface, we investigated whether TGFβ could induce OVE cells to undergo epithelial-mesenchymal transition. OVE cells grown in an adherent tissue culture dish form a sheet of adherent cells that are connected to each other by junction molecules. These junction molecules help to give the cells their cuboidal shape. To determine the effect of TGFβ on cell morphology, OVE cells were treated with 10 ng/ml TGFβ and monitored daily by light microscope. Cell morphology started to change after three days of TGFβ treatment when they began to acquire a more spindle shape (Figure 3-6C).

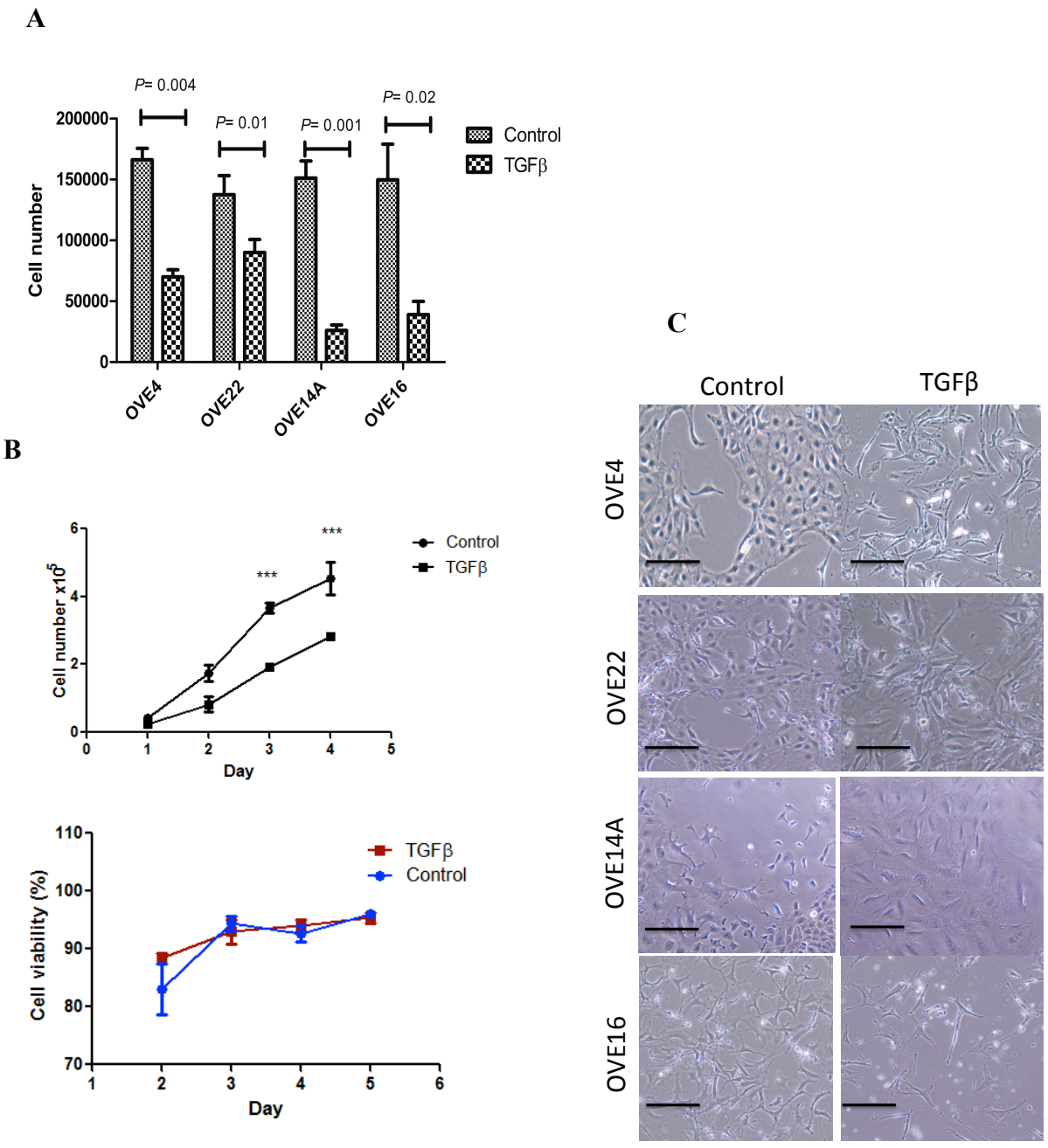

Figure 3-6: OVE cells respond to TGFβ.
A) TGFβ treatment for 7 days inhibited cell proliferation in all OVE clonal cell lines. (B) TGFβ treatment of OVE cells for four days shows decreased cell proliferation and no change in the cell viability (C), and induced a shift in morphology to a more fibroblast-like phenotype. Analysis was done using multiple t-test for three independent experiments.

Since cells undergoing EMT are usually more motile, we assessed cell migration and we found that TGFβ increased cell migration into wounds created in monolayers of OVE4, as assessed after 24 hours (Figure 3-7A).

To further confirm if TGFβ induced EMT in OVE cells, we investigated the expression of genes that are typically associated with EMT. Loss of adherent junction molecules such as E-cadherin, increased cytoskeletal proteins such as Vimentin, and induced expression of the transcription factor Snail are common mediators of EMT (Okamoto et al., 2009; Wang et al. 2015). TGFβ decreased E-cadherin proteins and mRNA and increased Vimentin expression, which likely helped to promote the fibroblast-like shape in OVE cells undergoing EMT. *Snail* mRNA was up-regulated after 7 days of TGFβ treatment and Snail protein levels were increased after 10 days of TGFβ treatment (Figure 3-7B&C).

To investigate if TGFβ released at ovulation might have similar effects on OVE cells *in vivo*, we induced superovulation in 25-day old mice and assessed the morphology and E-cadherin expression of the oviductal cells 1 and 2 hours after ovulation. OVE cell morphology was changed in some areas of oviduct with a shift in cells becoming more columnar and pseudo-stratified. IHC staining for E-cadherin showed that oviducts highly expressed E-cadherin and the level of expression did not appear to change after superovulation. The distribution of E-cadherin changed modestly such that some of the oviductal cells had the expression concentrated on the apical surface of the cells (Figure 3-8).

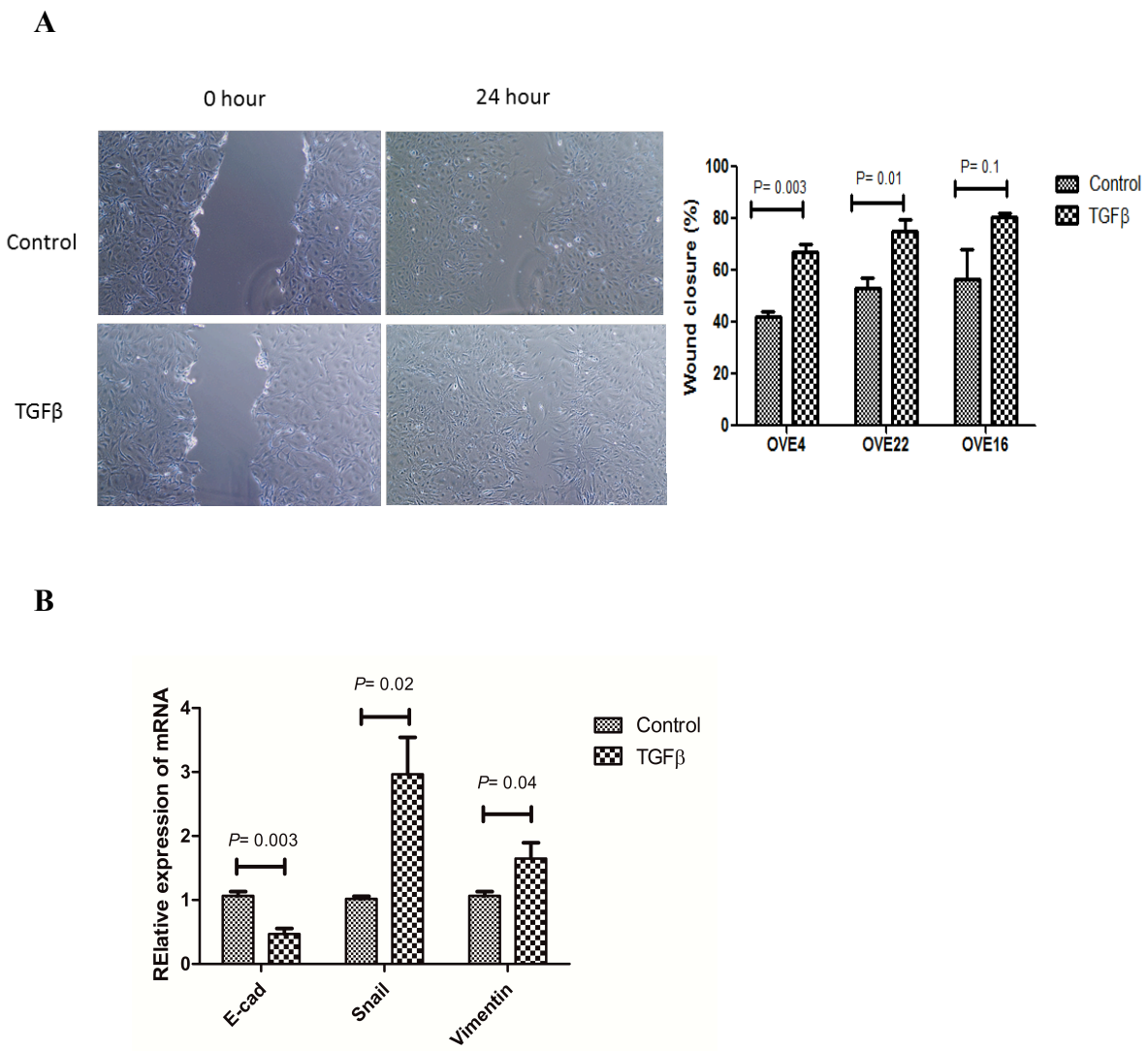

Figure 3-7: TGFβ increases characteristics of EMT in OVE cells

A) Scratch assays for OVE cells pretreated with TGFβ shows that TGFβ enhances the migration of OVE cells into the wound. The histogram shows the percentage of wound closure with and without TGFβ for three OVE clonal cells (N=3). B) Relative expression of mRNA encoding for epithelial and EMT genes (*E-cad, Snail and Vimentin*) in OVE4 cells after 7 days of treatment with or without TGFβ. Analysis was done using multiple t-tests for three independent experiments.

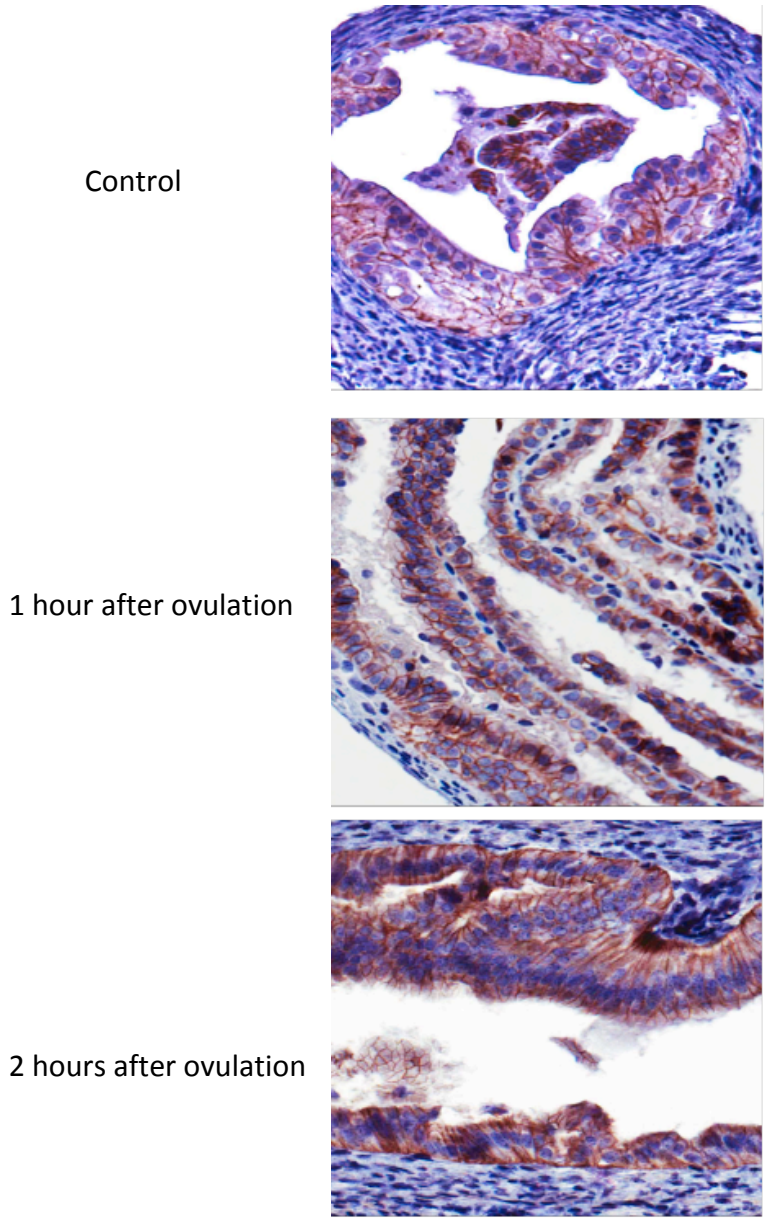

Figure 3-8: E-cadherin expression in the oviduct of superovulated mice
Mouse oviducts collected after superovulation showed modest changes in cell morphology at 2 hours after ovulation. There was no evident change in the level of E-cadherin expression. Arrows indicate the dark staining on the apical surface of the oviductal cells.

3.5 TGFβ enhances stem cell characteristics

To determine if TGFβ affected any of the stem cell characteristics in the OVE cell lines, sphere formation assays were performed in low attachment plates with OVE cells treated with or without 10ng/ml TGFβ for two weeks. For each cell line, a subset of the cells was able to self-renew and form spheres in suspension. TGFβ had no effect on the number of spheres, but significantly increased the size of the spheres in three of the OVE clones (Figure 3-9A&B).

To test further the possible effects of TGFβ on enhancing stemness, the expression of several stem cell markers was assessed after 7 days of TGFβ treatment, including *CD44, Sca-1, CD133, Oct3/4, Aldh* and *Lgr5*. TGFβ up-regulated the levels of *CD44* and *Sca-1* mRNA, with a particularly notable 5-fold increase in CD44 (Figure 3-10A). When the expression of CD44 was examined further, TGFβ was found to increase the fraction of CD44-expressing cells, as determined by flow cytometry using a pan CD44 antibody (Figure 3-10B) and by immunofluorescence (Figure 3-10C). Using an antibody that detects all CD44 isoforms, western blot analysis showed that CD44v (230KD) was up-regulated after 7 days of TGFβ treatment of OVE4 and OVE16 cells, whereas CD44s (90KD) was up-regulated after 20 days of TGFβ treatment (Figure 3-10D).

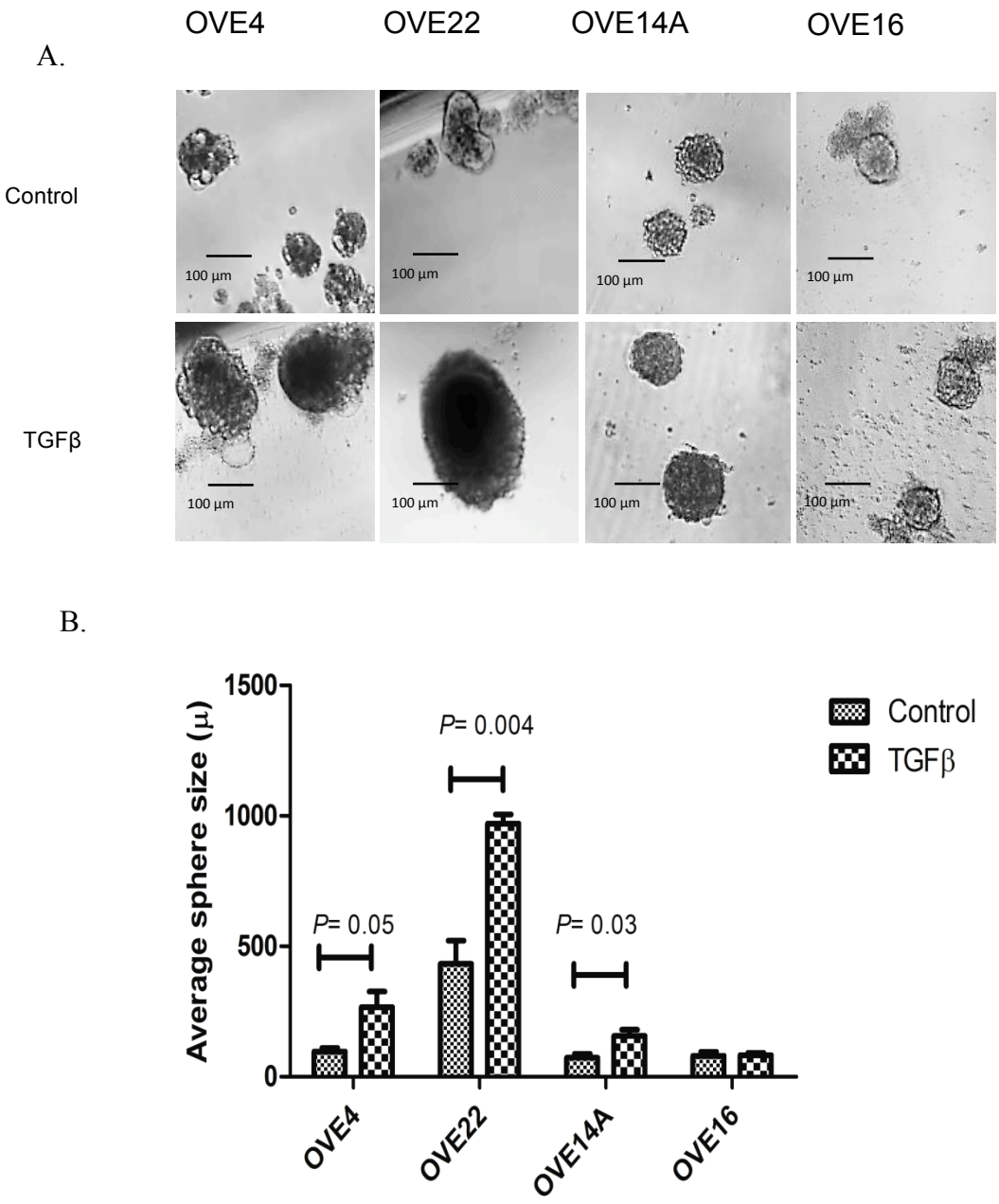

Figure 3-9: TGFβ induces sphere formation capacity in OVE cells.
A) OVE cell lines form spheres in low attachment plates that are increased in size by treatment with TGFβ of OVE4, OVE22 and OVE14A clones. B) Quantitative assessment of the average sphere size formed by OVE clones. Analysis was done using multiple t-tests for three independent experiments.

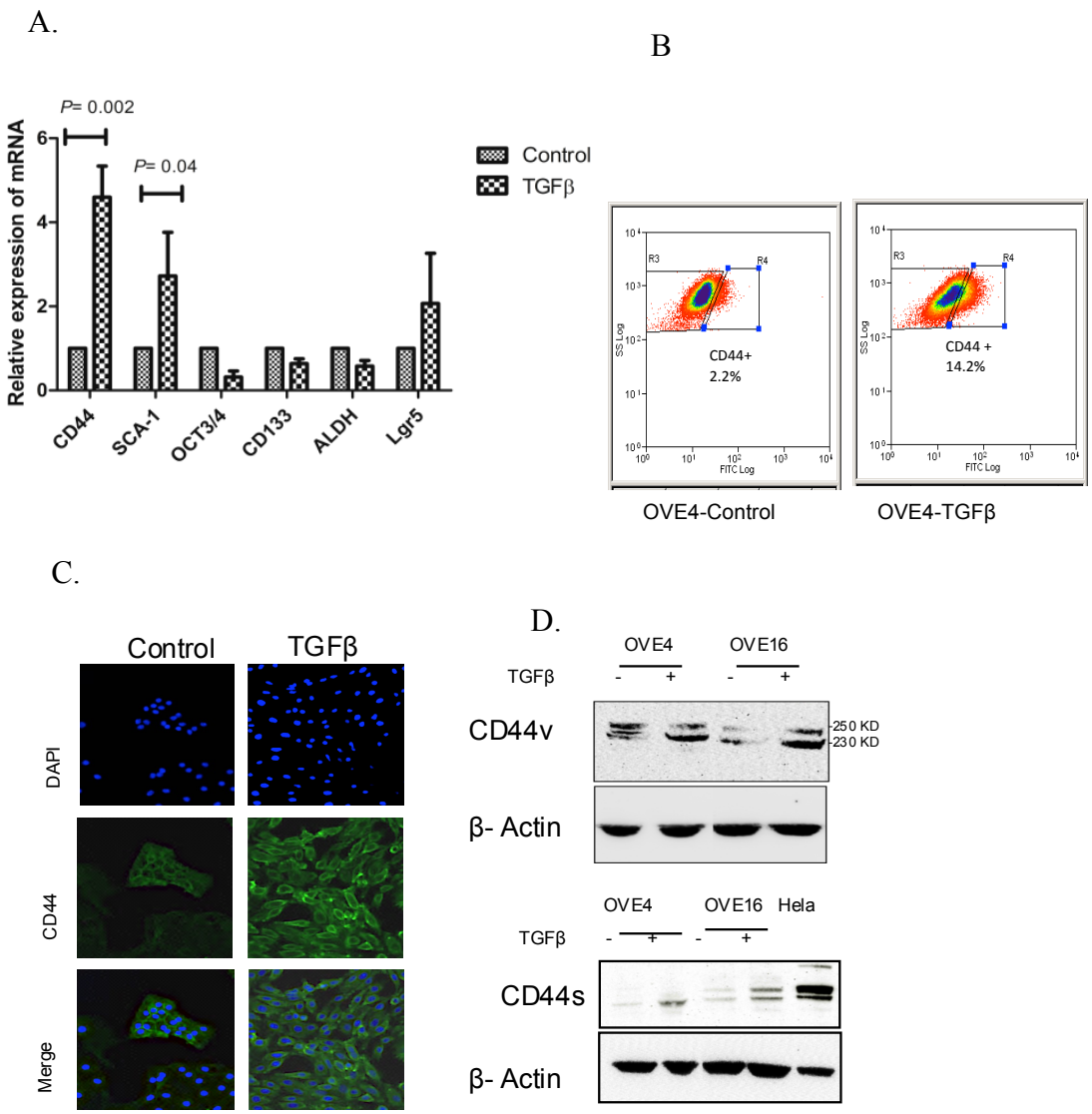

Figure 3-10: TGFβ increases the expression of stem cell associated genes in OVE cells.

A) Relative expression of mRNA encoding for stem cell markers in OVE4, TGFβ significantly up-regulates *CD44* and *Sca-1* mRNA. Analysis was done using multiple t-tests for three independent experiments. (B) Flow cytometric analysis showed an increased number of cells with CD44 expression after TGFβ treatment. (C) Immunofluorescence microscopy revealed the presence of intense staining of CD44 in OVE cells after TGFβ treatment for 4 days. (D) Western blots show increased expression of CD44v after 7 days of TGFβ treatment and CD44s after 20 days of TGFβ treatment. Blots are representative of one independent experiment.

3.6 TGFβ decreases PAX2 expression

We have shown above that TGFβ promotes OVE cells to undergo EMT and the epithelial cells changed to a more fibroblast-like morphology. Since PAX2 has an established role in epithelial differentiation of the Mullerian duct system (Mansouri et al.,1996), we examined whether TGFβ affects the differentiation status of OVE cells by modulation of PAX2 expression. PAX2 expression was determined after 7 days of OVE cell treatment with 10 ng/ml TGFβ. Interestingly, we found that TGFβ treatment led to a significant reduction in the levels of mRNA encoding for *Pax2*, as assessed by qPCR, for two of the OVE clonal cell lines (OVE4 and OVE16), and with a strong trend in OVE22 cells (Figure 3-11A). PAX2 protein was suppressed by TGFβ treatment of the two OVE clonal cell lines tested (OVE4 and OVE22; Figure 3-11B).

In order to know which TGFβ signaling pathway is associated with PAX2 reduction, we performed a TGFβ treatment time course for 7 days. We found that TGFβ decreased PAX2 protein at day 2 and for 7 days. The suppression of PAX2 was associated with continues phosphorylation of SMAD2 (Figure 3-11C).

To know if TGFβ signaling to induce EMT and increase stem cell characteristics is mediated by loss of PAX2, we performed qPCR for EMT markers and stem cell markers for OVE 4 cells treated with and without TGFβ. We found that TGFβ was able to suppress PAX2, down regulates epithelial markers, upregulated EMT and increase stem cell marker (CD44) in the first day (Figure 3-11D)

This chapter of results displays evidences to support the stem cell existence within OVE cells and TGFβ effects on OVE cells to induce EMT and stemness, and decrease

PAX2 expression, suggesting that PAX2 may mediate the TGFβ effect on the EMT and stemness. To better understand the role of PAX2 in EMT and stemness, PAX2 expression was suppressed to investigate EMT and stem cell characteristic with loss of PAX2.

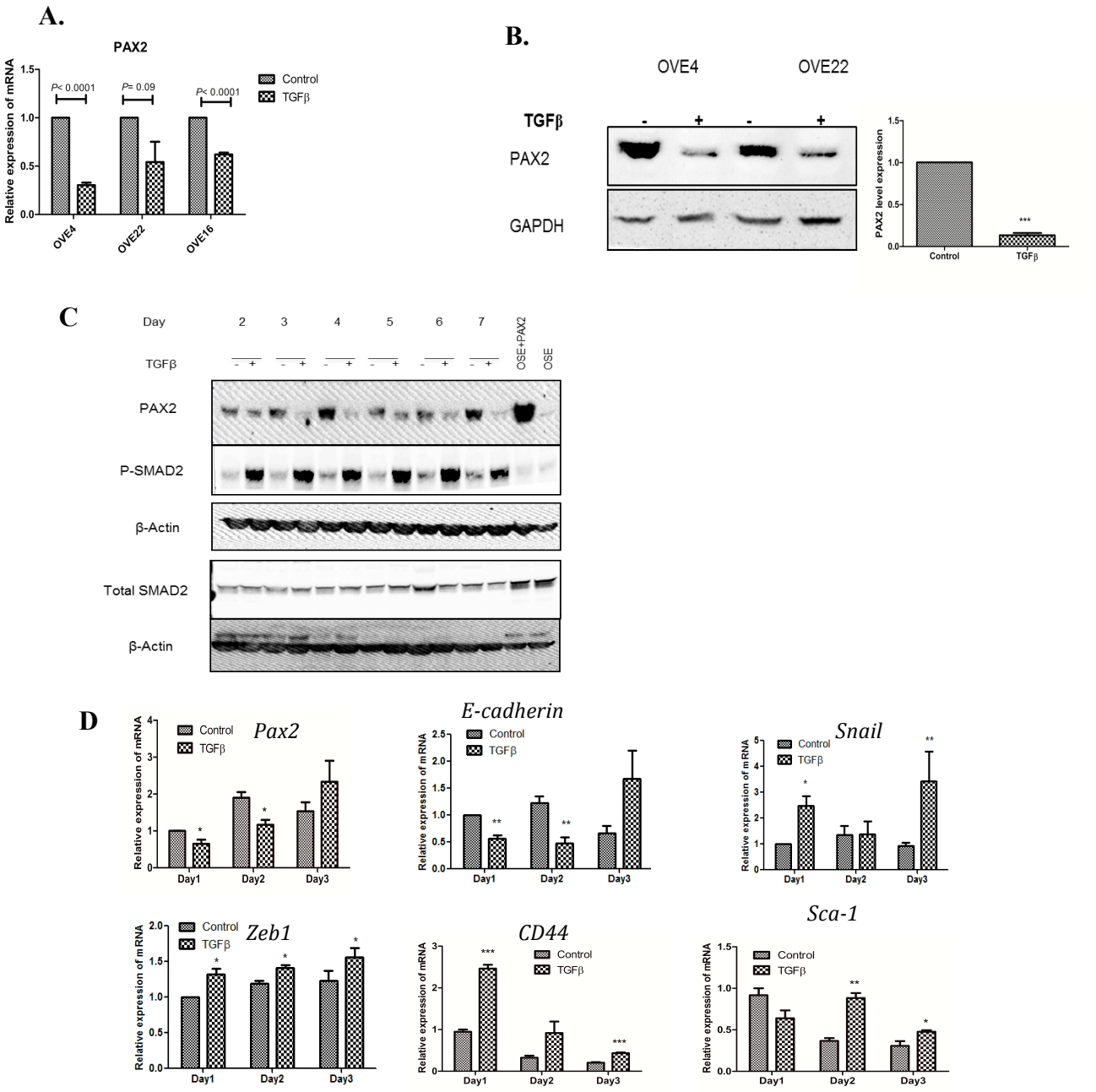

Figure 3-11: TGFβ decreases Pax2 in OVE cells.

A) Relative mRNA expression of *Pax2* in three OVE clonal cells treated with TGFβ showed a significant decrease in *Pax2* mRNA in two of the lines, and a strong trend in the third line. (B) Western blots showed decreased expression of PAX2 after 7 days of TGFβ treatment of OVE4 cells. PAX2 expression in western blots were analyzed using t-test of densitometric measurements for three independents experiments. (C) Western blot representative of two independent experiments with OVE4 cells shows that PAX2 suppression by TGFβ for 7 days is associated with SMAD2 phosphorylation. (D) qPCR experiments for OVE4 treated with TGFβ for 3 days shows decreased expression of *Pax2* mRNA in the first day of treatment associated with EMT and expression of stem cell markers. Analysis for qPCR experiments was done using t-tests (N=3).

Chapter 4: Results (Part II)

PAX2 negatively regulates stemness in OVE cells and OSE cells

Since TGFβ induced the cells to undergo EMT and increased expression of SCA-1 and CD44, we hypothesized that loss of PAX2 may mediate at least some of the TGFβ effects on EMT and stemness. To better understand the role of PAX2 in these processes, the consequences of suppression of its expression were assessed in OVE cells.

4.1 PAX2 negatively regulates CD44 in OVE cells

Flow cytometric analysis for CD44 in all OVE clonal cells showed that the percentage of cells that express CD44 varies among the cell lines (Figure 4-1). Interestingly, OVE14A clonal cells are PAX2 negative and they have the highest fraction of cells expressing CD44. This observation, in combination with the results in Chapter 3 showing that TGFβ had opposite effects on the expression of CD44 and PAX2, suggested a possible inverse relationship between PAX2 and CD44 in OVE cells, a hypothesis that we explored further.

We first selected two OVE clonal cell lines (OVE4 and OVE14A) to examine the expression of CD44 by immunofluorescence. OVE4 cells express CD44 on the surface of some cells, whereas OVE14A cells express CD44 on both the cell surface and in the cytoplasm (Figure 4-1C). One interpretation of this result is that OVE14A cells may express different isoforms of CD44 including the standard form of CD44 which may specify the transmembrane domain and cytoplasmic domain of CD44 protein. To confirm the differential expression of CD44 and the other stem cell marker, SCA-1, in OVE14A vs. OVE4 cells, qPCR was performed and showed that OVE14A cells express higher

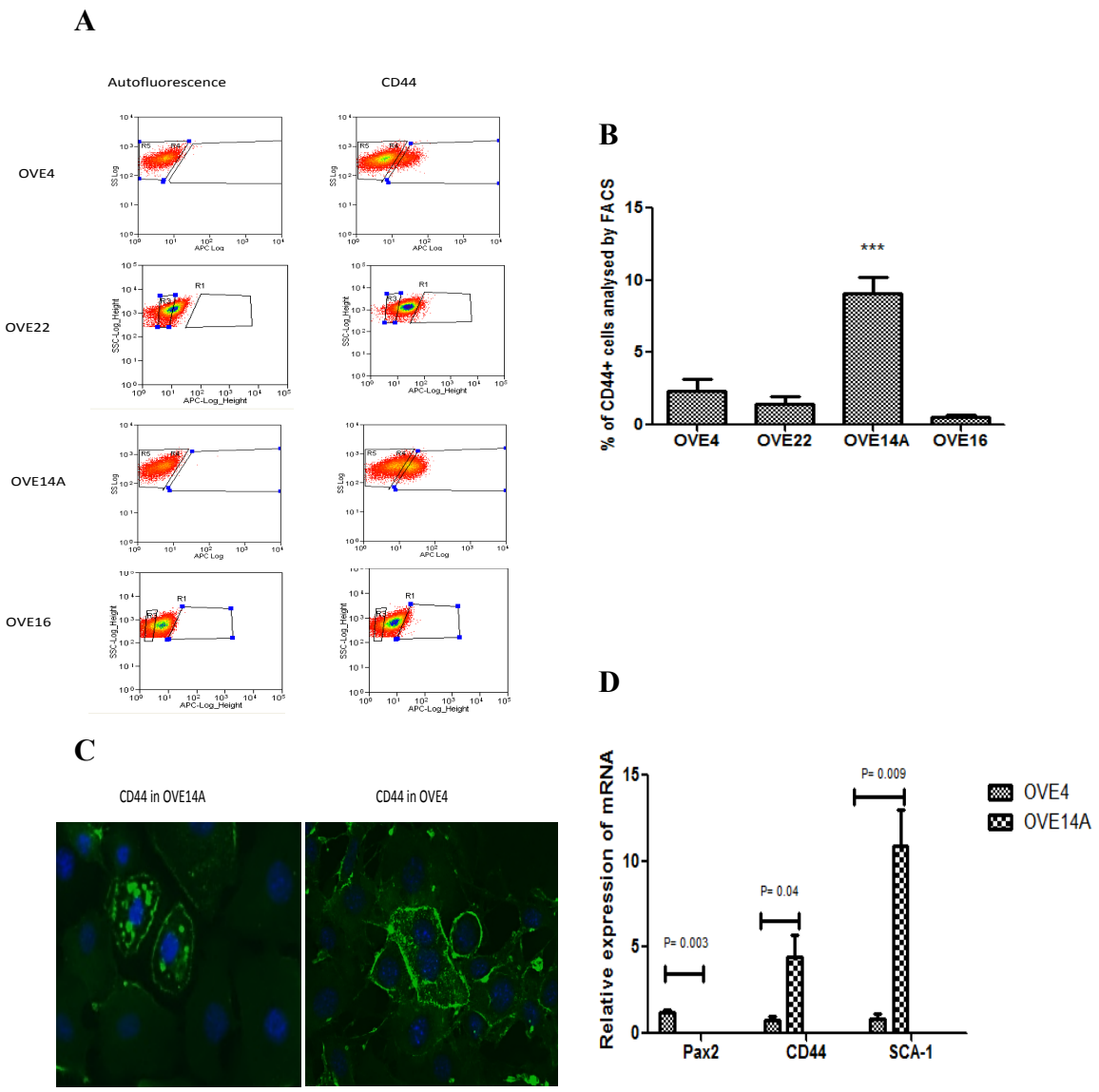

Figure 4-1: CD44 expression is highly expressed in PAX2-null OVE cells.
A) Flow cytometric analysis for OVE cells labeled with CD44 antibody shows that OVE14A highly expresses CD44 relative to the other four OVE cell lines. B) Quantitative analysis of the flow cytometry data. One way ANOVA analysis $P<0.0001$, $n=3$. C) Immunofluorescence for two OVE clones, OVE4 and OVE14A, displayed CD44 expression in OVE4 only on the surface of cells, whereas in OVE14A, CD44 is present on the cell membrane and in the cytoplasm. qPCR analysis for stem cell markers in OVE4 and OVE14A shows that OVE14A highly expresses *CD44* and *Sca-1* mRNA compared to OVE4 and no expression of *Pax2* mRNA. Gene expressions were analyzed by t-test on data obtained from three independent experiments.

levels of CD44 and SCA-1 mRNA compared to OVE4 (Figure 4-1D).

To determine if PAX2 expression negatively correlates with CD44 expression *in vivo*, serial sections of mouse fimbria were stained for CD44 and PAX2. As shown in Figure 3-5, immunohistochemistry confirmed that CD44 protein is localized to the basement membrane and is expressed in some basal cells. Those cells, however, do not express PAX2 (Figure 4-2A). Double staining of the mouse oviduct showed that the luminal epithelial cells in the distal end of the mouse oviduct express PAX2 and some CD44 is seen at the basal surface of the cells. However, the few small basal cells located under the epithelial cells express only CD44 (Figure 4-2B). Based on a previous study reporting that the basal cells may represent stem cells in the human fallopian tube (Paik et al., 2012), we considered that the CD44 expression in the luminal epithelial cells may represent the variant isoforms (epithelial isoforms) of CD44, whereas the basal cells expressing CD44 may express alternative isoforms associated with stem cell characteristics, which is a concept we next explored. We hypothesized that the expression of PAX2 and the stem cell isoform of CD44 may be mutually exclusive in the basal cells of the mouse oviduct.

A

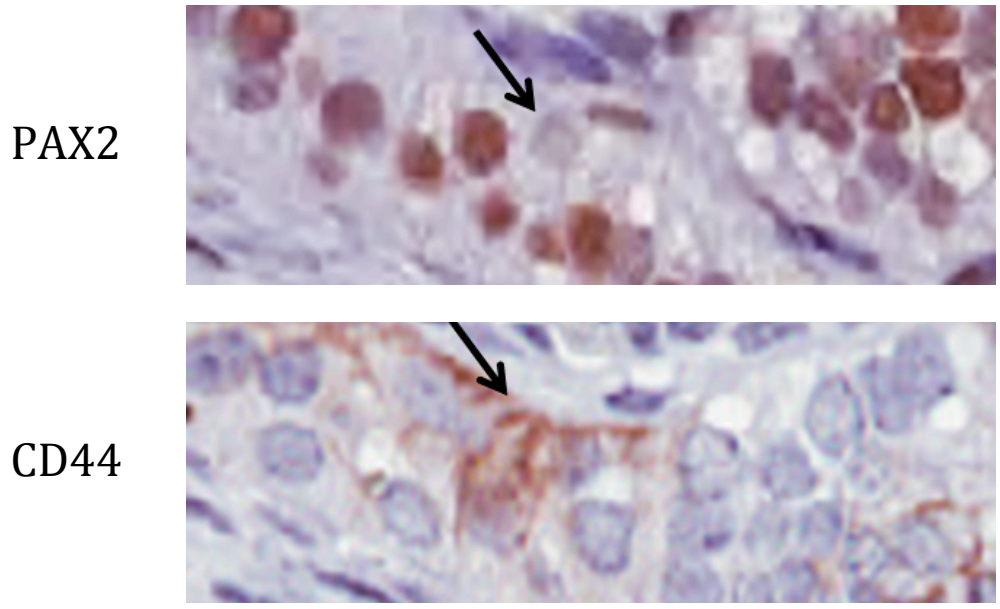

B

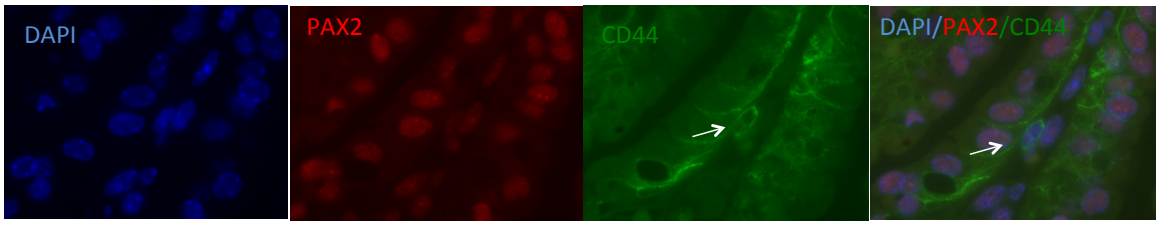

Figure 4-2: CD44 and PAX2 expression in mouse oviducts.
A) Immunohistochemical analysis of serial sections of mouse oviduct shows the expression of PAX2 in the luminal OVE cells and CD44 in the basement membrane. B) Immunofluorescent double staining for PAX2 and CD44 shows high expression of CD44 on the basement membrane. The arrows show a basal cell that is negative for PAX2 and positive for CD44.

To determine the requirement for PAX2 in maintaining the OVE cell state of differentiation vs. stemness, and to begin to explore how the loss of PAX2 in the fallopian tube in STICS may contribute to tumor initiation (Horn et al., 2013; Chen et al. 2010), we knocked down expression of *Pax2* using doxycycline-inducible shRNA (pLKO) in OVE4 and OVE16 cells. PAX2 expression was decreased by 50% in OVE4-pLKO and 70% in OVE16-pLKO in doxycycline-treated cells compared to transfected cells without doxycycline. Inhibition of *Pax2* expression was associated with an increase in *CD44v* expression in OVE4-pLKO and OVE16-pLKO in sub-confluent cell culture (Figure 4-3A&B). Knockdown of *Pax2* in OVE4-pLKO cells resulted in a significant increase in *CD44*, *Sca-1* and *CD133* mRNA (Figure 4-3C), with no effect on the levels of *Aldh* or *Lgr5* mRNA. Quantitative analysis of sphere formation by both OVE4-pLKO and OVE16-pLKO cells showed increased sphere-forming capacity after PAX2 knockdown only in OVE4-pLKO (Figure 4-3D).

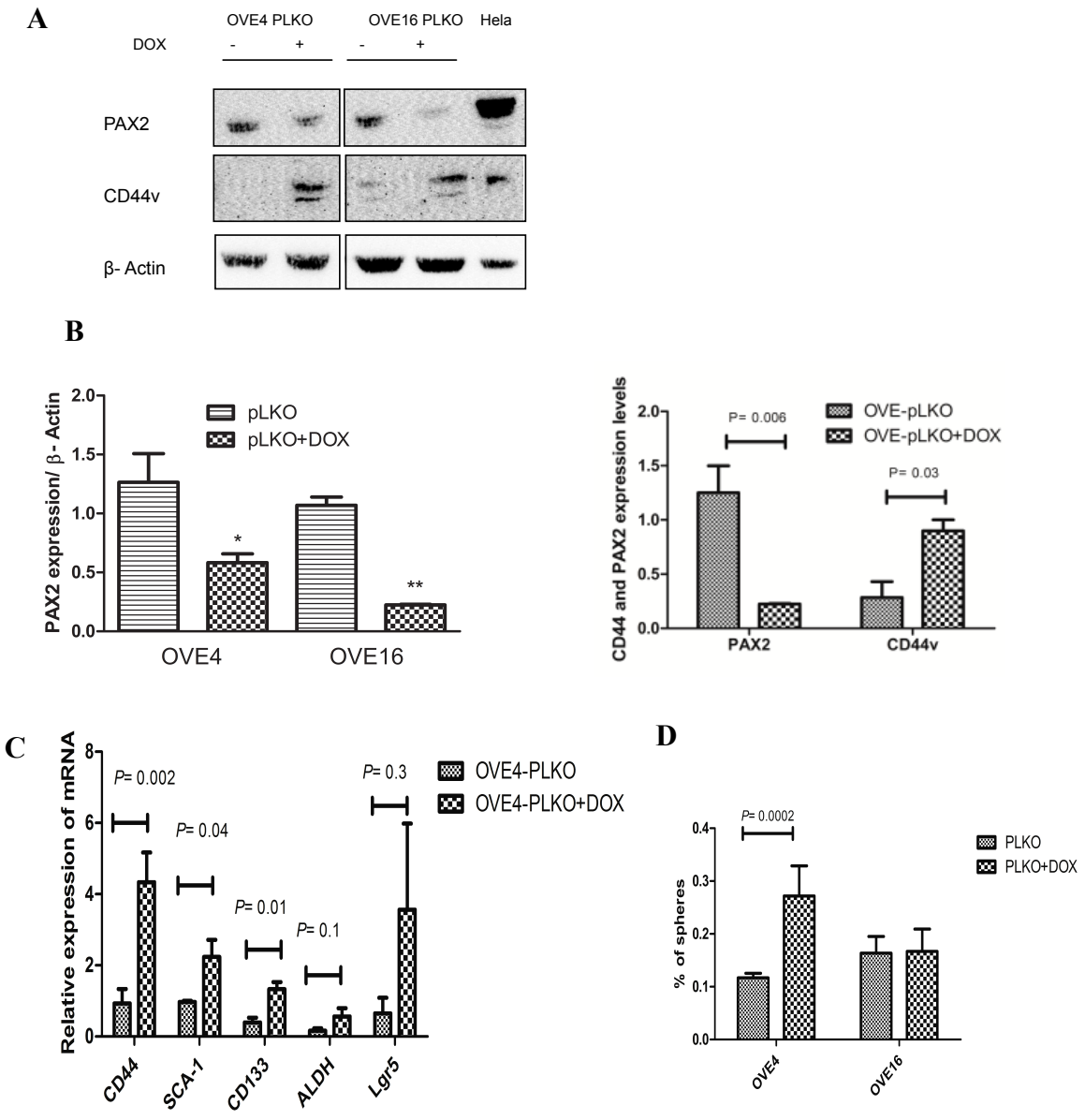

Figure 4-3: Loss of PAX2 enhanced stem cell characteristics in OVE cells.
A) Western blots show PAX2 knockdown in two OVE clones and an associated increase in CD44v abundance. Hela cells were used as a positive control. B) Histograms show densitometric analysis of PAX2 and CD44 levels that were normalized to β-actin (N=3). C) Determination of relative expression of mRNA encoding stem cell genes shows up-regulation of *CD44*, *Sca-1*, and *CD133* mRNA, but not *Aldh* or *Lgr5* mRNA, after PAX2 knockdown. D) Quantitative determination of the percentage of spheres relative to the total number of plated cells before and after PAX2 knockdown. Groups with and without knockdown were compared by t-test analysis of three independent experiments.

4.2 PAX2 negatively regulates CD44 and stemness in mouse OSE cells (MOSE)

PAX2 is not expressed in OSE cells *in vivo*, whereas it is expressed in oviductal epithelium, despite evidence that these cells derive from common precursors in the coelemic epithelium (Auersperg et al., 2011). To better understand the role of PAX2 in promoting epithelial differentiation and inhibiting stemness, we forced *Pax2* expression in poorly differentiated MOSE cells (M1102) which do not express PAX2. We have previously shown that M1102 cells have a subpopulation with stem cell characteristics that include SCA-1 expression and sphere formation (Gamwell et., 2012). M1102 cells were transduced with a construct expressing loxP-flanked *Pax2* as shown by western blot (Figure 4-4A). In M1102 cells expressing PAX2, sphere formation was significantly reduced, compared to parental cells and the vector control. When the *Pax2* gene was deleted by treatment of the cells with AdCre, the capacity for sphere formation was restored (Figures 4-4B and C). Since we have shown in Figure 4-3 that loss of PAX2 is associated with increased CD44 expression in OVE cells, we investigated CD44 expression after induced PAX2 expression in MOSE to confirm the regulatory role of PAX2 on CD44 expression. The expression of CD44 isoforms was analyzed by western blot, which revealed a significant reduction in both variant and standard isoforms of CD44 (Figure 4-5A&B).

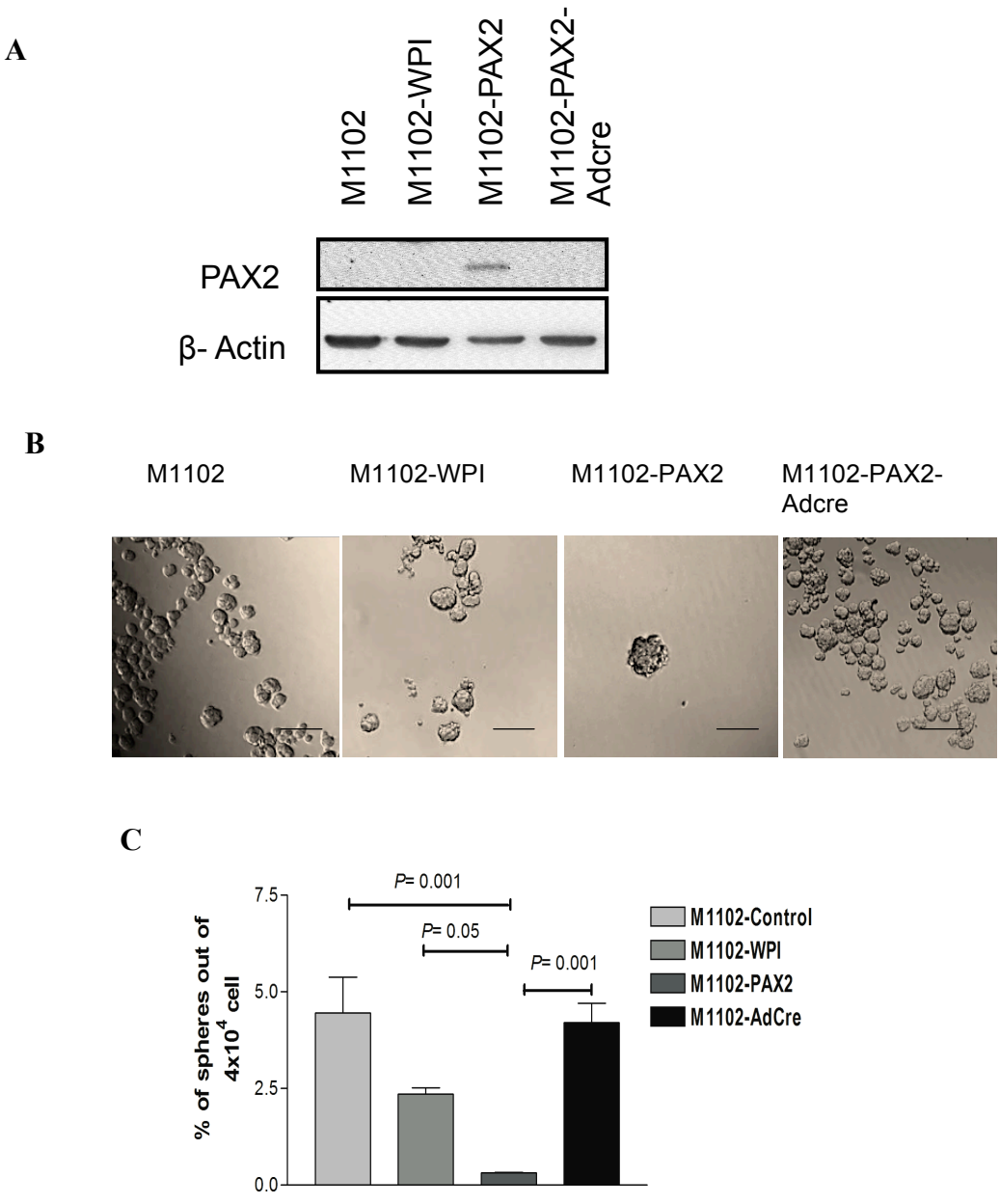

Figure 4-4: Pax2 decreases sphere-forming capacity in MOSE cells.

A) Western blot shows the overexpression of PAX2 in the MOSE cell line, M1102, and the down-regulation of PAX2 after AdCre treatment. B) Sphere formation assay for M1102 cells grown in suspension results in relatively few spheres from cells with PAX2 overexpression. C) Quantitative analysis shows a significant decrease in sphere number after PAX2 is expressed in M1102 cells. Percentages were compared by one way ANOVA statistical test for three independent experiments.

To confirm these results, immunofluorescence to detect PAX2 and CD44 was performed. M1102 control cells are PAX2-null, whereas CD44 is highly expressed in cell clusters. In contrast, M1102 cells with forced expression of PAX2 are highly proliferative and present weak CD44 signals distributed throughout the monolayer. Knockout of PAX2 with AdCre abolished PAX2 expression and restored CD44 expression in clusters of cells (Figure 4-5C).

To further examine if PAX2 down-regulates stem cell characteristics in MOSE cells, we investigated the expression of other stem cell genes that have been reported to be expressed on the surface of the ovary (Hummitzsch et al., 2015). qPCR analysis was performed to detect *Sca-1, Lgr5, Nanog* and *CD133* mRNA. We found that induced PAX2 expression significantly decreased mRNA encoding for *Sca-1* and *Lgr5* whereas *Nanog* mRNA was not affected (Figure 4-6). MOSE cells do not express mRNA encoding for *CD133* and forcing PAX2 expression in those cells did not induce expression.

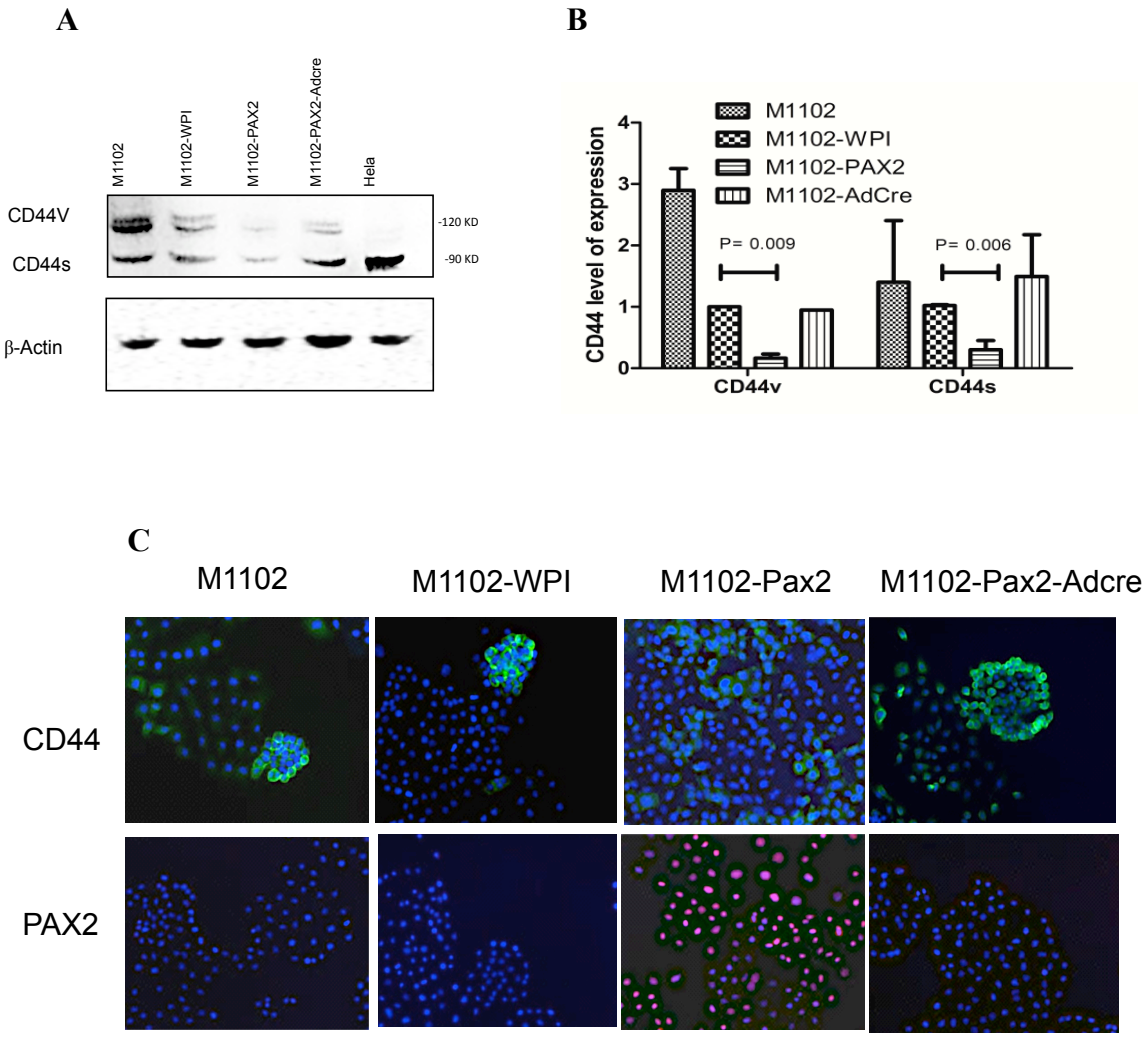

Figure 4-5: PAX2 down-regulates CD44 expression.
A) Representative western blot shows induced expression of *Pax2* results in decreased abundance of both variant and standard isoforms of CD44. (B) Histograms show densitometric analysis of CD44 levels that were normalized to β-actin (N=3). (C) Immunofluorescence staining for CD44 and PAX2 shows that expression of PAX2 in M1102 is associated with decreased CD44 expression.

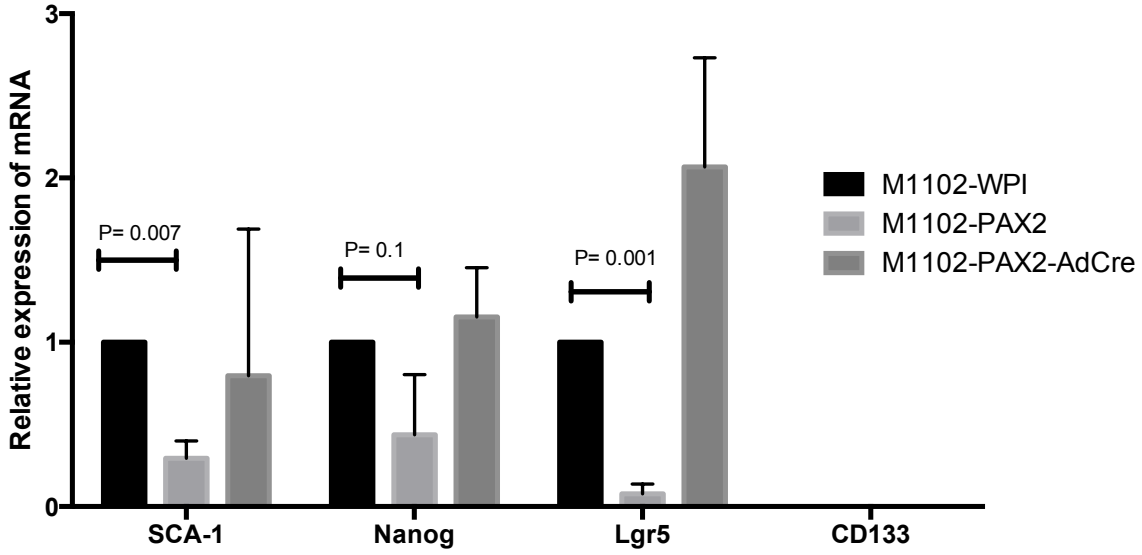

Figure 4-6: PAX2 suppressed expression of stem cell markers.
qPCR analysis for stem cell markers in MOSE cells (M1102) with and without forced expression of PAX2 shows significant down-regulation of *Sca-1* and *Lgr5* mRNA, and no effect on *Nanog*. CD133 mRNA was undetectable. Gene expressions were analyzed by one-way ANOVA test on data obtained from three independent experiments.

4.3 PAX2 enhances cell differentiation in OVE cells to form luminal structures

The suppression by PAX2 of stem cell characteristics in both OVE and OSE cells suggests that it may play an essential role in maintaining the epithelial differentiation of OVE cells. OVE cells were therefore cultured in matrigel using methods previously used to assess mammary epithelial cell differentiation (Debnath et al., 2003). After 14 days in 3D culture in matrigel, OVE cells formed differentiated structures with a hollow lumen that resemble the oviduct structure (Figure 4-7A). The luminal structures express E-cadherin localized to the membrane and the nuclei clearly express the OVE markers PAX8 and PAX2 (Figure 4-7B). These hollow lumen structures were similar to those observed previously when generated by MCF10A cells, where they are known as acini (Debnath et al., 2003).

Interestingly, not all OVE clonal cell lines were able to form luminal structures in 3D culture. Only OVE cells resembling ciliated cells with clear epithelial morphology and high expression of PAX2, such as OVE4 cells, were able to form efficient luminal structures. PAX2 expression and ciliated cells that express β-tubulin were identified in OVE4 clonal cells (Figure 4-7C). Although generated as a clone from a single cell, OVE4 cells have mixed populations of epithelial and mesenchymal-like cells, but the phenotype of the luminal structures suggests that it is the ciliated epithelial cells that contribute to the formation of these structures in the 3D culture. In contrast, OVE cells with negative or low expression of PAX2, such as OVE14A and OVE16, did not form luminal structures in 3D culture. Remarkably, the OVE cells that were able to form luminal structures had limited capacity to form spheres in suspension (Figure 4-8A). The results

suggest a positive correlation of PAX2 expression with epithelial morphology and the ability to differentiate into luminal structures.

To confirm that PAX2 is important for epithelial differentiation, we investigated the formation of luminal structures by OVE4-PLKO cells after *Pax2* knockdown with doxycycline. Interestingly, *Pax2* knockdown in OVE4-PLKO cells disrupted the formation of luminal structures, resulting instead in irregular spheres (Figure 4-8B). The percentage of cells that were able to form luminal structures after *Pax2* knockdown was significantly reduced (Figure 4-8C), supporting the concept that PAX2 is an important transcription factor for the maintenance of the epithelial differentiated state of OVE cells.

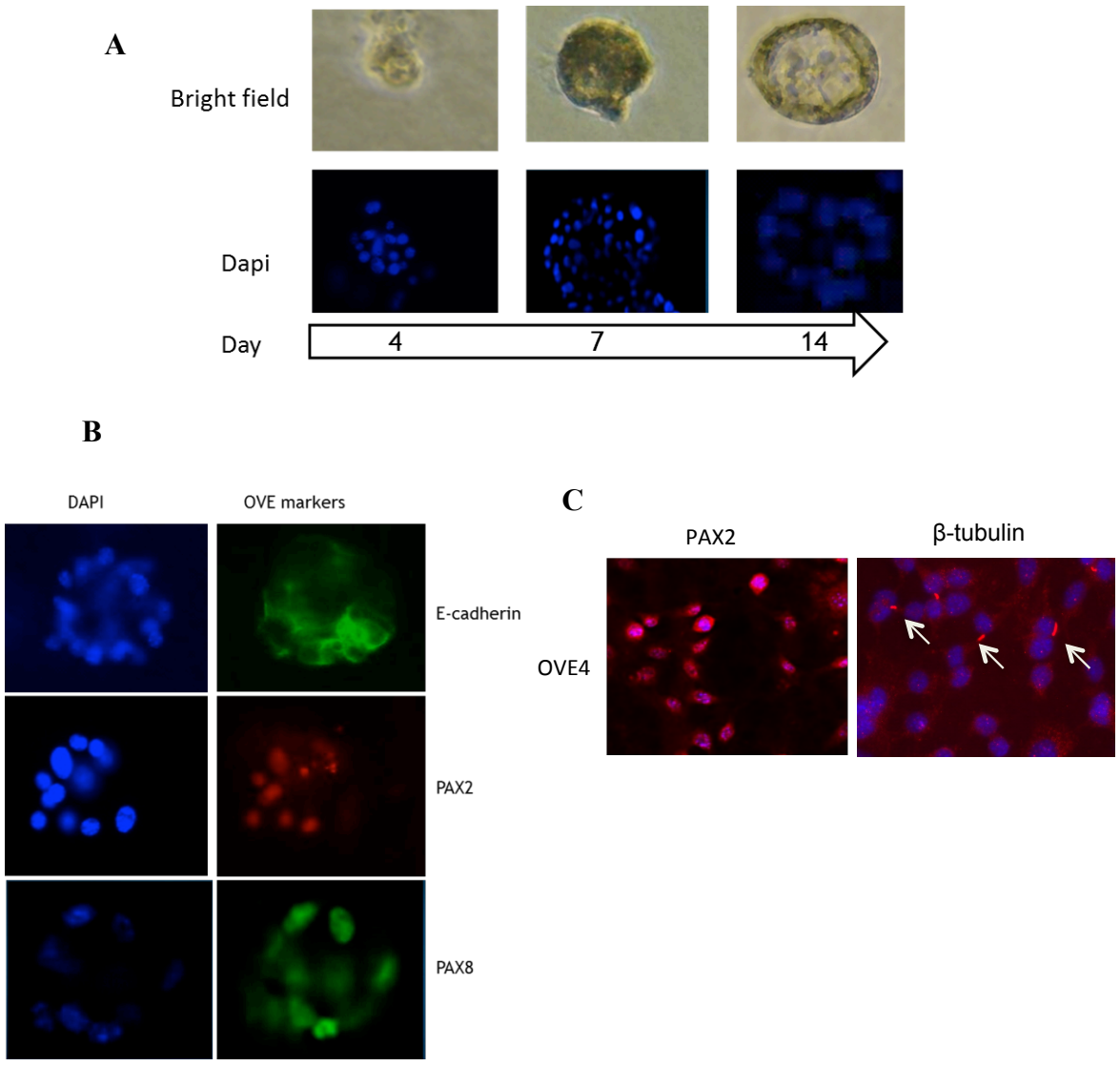

Figure 4-7: Pax2 induces cell differentiation in 3D cultures, enabling OVE to form luminal structures.

A) The formation of luminal structures in matrigel started with small spheres by day 4 and ended with hollow-lumen spheroids by day 14. (B) OVE4 luminal structures expressed OVE markers (E-cadherin, PAX2 and PAX8). (C) Immunofluorescence staining in a monolayer culture of OVE4 cells for PAX2 and β-tubulin identifies cilia on the surface of some epithelial cells.

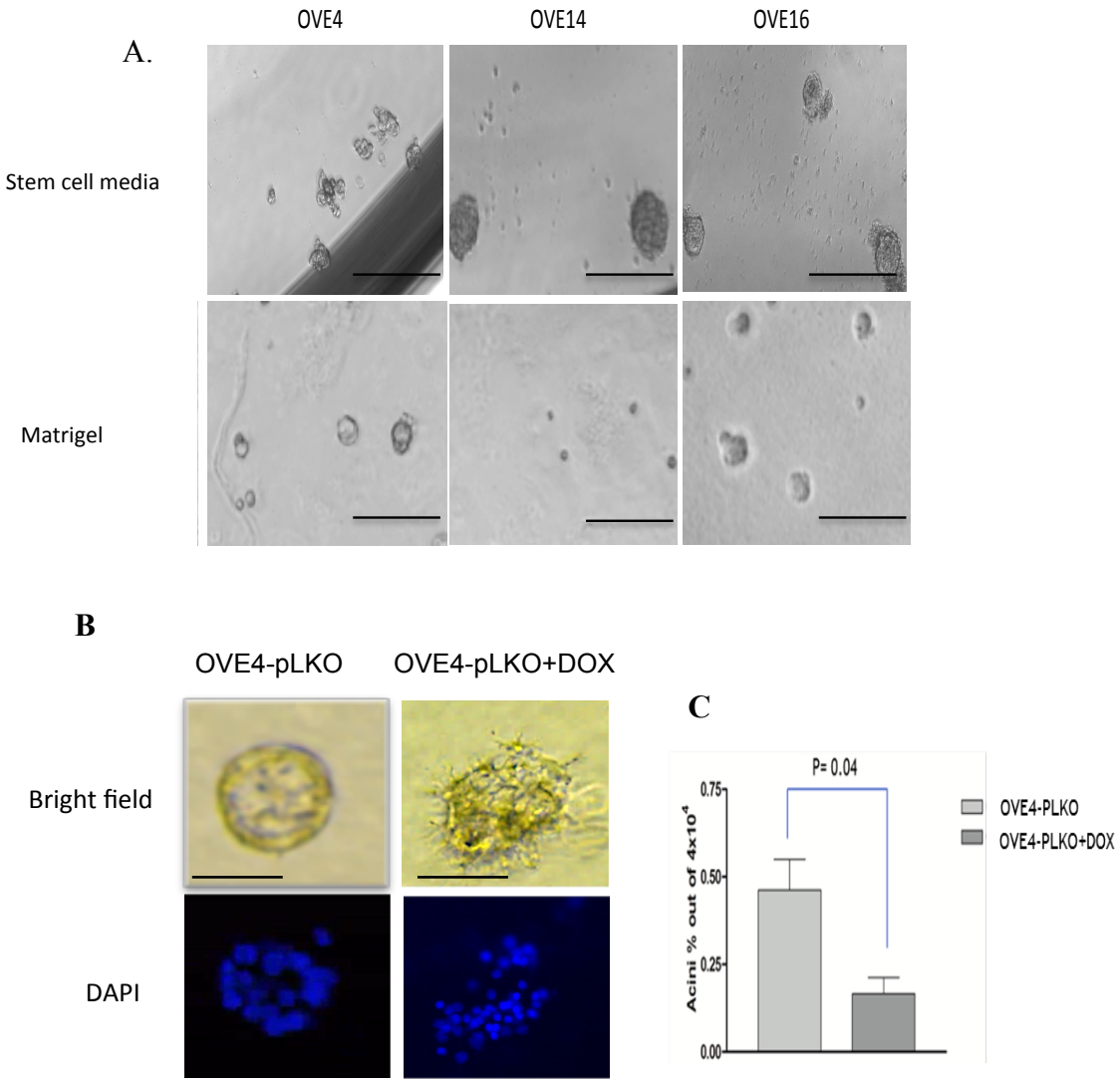

Figure 4-8: PAX2 positively regulates OVE differentiation.
A) OVE clonal cells grown in suspension in stem cell media vs. matrigel showed that OVE4 cells were able to differentiate to form luminal structures in matrigel, but they had weak capacity to form spheres when grown in suspension in stem cell media (scale bars = 400 µm). In contrast, OVE14A and OVE16 cells had better capacity for sphere formation and reduced ability to develop into luminal structures. B) Knockdown of PAX2 disrupted the formation of luminal structures by OVE4 cells, and (C) significantly decreased the percentage of cells able to form luminal structures. Scale bars = 100 µm. The results were compared by t-test analysis of data obtained from three independent experiments.

Chapter 5: Results (Part III)

PAX2 induces vasculogenic mimicry in OSE cells and ovarian cancer

5.1 PAX2 induces vascular channels *in vitro* in MOSE cells

PAX2 plays important role during embryogenesis, particularly in the formation of the kidney and Mullerian duct. In the kidney, PAX2 is involved in the branching and formation of tubular structures that will develop into nephrons (Narlis et al., 2007). Likewise, morphogenesis of the Mullerian duct requires invagination of epithelial cells and elongation of the structure to form the oviduct (Stewart et al., 2012). The role of PAX2 in Mullerian duct morphogenesis is poorly studied, but the results of the previous chapter suggest that PAX2 may play a critical role in epithelial cell differentiation and organization into luminal structures.

Since knockdown of PAX2 impaired the ability of OVE to form luminal structures, we explored the possibility that forced expression of PAX2 in OSE cells might allow them to gain this capacity. M1102-PAX2 cells were plated in 3D culture of a matrigel and Human Umbilical Vein Endothelial Cells (HUVEC) cells were used as a positive control. We found that M1102–PAX2 cells formed highly branched and elongated tubular channels that mimic the vascular channels formed by HUVEC cells (Figure 5-1A). This ability to form patterned vascular channels has been reported previously for aggressive cancerous cells and has been termed vasculogenic mimicry (VM) (Maniotis et al., 1999). Interestingly, we found that the formation of tubular channels is highly dependent on cell density. The higher number of cells plated formed very organized

branched vascular channels within 48 hours (Figure 5-1A). However, the parental cells and control M1102 cells did not form these tubular channels and deletion of *Pax2* by adding AdCre to the cells decreased their ability to form these channels (Figure 5-1B).

To better understand if PAX2 induces cell differentiation into endothelial cells or if PAX2 induces vasculogenic mimicry, the tubular channels were stained with Periodic acid–Schiff stain (PAS) to label the remodeling extracellular matrix formed by the M1102-PAX2 cells. The glycogen in the extracellular matrix first reacts with the periodic acid stain, which labels the tissue with dark purple color. Then, the oxidized glycogens (aldehydes) are detected by the Schiff stain which results in pink color in the tissue. We found that the vascular channels formed by M1102-PAX2 cells are PAS positive, which indicates the existence of extracellular matrix supporting the channels, whereas spheres formed by control M1102 cells are PAS negative (Figure 5-2A). However, the vascular channels formed by M1102-PAX2 cells are CD31 negative, which means that PAX2 does not appear to induce MOSE cells to differentiate into endothelial cells, but can induce MOSE cells to form a pattern of vascular-like channels.

SKOV3 cells were used as a positive control for VM since it has been reported that they are able to form VM in 3D culture (Millimaggi et al., 2009). Interestingly, we found that, although SKOV3 cells readily formed vascular-like channels, a few of the cells within those channels expressed CD31 (Figure 5-2B). This supports previous observations of the ability of some ovarian cancer cells to differentiate into endothelial cells as reported previously (Su et al., 2008).

Overexpression of PAX2 alone is not able to induce OSE cell transformation into

cancer (Al-Hujaily et al., 2015), but the ability of PAX2 to promote VM suggests that tumors expressing PAX2 might be more aggressive through their development of VM in tumors, thereby augmenting tumor blood supply without angiogenesis. We therefore analyzed the ability of PAX2 to promote VM in a mouse ovarian cancer cell line, RM. RM cells were generated by expression of activated K-RAS and C-Myc in MOSE cells and they formed aggressive tumors when injected into mice. Overexpression of PAX2 in RM (RM-PAX2) cells resulted in even more aggressive tumors, where mice reached an average endpoint of 11 days compared to 16 days for RM cells that do not express PAX2 (Al-Hujaily et al., 2015). To determine whether PAX2 might contribute to tumor progression by inducing VM, we assessed the ability of RM-PAX2 cells to form tubular channels in matrigel and compared them to their control cells (RM, RM-WPI, RM-PAX2-AdCre). The control, PAX2-non-expressing RM cells were all inefficiently able to form vascular channels in matrigel; however, the forced expression of PAX2 in these cells significantly enhanced the formation of vascular channels compared to the controls (Figure 5-3).

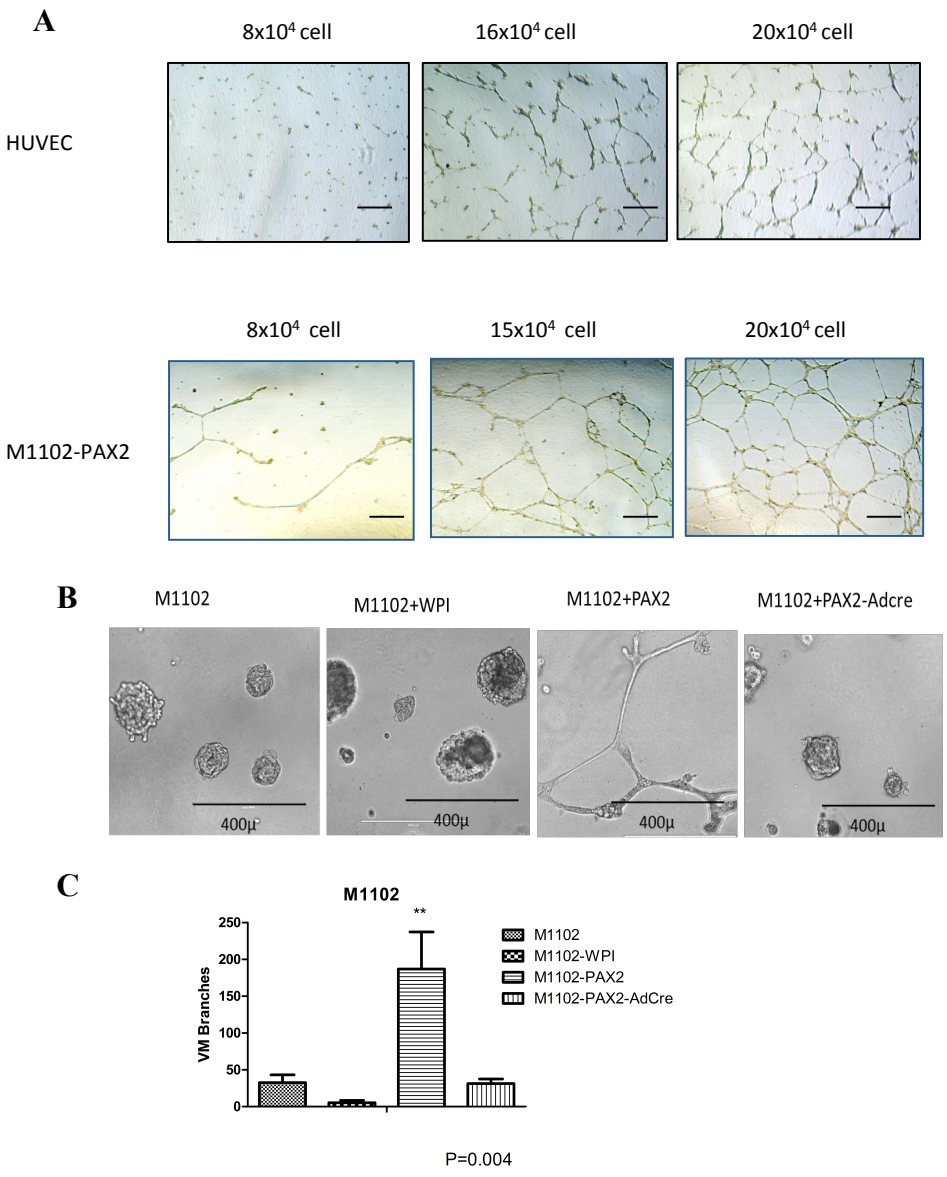

Figure 5-1: PAX2 induced the formation of vascular-like channels in 3D culture.
A) The vascular channels formed by HUVEC endothelial cells and by M1102-PAX2 cells were highly dependent on cell density after 48 hours of incubation. B) M1102-PAX2 cells generated vascular channels, where M1102 cells without PAX2 expression developed only cell aggregations. C) Quantitative analysis of the vascular channel branches shows a significant increase in M1102-PAX2 cells compared to the control groups. Analysis was done using one way ANOVA for three independent experiments, **p<0.01

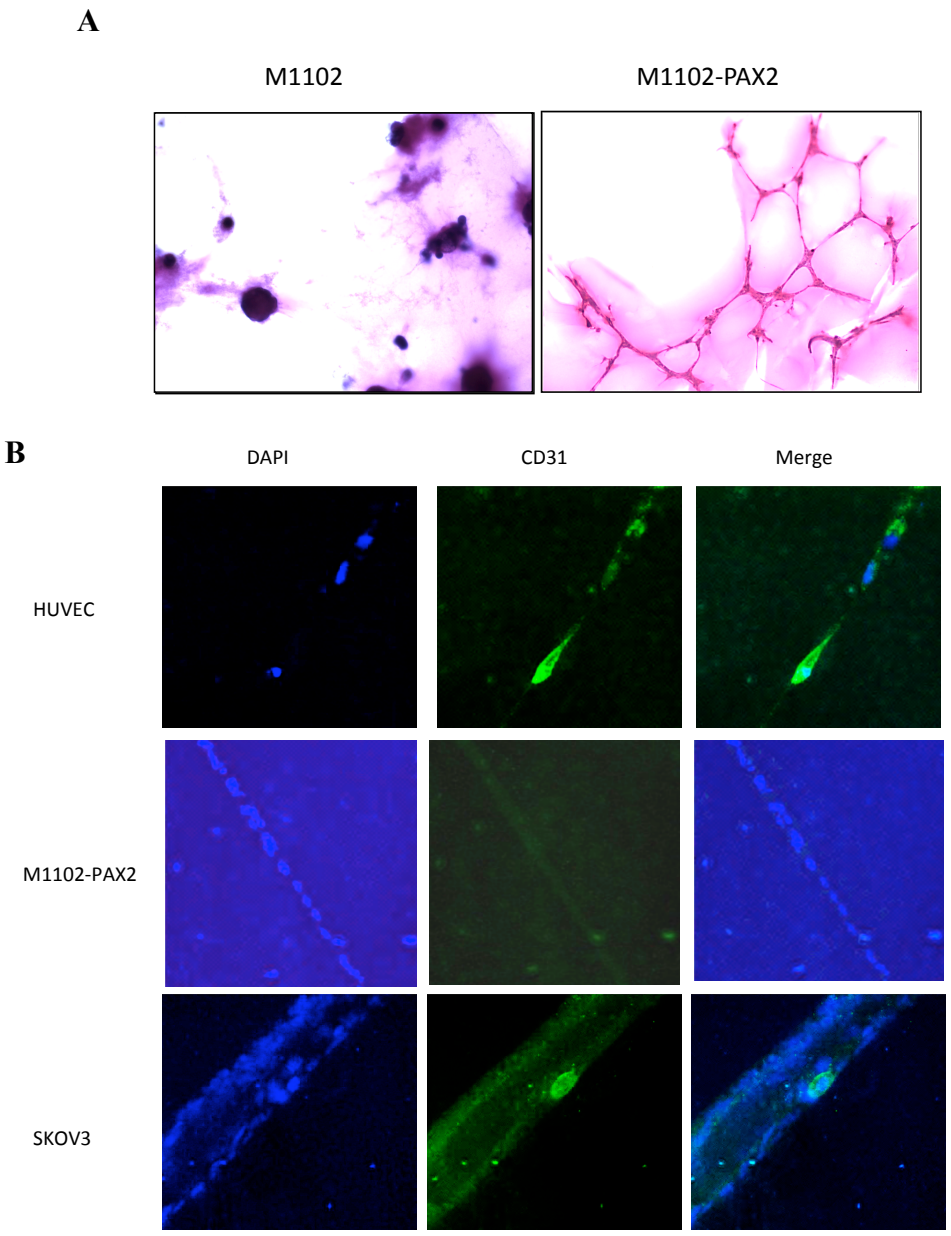

Figure 5-2: M1102-PAX2 cells formed vascular-like channels.
A) PAS staining for the vascular channels formed by M1102-PAX2 cells shows pink positive staining compared to the control cells that do not express PAX2. B) Immunofluorescence staining for CD31 in the vascular channels formed by HUVEC endothelial cells, M1102–PAX2 cells, and the ovarian cancer cell line SKOV3. M1102-PAX2 vascular channels were negative for CD31 compared to HUVEC as a positive control. A few cells expressing CD31 were identified in the vascular channels formed by SKOV3 cells.

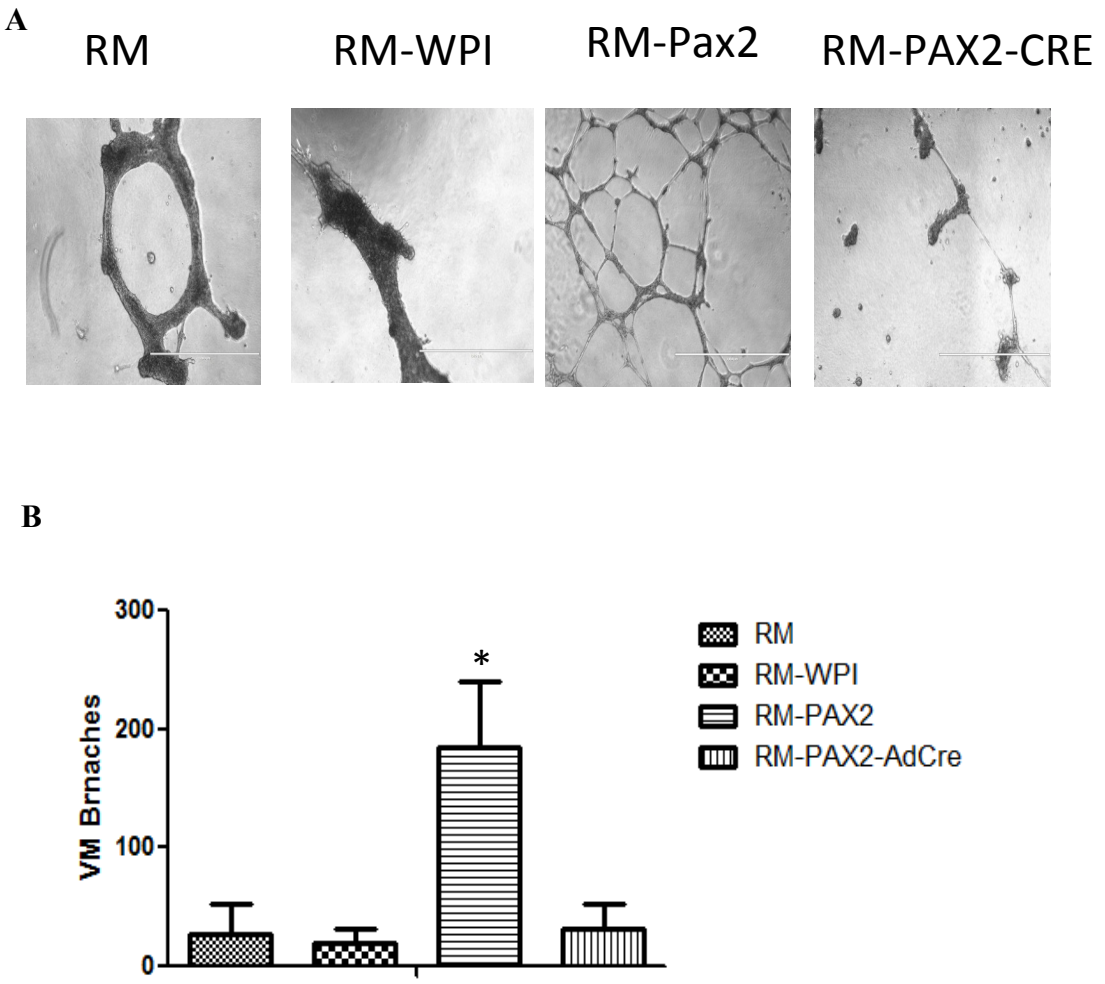

Figure 5-3: PAX2 induced vascular-like channel formation in RM cells in 3D culture.

A) RM-PAX2 cells differentiated in matrigel to form vascular-like channels, whereas none of the control cells were able to form organized web-like tubular channels. B) Quantitative analysis of the number of vascular channel branches formed by RM-PAX2 cells shows that they are significantly more abundant than the control groups. Analysis was done using one way ANOVA for three independent experiments, *$p<0.05$.

5.2 PAX2 enhances vascular channel formation *in vivo* in a tumor formed by an ovarian cancer cell line

To further understand the role of PAX2 in inducing tumor progression in ovarian cancer, RM (transformed mouse OSE cells) with vector control (RM-WPI) cells and RM cells with forced expression of PAX2 (RM-PAX2) were injected into the peritoneal cavity of immune-compromised mice. Both RM-WPI and RM-PAX2 cells were able to develop tumors in the injected mice. The tumors were isolated from the mice, fixed and paraffin-embedded for immunohistochemical analysis. The tumor sections were stained for PAS to identify all vascular channels in the tumors whether formed by endothelial cells or by cancer cells. We found that RM-PAX2 tumors have numerous small PAS positive vascular channels, whereas RM-WPI tumors lacked small vascular channels and PAS stain labeled primarily the large vascular channels. In addition, CD31 staining was performed in the same tumors and RM-PAX2 tumors were found to have a high density of CD31-labeled vessels compared to RM-WPI tumors, suggesting that PAX2 enhances angiogenesis in these ovarian cancers (Figure 5-4).

To investigate if PAX2 induces vasculogenic mimicry (VM) in ovarian tumors, we performed double staining for PAS and CD31 on the same sections. RM-PAX2 tumors had both of types of vascular channels, those formed by endothelial cells which present as PAS-positive and CD31-positive, and small vascular channels that were not formed by endothelial cells, which were PAS-positive and CD31-negative (Figure 5-5). Since VM has been identified as PAS-positive/CD31-negative staining (Folberg et al, 2000), these results indicate that PAX2 may enhance tumor progression by inducing VM.

To confirm whether the cancer cells expressing PAX2 are the cells forming the vascular channels, we stained for PAX2 in the tumors developed by RM-WPI and RM-PAX2 cells. Tumors arising from RM-PAX2 cells had vascular channels lined with cells expressing PAX2. However, RM-WPI tumors were negative for PAX2, as expected (Figure 5-6). These observations imply that cancer cells expressing PAX2 can contribute to vascular channel formation in ovarian cancer.

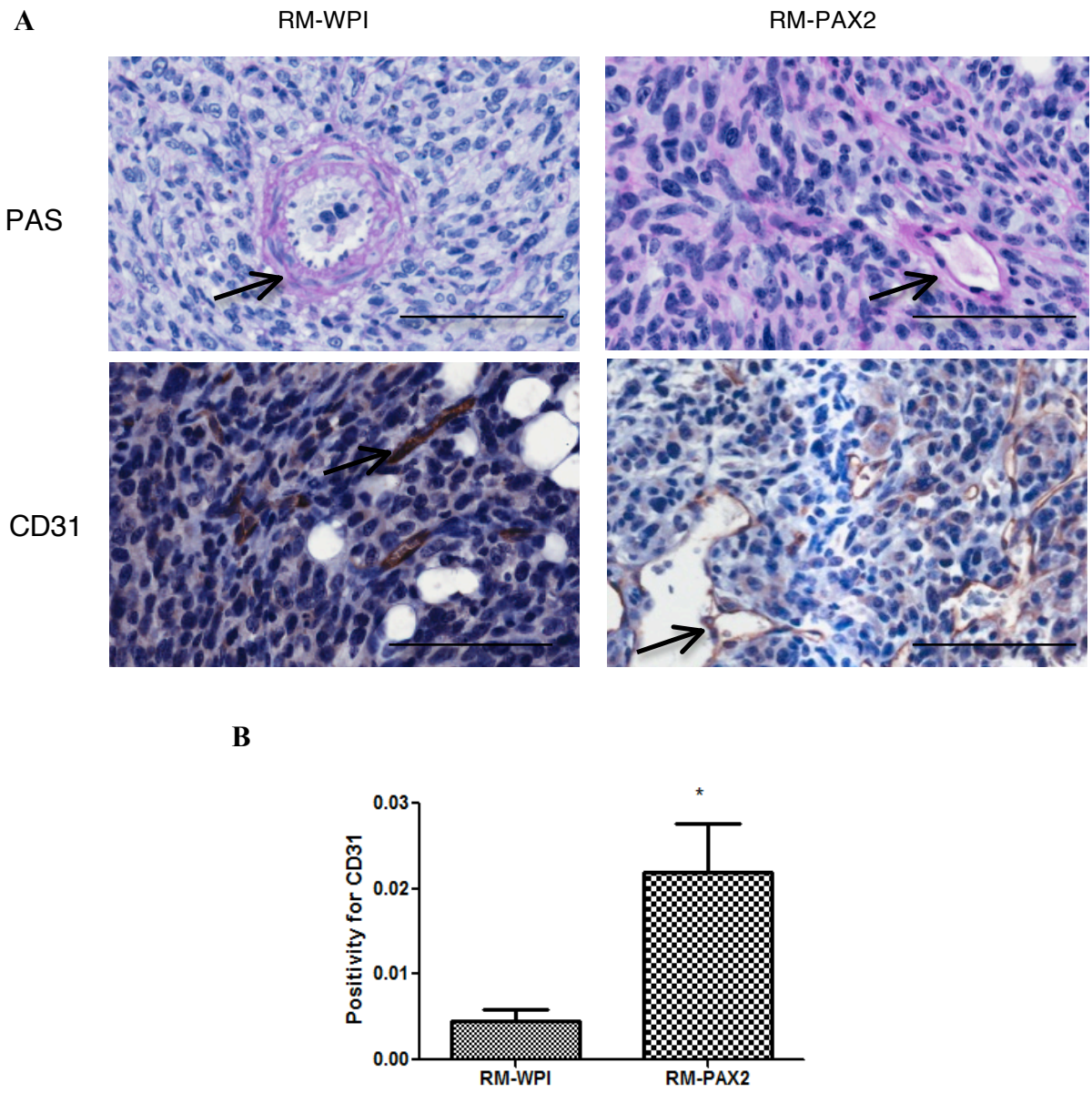

Figure 5-4: Immunohistochemistry for CD31 and PAS staining of tumors formed by RM cells and RM cells with forced expression of PAX2.
A) The upper panel of tumors derived from RM-WPI and RM-PAX2 cells shows vascular channels positive for PAS staining. The lower panel shows CD31 staining in numerous vascular channels in a RM-PAX2 tumor, indicating that PAX2 enhances angiogenesis. B) Quantification of immunohistochemical detection of CD31 shows increased CD31 positivity in RM-PAX2 compared to RM-WPI tumors. The scale bar is 100µm. Analysis was done using t-test analysis for three different fields of three different sections of the same tumor (*$p<0.05$).

Bright field image Analyzed image

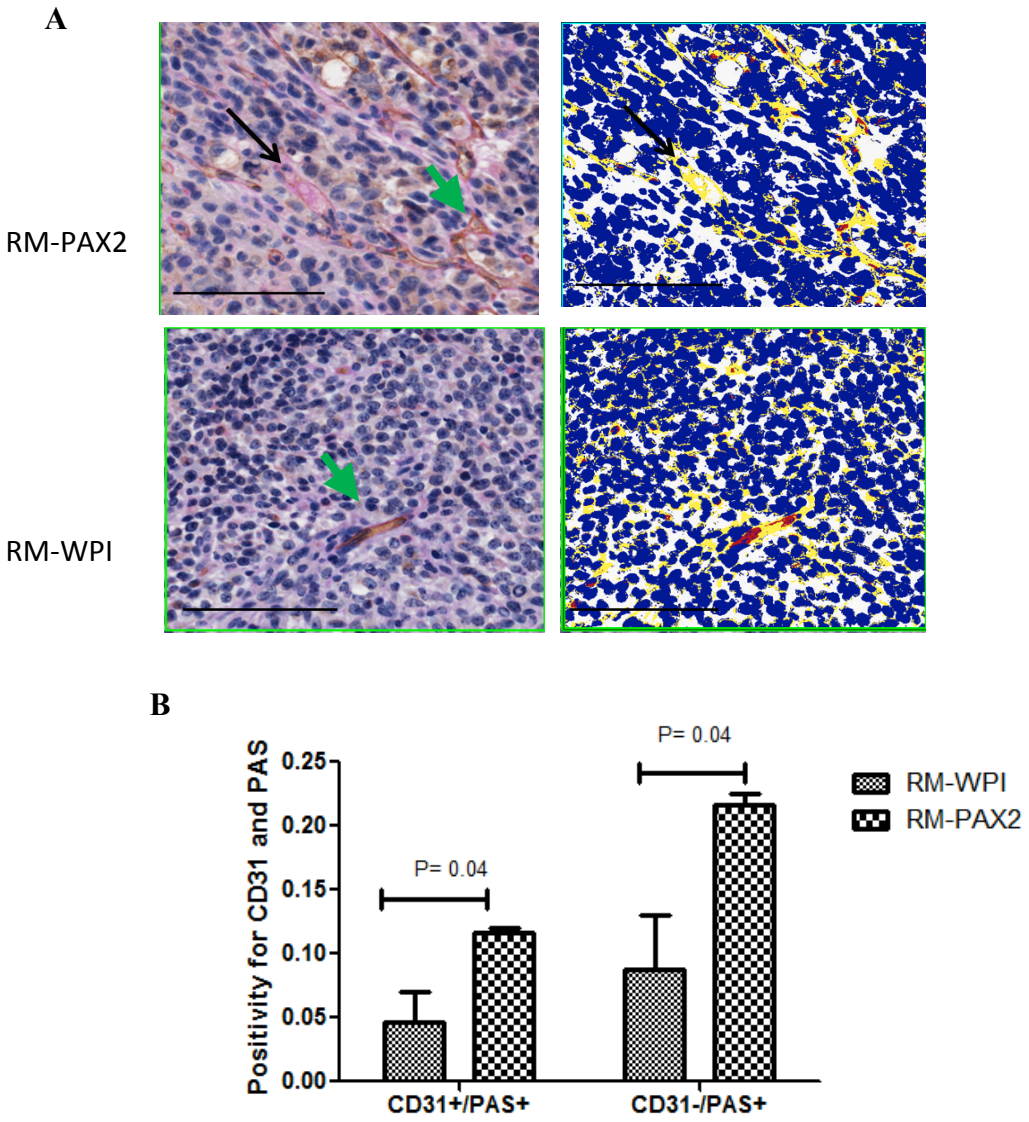

Figure 5-5: Double staining for PAS and CD31 in RM-PAX2 and RM-WPI tumors. Double staining for CD31 and PAS shows vascular channels that are PAS+/CD31+ (green arrow) in both RM-PAX2 and RM-WPI tumors, and PAS+/CD31- vascular channels (black arrow) in RM-PAX2 tumors, indicating the existence of VM in RM-PAX2 tumors. The scale bar is 100µm. B) Quantification of immunohistochemistry shows increased positivity for CD31+/PAS+ (red color) and CD31-/PAS+ (yellow color) in RM-PAX2 tumors compared to RM-WPI tumors. Analysis was done using t-test analysis for three different fields on three sections of the same tumor.

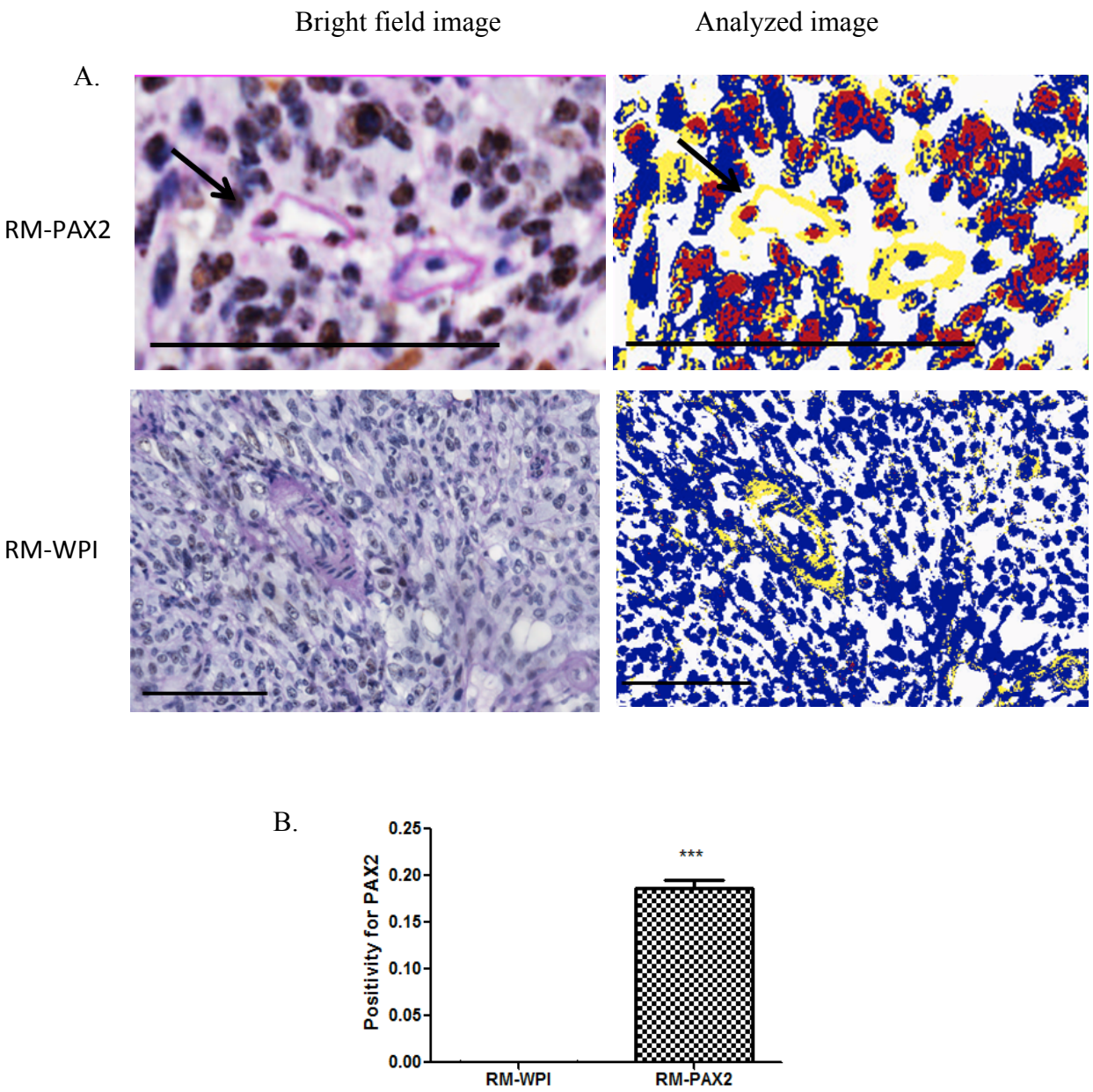

Figure 5-6: PAX2 is expressed in cells that line the vascular channels.
A) Double staining for PAS and PAX2 in RM-PAX2 and RM-WPI tumors shows, on the left, PAS-positive (pink) vascular channels with some cells lining the channels in RM-PAX2 tumors being positive for PAX2 (brown; arrow). The pictures on the right are the measurements of staining intensity; red color is PAX2 and yellow color is PAS. The scale bar is 100µm. B) Quantification of immunohistochemical detection of PAX2 shows increased PAX2 positivity in RM-PAX2 tumors compared to RM-WPI tumors. Analysis was done using t-test analysis for three different fields of three sections from the same tumor (***$p<0.001$).

Chapter 6: Results (Part IV)

Consequences of loss of *Trp53* alone or in combination with *Brca1* in oviductal epithelial cells

6.1 Isolation and characterization of OVE cells from mice with conditional expression of *Trp53* and/or *Brca1*

Early lesions in the fallopian tube that are thought to lead to HGSC are commonly detected in women with *BRCA1* mutation, and those lesions often acquire mutations in *TP53* (Lee et al., 2007). The *TP53* mutation is often associated with loss of PAX2 expression in STICs (Chen et al., 2010). To determine the effect of *Trp53* and *Brca1* mutations on OVE cell behavior and gene expression, clones of OVE cells were established from transgenic mice having flanked *loxP* sites located in the *Trp53* or/and *Brca1* genes. The *loxP* sites in the *Trp53* gene are located between exons 1 and 10, and the *loxP* sites in the *Brca1* gene are located between exons 4 and 13. In both cases, Cre-mediated deletion should result in excision of the DNA segments flanked by the *loxP* sites. After a few passages, the morphology of the clonal cells was assessed and each clone was found to have different morphologies (Figure 6-1A).

To characterize the new OVE clonal cells, the expression of several genes encoding epithelial and OVE markers as well as the tumor suppressor genes *Trp53* and *Brca1* were determined (Figure 6-1B). All clonal cells express mRNA encoding for the epithelial markers *Krt19* and *Cdh1*. However, the floxed *Brca1* clone 2 cells (BRCA1-C2-flox) cells have very high levels of expression of mRNA encoding *Krt19* and *Cdh1,* which reflects their more epithelial morphology compared to the other OVE clonal cells. In addition, the BRCA1-C2-flox cells have very high expression of the marker of ciliated

cells FOXJ and low levels of OVGP, a marker of secretory cells. Accordingly, the gene expression and epithelial morphology of these cells suggests that they are ciliated cells.

In contrast, the secretory cell marker OVGP was highly expressed in P53-flox and P53/BRCA1-flox cells, which also have lower levels of expression of the ciliated cell marker FOXJ, the latter of which may contribute to the more mesenchymal morphology. In addition, we investigated the expression of the transcription factors *Pax8* and *Pax2*, which is commonly found in OVE cells *in vivo*. *Pax8* mRNA was evenly expressed among all the OVE clonal cells, but the expression of PAX2 was much more varied. The mRNA encoding for *Pax2* was highly expressed in the floxed *Brca1* clone 1 (BRCA1-C1-flox), whereas BRCA1-C2-flox cells have lower levels of expression. P53-flox clonal cells had barely detectable expression of *Pax2* mRNA, whereas P53/BRCA1-flox cells expressed no detectable *Pax2*. Assessment of the expression of *Trp53* and *Brca1* mRNA confirmed detectable levels in all OVE clonal cells.

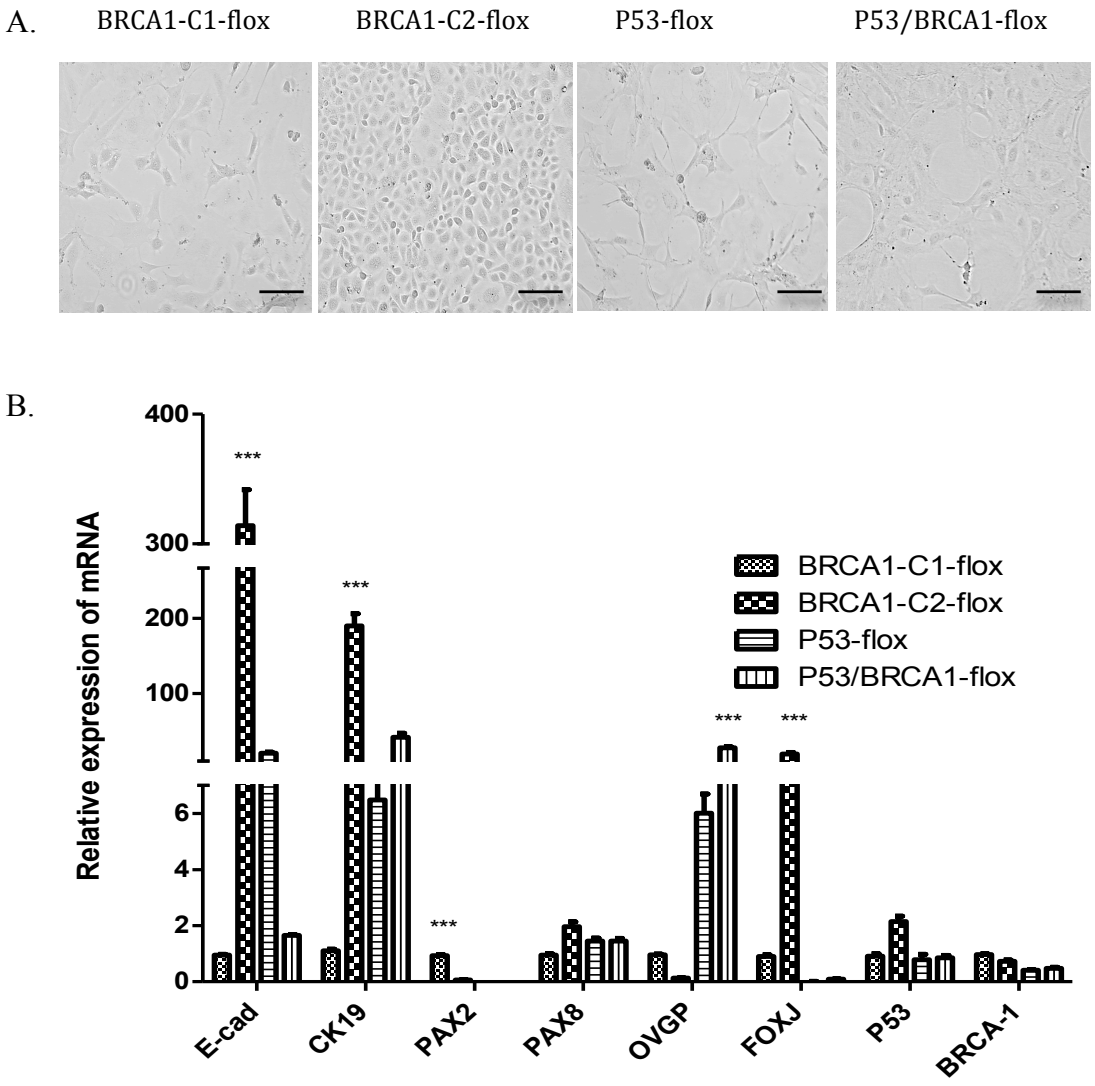

Figure 6-1: OVE clonal cells have different cell morphology and gene expression.
A) Microphotographs of OVE clonal cells showing the epithelial morphology of BRCA1-C2-flox cells and more mesenchymal morphology of the other three cell lines. Scale bar 100μm. B) qPCR analysis shows variable gene expression for epithelial markers, OVE markers and tumor suppressor genes among the four cell lines. In line with their morphology BRCA1-C2-flox clonal cells express higher levels of transcripts for epithelial markers and markers of ciliated cells, relative to the other cell lines. P53-flox and P53/BRCA1-flox cells express lower levels of mRNA for epithelial markers and higher levels of the secretory marker, OVGP. PAX8 mRNA is equally expressed in all OVE clonal cells, whereas PAX2 is expressed only in the BRCA1-C1-flox cells. Analyses were performed using multiple t-test analysis for three independent experiments (***$p<0.001$).

6.2 Conditional inactivation of *Trp53, Brca1* and *Trp53/Brca1*

To determine the effect of loss of *Trp53* and *Brca1* on OVE cells, we treated OVE clonal cells with AdCre to inactivate *Trp53* and/or *Brca1*. The control cells were treated with AdGFP. PCR was used to confirm DNA recombination at the loxP sites and showed that in *Trp53*, exons 1 to 10 were deleted efficiently. However, recombination of the *Brca1* gene at exons 4 to13 was less efficient, retaining detectable unrecombined populations of BRCA1-C1-flox, BRCA1-C2-flox and P53/BRCA1-flox cells, even after treatment with AdCre (Figure 6-2A).

To confirm that the cells had both *loxP* sites flanking exons 4 to 13 of *Brca1*, the gene was sequenced and identified to have *loxP* sites in the right locations. For further confirmation, quantitative qPCR and western blots were performed to determine the levels of *Brca1* mRNA and protein. For qPCR, primers for exons 11-12 of the *Brca1* gene were used, which should be deleted after AdCre treatment. mRNA encoded by these exons was significantly down-regulated after AdCre treatment in BRCA1-C2 clonal cells and modestly decreased in P53/BRCA1 clonal cells (Figure 6-2B). Western blots showed that OVE cells treated with AdCre have decreased BRCA1 expression in both BRCA1-C2 and in P53/BRCA1 cells (Figure 6-2C). However, in BRCA1-C1-AdCre cells, recombination was detected in genomic DNA, but the decrease in abundance of *Brca1* transcripts did not reach significance. Therefore, BRCA1-C1 cells were excluded from further studies. Since the BRCA1 gene did not show complete inactivation in all OVE cells, we proceeded with further experiments knowing that *Brca1* is inactivated in only a subpopulation of the BRCA1-C2 and P53/BRCA1 clonal cells under study.

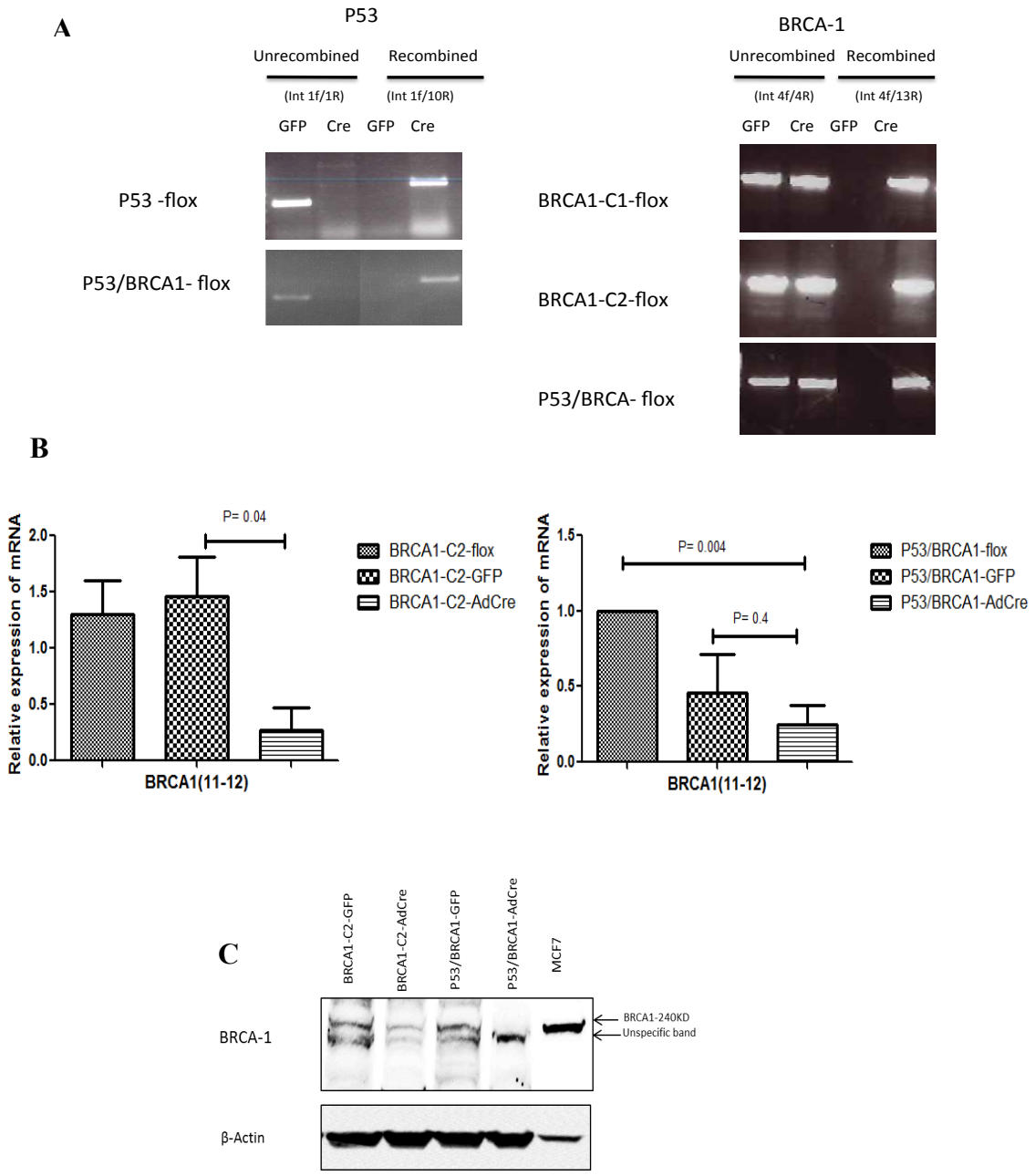

Figure 6-2: Conditional inactivation of *Trp53* and *Brca1* in OVE cells.
A) Gel electrophoresis shows the recombination of both *Trp53* and *Brca1* DNA after exposure to AdCre. B) qPCR analysis for *Brca1* mRNA shows a significant decrease in BRCA1-C2-AdCre (left panel) and modestly in P53/BRCA1-AdCre (right panel). Analyses were done using one-way ANOVA for three independent experiments. C) Protein analysis shows the decreased expression of BRCA1 protein in BRCA1-C2-AdCre and P53/BRCA1-AdCre.

6.3 Analysis of OVE cells after loss of *Brca1* or/and *Trp53*

To assess the consequences of *Trp53* and *Brca1* inactivation in OVE cells, cell morphology was investigated after AdCre treatment and compared with the cells treated with AdGFP. *Brca1* inactivation alone significantly changed cell morphology to become more mesenchymal compared to the control cells (Figure 6-3). In contrast, OVE cells with combined mutation of *Trp53* and *Brca1,* or with *Trp53* mutation alone did not show any changes in cell morphology, perhaps because these cells already had a more mesenchymal phenotype.

To determine if inactivation of *Brca1* and *Trp53* is associated with any other changes in cell behavior, cell proliferation for the three cell lines with *Brca1* or *Trp53* mutation alone or in combination was analyzed. Proliferation of OVE cells with reduced BRCA1 did not change compared to their control. However, *Trp53* inactivation in OVE cells, with or without loss of *Brca1*, significantly increased cell proliferation within four days (Figure 6-4A). Likewise, colonies were formed in soft agar when *Trp53* was inactivated in OVE cells, whereas the single inactivation of *Brca1* did not alter the cell capability to form colonies in soft agar. Mutations in both *Trp53* and *Brca1* enabled the cells to form large colonies (Figure 6-4B&C). Thus, these data indicate that loss of P53 alone or in combination with loss of *Brca1* increases cell proliferation and colony formation, whereas loss of *Brca1* alone changes only cell morphology.

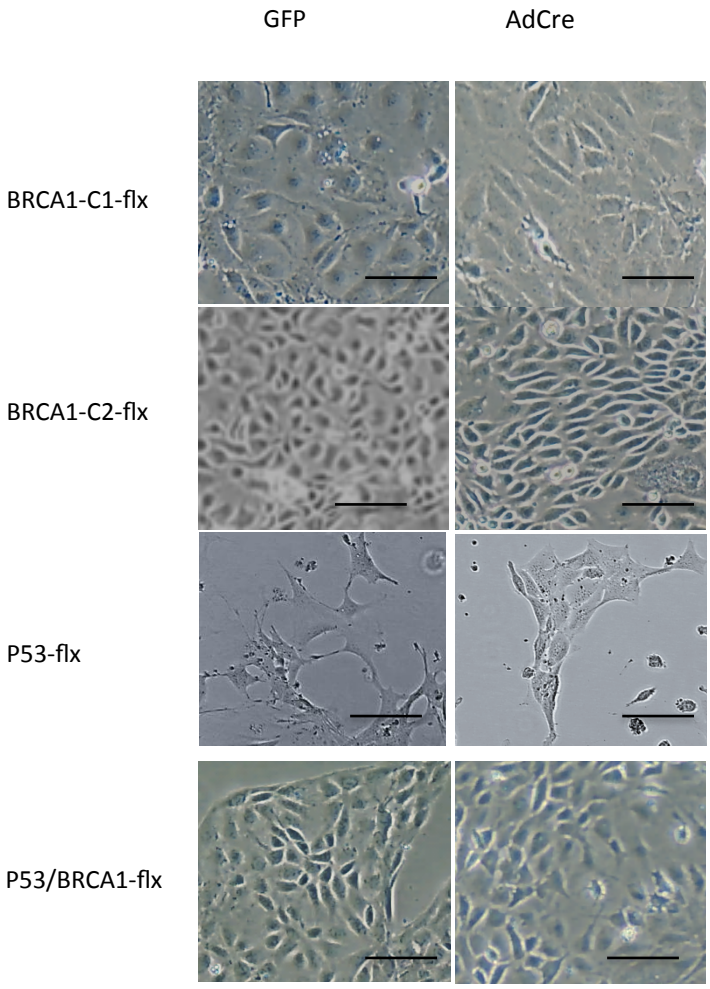

Figure 6-3: Microphotograph of OVE clonal cells with conditional inactivation of *Trp53* and/or *Brca1* shows differences in cell morphology with loss of *Brca1*. Scale bar is 100μm.

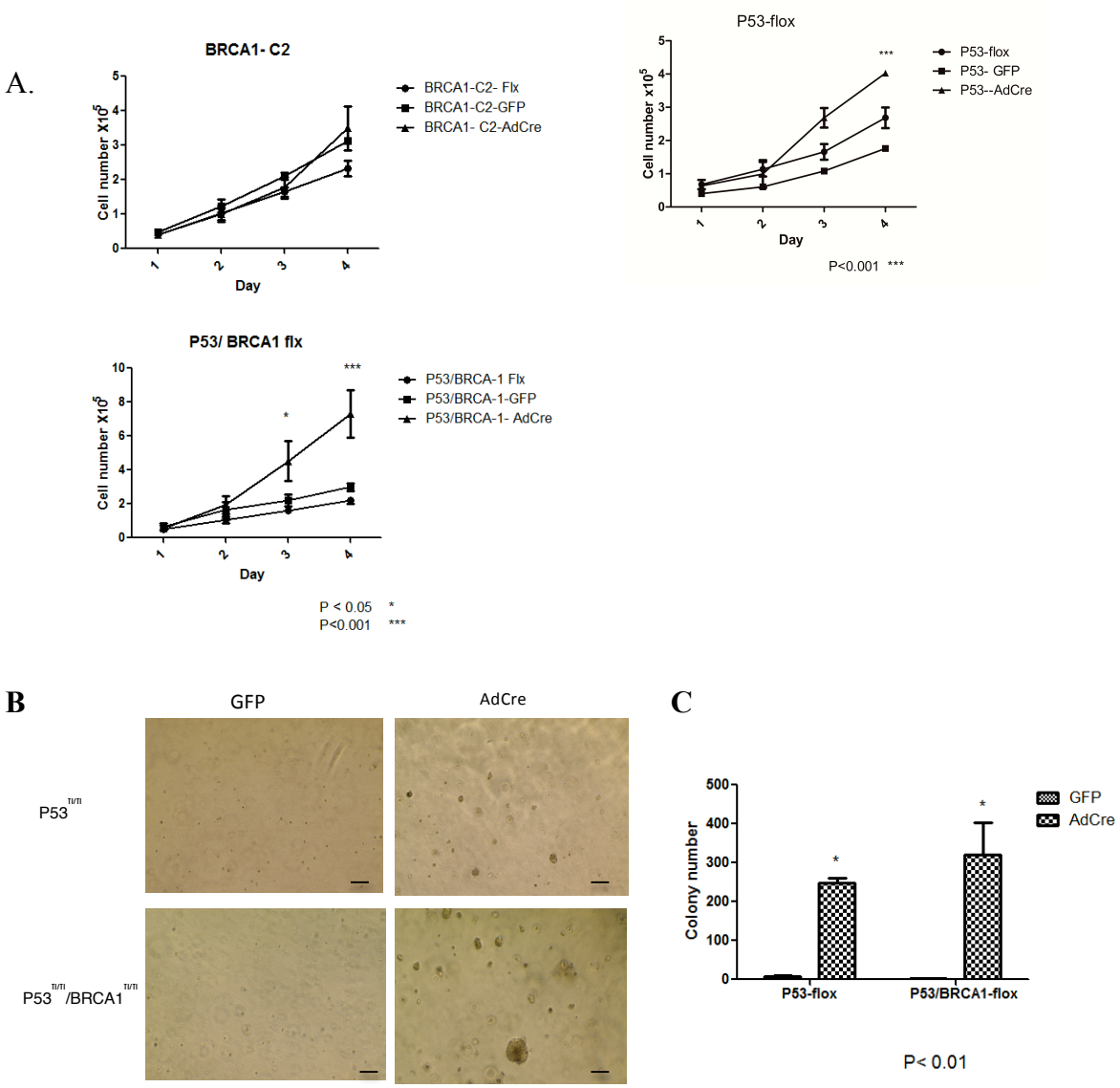

Figure 6-4: Loss of *Trp53* alone or in combination with *Brca1* increases cell proliferation and colony formation.

A) Proliferation assays show significant increases in the rate of cell proliferation after *Trp53* knockout with and without *Brca1* inactivation, but not with *Brca1* inactivation alone. Analyses were done using one-way ANOVA for three independent experiments. B) Microphotographs show the capacity for colony formation after *Trp53* knockout and after *Trp53* and *Brca1* knockout; scale bar is 100μm. C) Quantitative analysis of the number of colonies. Analysis was done using multiple t-test analysis for three independent experiments (*p<0.05, ***p<0.001).

6.4 Loss of *Trp53* alone or in combination with *Brca1* induced OVE cells to undergo an epithelial-mesenchymal transition.

BRCA1-C2-flox cells have an epithelial morphology and high expression of the epithelial markers E-cadherin and CK19 (Figure 6-1). Inactivation of *Brca1* with AdCre treatment did not change the abundance of transcripts encoded by *Krt19* and *Cdh1*. Although loss of *Brca1* changed the cell morphology to become more mesenchymal, the mRNA expression for the EMT marker, *Snail,* was not altered by loss of *Brca1*, suggesting that the reduction in BRCA1 was not sufficient to induce EMT in these OVE cells (Figure 6-6A). In contrast, *Trp53* knockout significantly down-regulated the mRNA encoding the epithelial markers CK19 and E-cadherin and up-regulated *Snail* transcripts (Figure 6-6B), indicating that loss of *Trp53* effectively induces EMT in OVE cells. Interestingly, the combined mutation of *Trp53* and *Brca1* decreased the epithelial markers but did not increase *Snail* transcripts (Figure 6-6C).

To determine if OVE cells gained another indicator of EMT, their migration ability was analyzed after inactivation of *Trp53* and/or *Brca1*. The migration of OVE cells was not affected by loss of BRCA1 alone; however, inactivation of *Trp53* alone or in combination with *Brca1* increased migration of OVE cells toward the gap (Figure 6-7). This enhanced migration was evident within 18 hours of creating the scratch-wound and was therefore not likely a result of increased cell proliferation since the slow doubling time of these cells does not reveal any differences in growth rates for at least 48 hours (Figure 6-4).

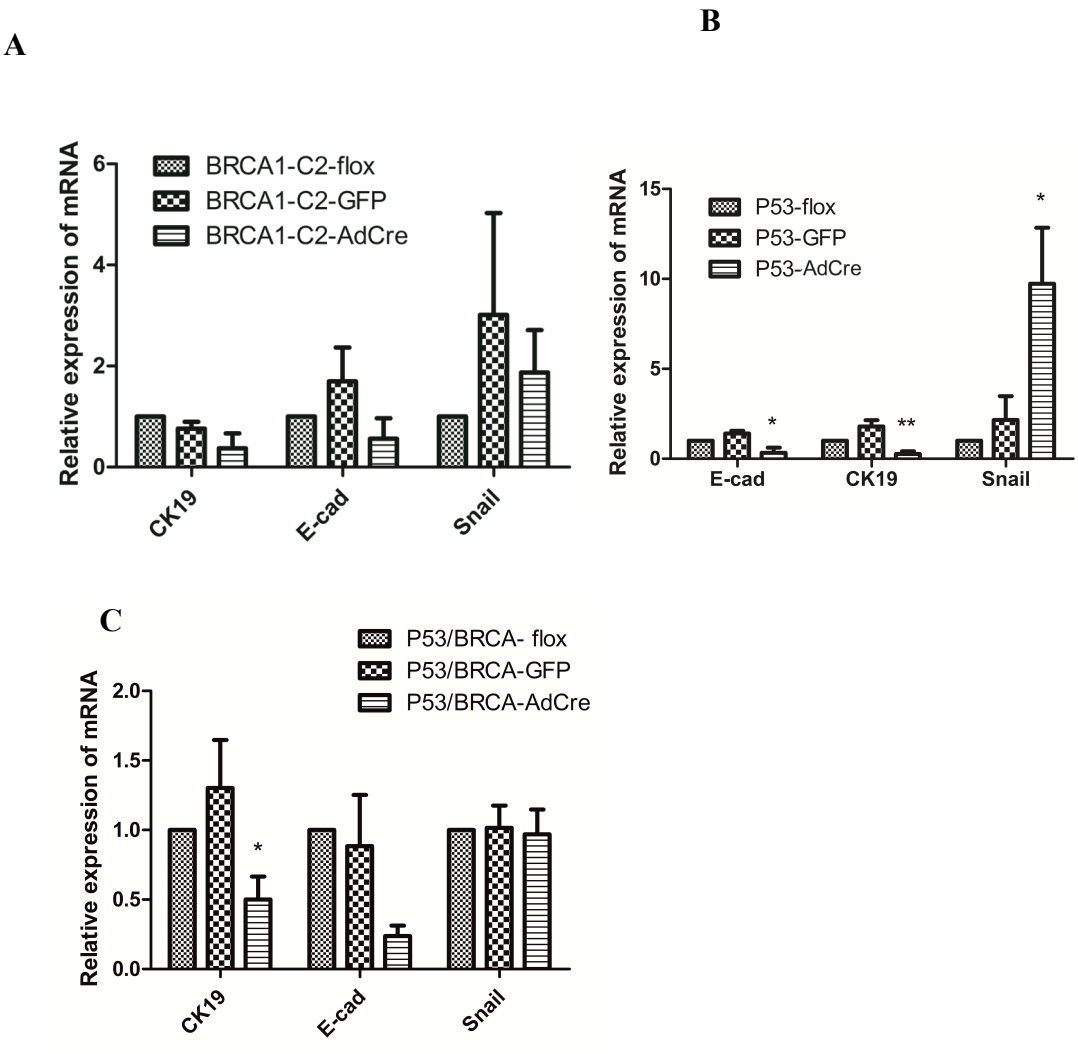

Figure 6-5: Loss of *Trp53* alone or in combination with loss of *Brca1* induced OVE cells to undergo an epithelial-mesenchymal transition.
A) qPCR analysis shows modest, but not significant, down-regulation in the transcripts for epithelial markers after inactivation of *Brca1*. B) Inactivation of *Trp53* decreased the mRNA for epithelial markers and increased the expression of the EMT marker, Snail. C) Combined inactivation of *Trp53* and *Brca1* decreased the abundance of transcripts for epithelial markers but had no effect on levels of *Snail* mRNA. Analyses were done using one-way ANOVA analysis for three independent experiments (*$p<0.05$).

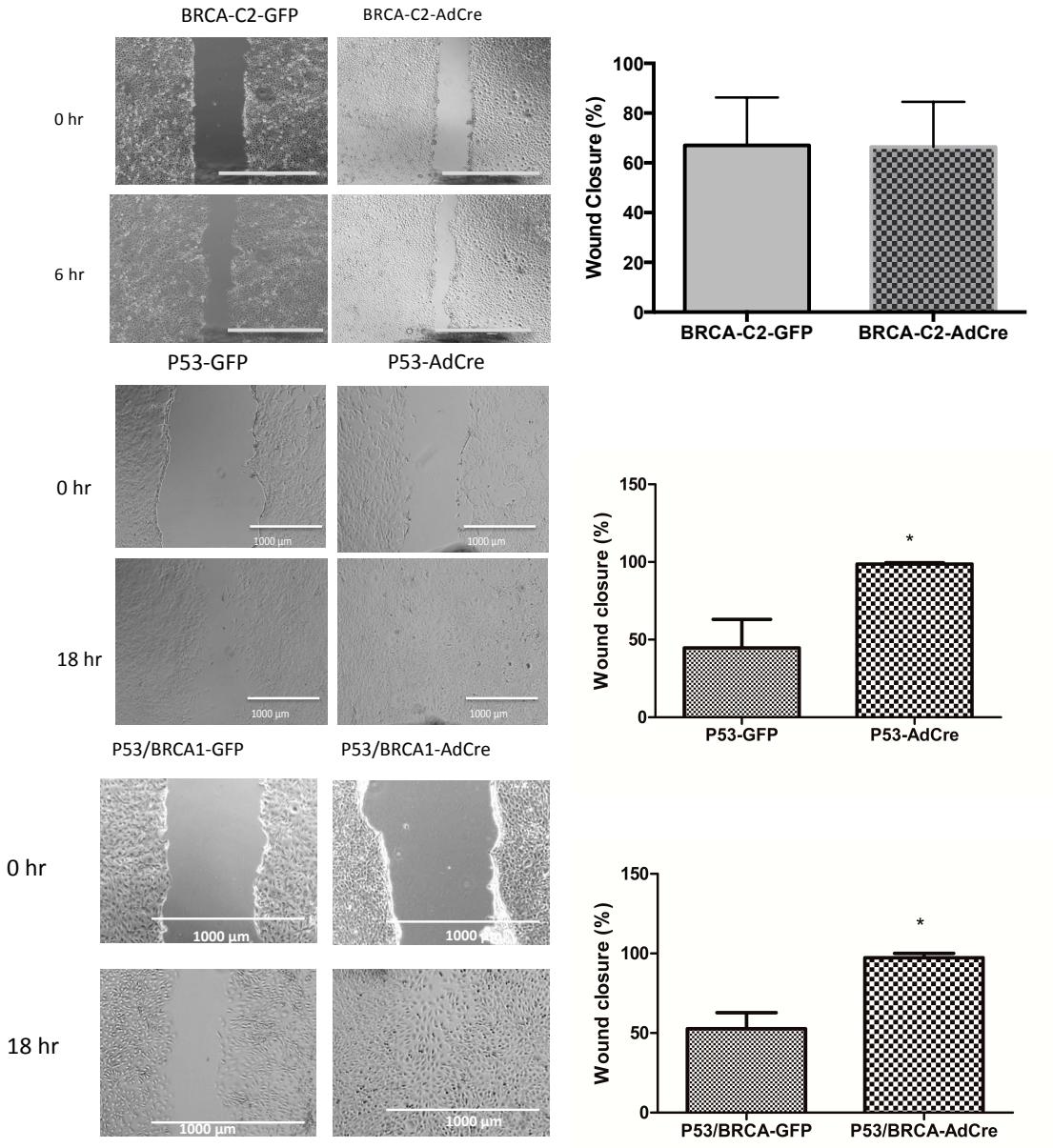

Figure 6-6: Migration assay of OVE cells after loss of *Trp53* and /or *Brca1*
Photomicrographs and analysis of wound healing shows enhanced cell migration with loss of P53, with and without concurrent loss of BRCA1. Scale bar is 1000µm. Results are representative of three independent replicates and the analyses were performed using t-tests (*$p<0.05$).

6.5 Loss of *Trp53* enhances sphere-forming capacity and expression of the stem cell markers CD44 and SCA-1

To investigate if inactivation of *Trp53* or/and *Brca1* and the associated shift to a more mesenchymal phenotype would also alter the stem/progenitor-like state of the OVE cells, sphere formation assays were performed and the sphere sizes were determined (Figure 6-7A). The more epithelial BRCA1-C2-flox clonal cells were not capable of forming spheres in suspension but they differentiated in matrigel and formed luminal structures (Figure 6-7B). Inactivation of *Brca1* did not induce sphere-forming capacity in these cells. OVE clones that are epithelial and express high levels of E-cadherin, CK19 and markers of ciliated cells (FoxJ) were less able to form spheres, whereas OVE clones that have a less epithelial morphology and express lower levels of E-cadherin and CK19 and higher levels of the secretory marker OVGP were more capable of forming spheres in suspension.

Assessment of stem cell marker expression revealed that BRCA1-C2-flox cells express very low levels of the stem cell genes *CD44*, *Sca-1* and *Aldh1* and inactivation of *Brca1* had no effect on their expression (Figure 6-8A). Surprisingly, the loss of *Brca1* up-regulated the expression of *Nanog*, which has been reported to be a stem cell marker, including in ovarian cancers (Lee et al., 2012). However, the ability to form spheres was not correlated with *Nanog* expression in OVE cells or MOSE cells in this study.

The P53-flox OVE cells formed spheres in suspension and *Trp53* knockout did not change the number of spheres; however loss of *Trp53* increased the size of the spheres, possibly indicating the enhanced ability of OVE stem cells to proliferate in suspension compared to the control cells (Figure 6-7A). To determine if loss of *Trp53* increased the

expression of stem cell genes, qPCR was performed. *Sca-1* mRNA levels were found to be significantly up-regulated after loss of *Trp53*, with no change in *CD44* and *Aldh1* transcripts (Figure 6-8B). Surprisingly, the combination of *Trp53* and *Brca1* mutations did not change the number of spheres or sphere size, indicating there was no promotion of stemness. To confirm that, stem cell markers were analyzed by qPCR and we found that only *CD44* mRNA is up-regulated with loss of *Trp53* and *Brca1,* whereas no change in other stem cell markers was evident (Figure 6-8C).

6.6 Loss of *Trp53* decreases PAX2 expression and enhances SCA-1 positive population associated with colony formation.

Since *Trp53* mutation was associated with induced colony formation and increased *Sca-1* mRNA expression, we investigated if SCA-1 positive populations are associated with the ability to form colonies. We analyzed the proportion of SCA-1 positive OVE cells with and without *Trp53* knockout and found that the fraction of SCA-1 positive cells was highly upregulated with *Trp53* mutation (Figure 6-9A). To determine if SCA-1 is associated with the ability to form colonies, positive and negative populations from OVE cells with and without *Trp53* mutation were plated in soft agar. SCA-1 positive cells sorted from OVE cells with *Trp53* knockout formed more colonies than the SCA-1 negative population (Figure 6-9B&C).

To determine if *Trp53* mutation might also have an effect on PAX2 expression, western blot assays were performed for PAX2 expression in cells with and without *Trp53* mutation. Although PAX2 expression was barely detectable in P53-flox clonal cells, the *Trp53* knockout significantly decreased PAX2 expression (Figure 6-9D).

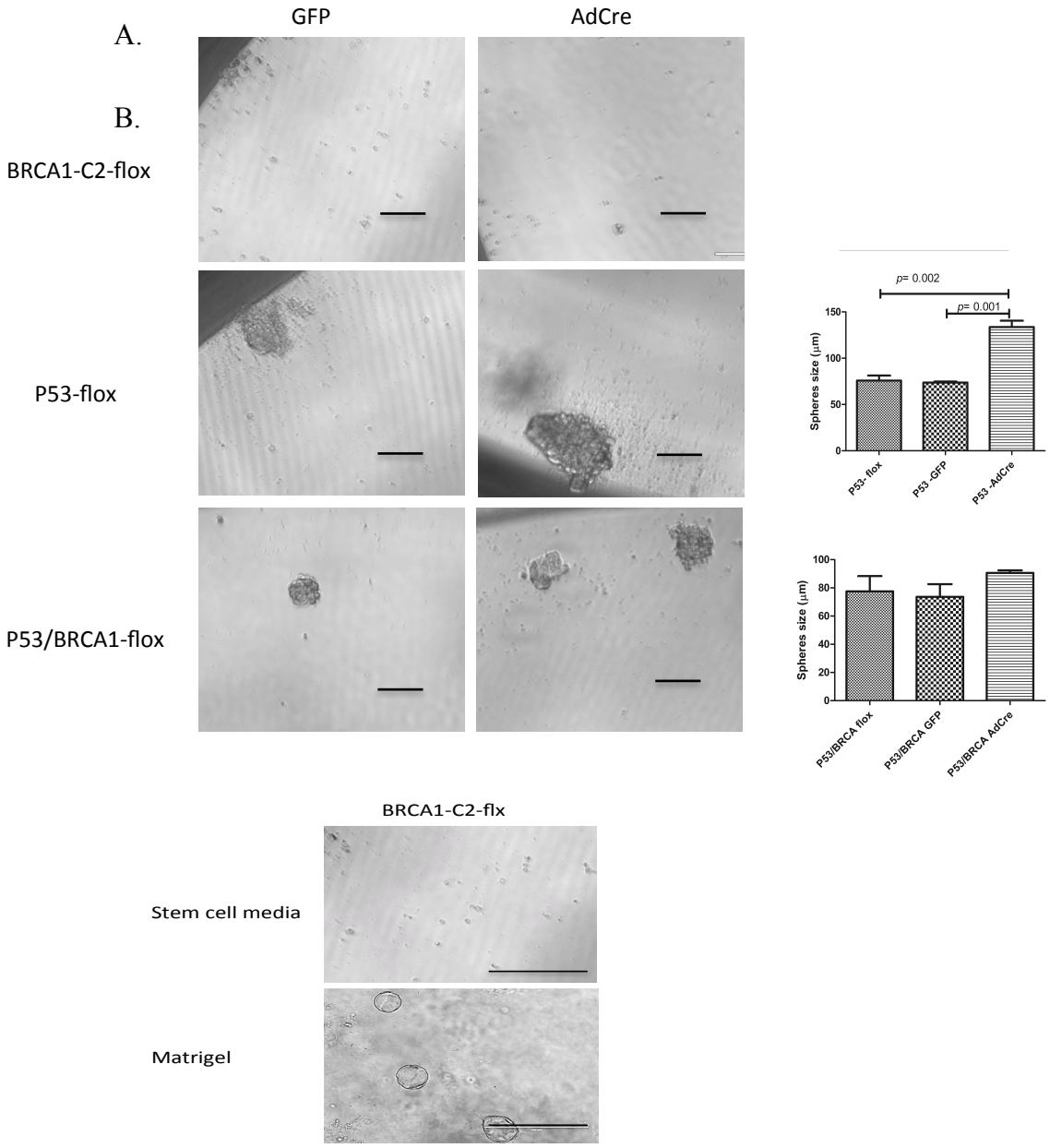

Figure 6-7: Sphere formation assays of OVE cells after inactivation of *Trp53* and/or *Brca1*.

A) Sphere formation assays in suspension culture for two weeks show that BRCA1-C2 clonal cells were not able to form spheres with or without BRCA1, whereas loss of P53 alone increased the size of the spheres. B) BRCA1-C2-flox cells were not able to form spheres in stem cell media but they differentiated and formed luminal structures in matrigel. The scale bar is 100µm. Analysis was done using one-way ANOVA (N=3).

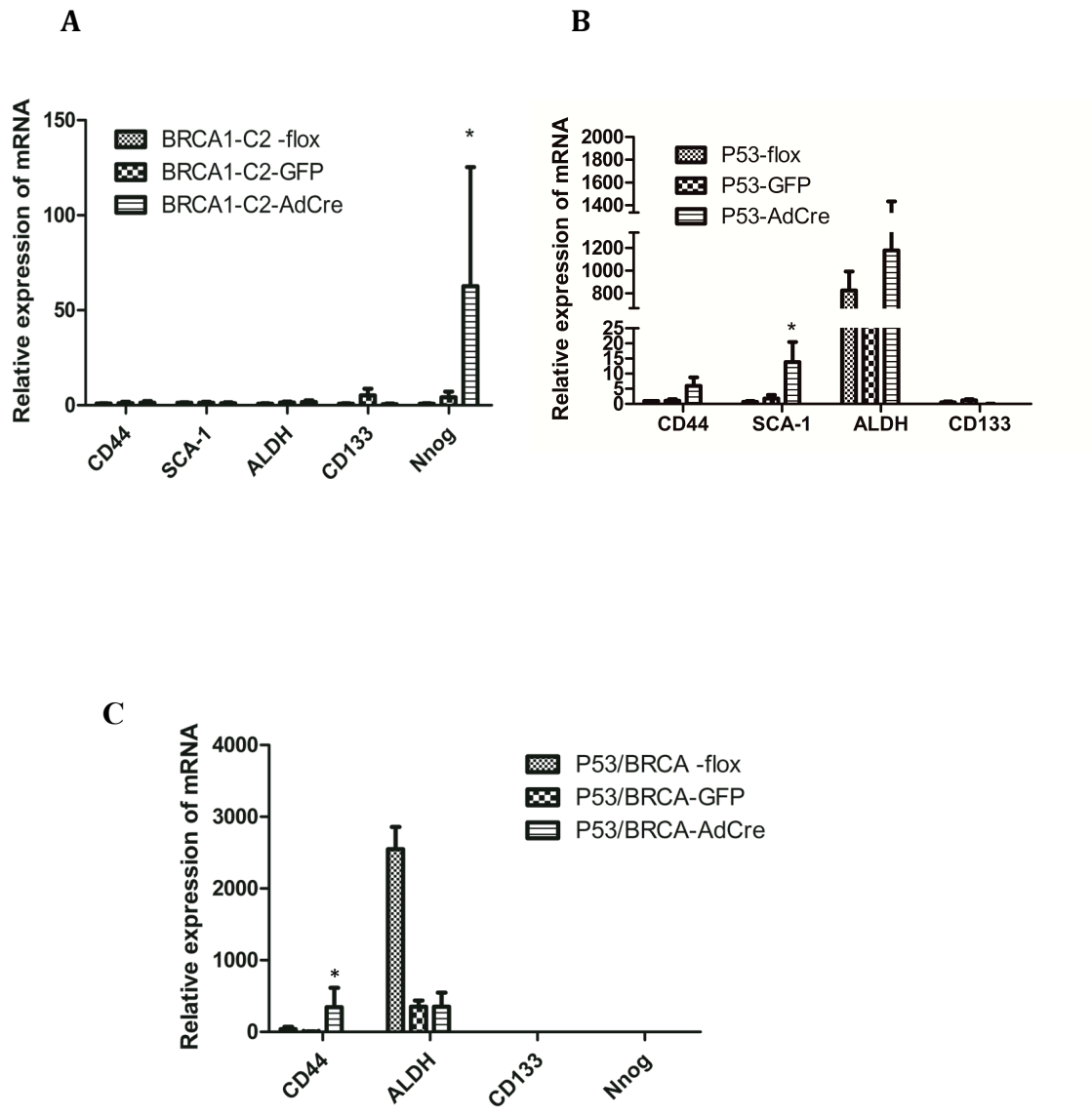

Figure 6-8: qPCR analysis of stem cell markers in OVE cells with inactivation of *Brca1*, *Trp53* and *Trp53/Brca1.*

A) Loss of BRCA1 did not change the expression of *CD44*, *SCA-1*, *Aldh1*, or *CD133*, but increased the expression of *Nanog*. B) Inactivation of *Trp53* significantly increased expression of *CD44* and *Sca-1*. C) Loss of both P53 and BRCA1 increased only *CD44*. One-way ANOVA were performed for three independent experiments (*$p<0.05$).

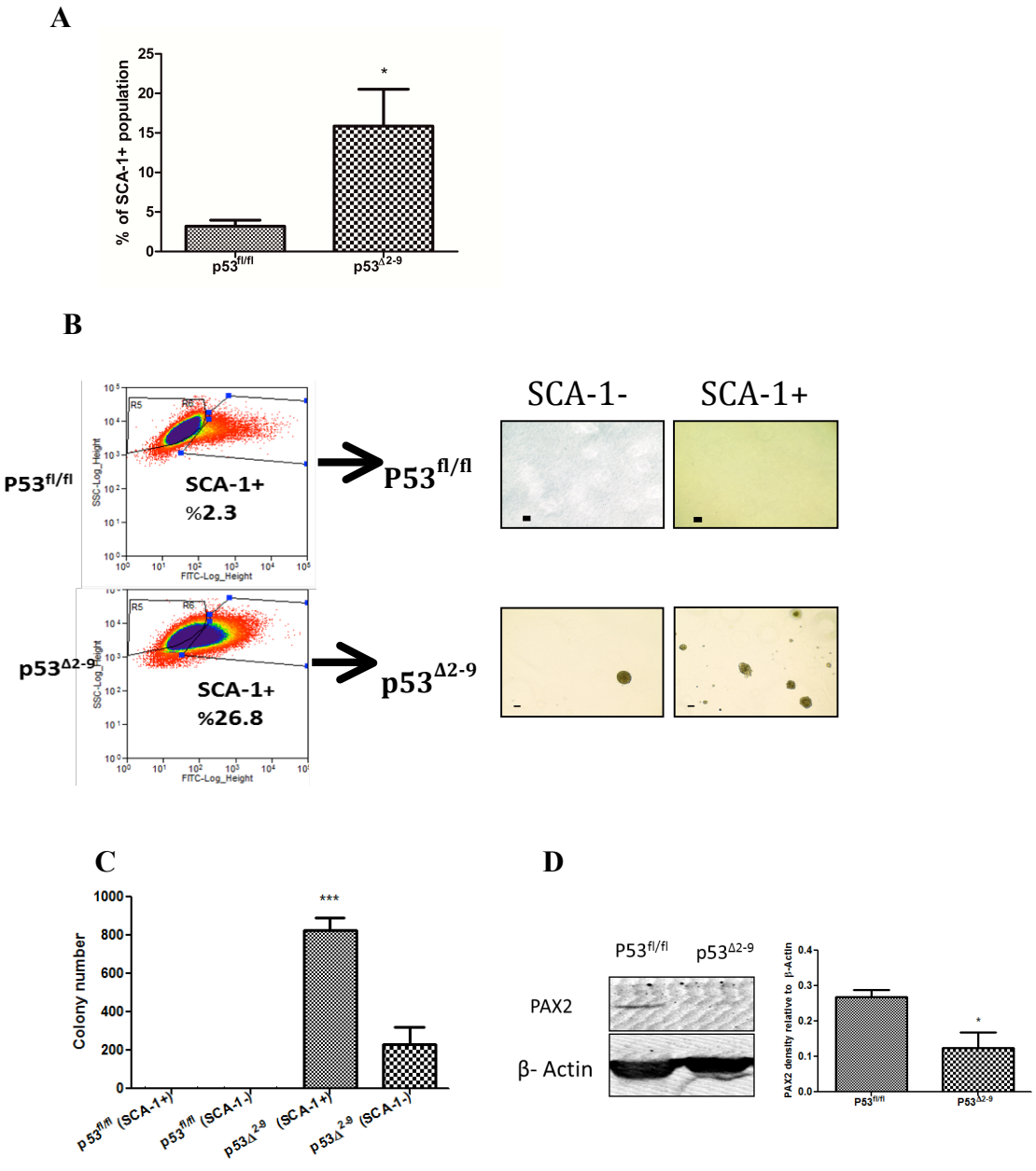

Figure 6-9: Inactivation of *Trp53* increased SCA-1+ population and decreased PAX2 expression.

A) Quantitative analysis of the SCA-1 positive fraction with *Trp53* mutation analyzed by flow cytometry (N=3). B) Colony formation assay for SCA-1 positive cells sorted by FACS from OVE with and without *Trp53* mutation, (C) quantitative analysis for the colony number (N=3). D) Representative western blot shows the decreased expression of PAX2 in OVE cells with *Trp53* mutation. The histogram shows densitometric analysis of PAX2 expression that was normalized to β-actin (N=3). Scale bar is 100 µm.

Chapter 7: Discussion

A growing number of studies have suggested that STICs within the distal end of the fallopian tube are precursor lesions for primary ovarian carcinoma (Chen et al., 2010; Koc et al., 2014; Sherman-Baust et al., 2014). Multiple gene mutations and gene alterations have been investigated to identify promising biomarkers for STIC (reviewed by Mehra et al., 2011). STICs are characterized by *TP53* mutation and loss of PAX2 (Chen et al., 2010; Ning et al., 2014); however, the mechanisms contributing to the changes in expression are unknown. The incidence of fallopian tube lesions may be increased by the repeated process of ovulation (Hennessy et al., 2009).

Both the ovary and adjacent fimbria are exposed to ovulatory follicular fluid containing inflammatory cytokines (Tone et al., 2012), creating a pro-inflammatory microenvironment on the surface of the ovary and the fimbria that could be suitable for DNA damage, EMT and stem cell stimulation (Zhou et al., 2012). Thus, we examined the effect of TGFβ as an inflammatory cytokine and report here its ability to induce EMT in OVE cell lines, as well as to suppress PAX2 expression. We have demonstrated that PAX2 promotes epithelial differentiation in both OVE cells and MOSE cells and enables OVE cells to form luminal structures in 3D culture. In agreement with that function, PAX2 knockdown reduces epithelial differentiation and enhances some features associated with stem or progenitor cells. PAX2 regulates CD44 and SCA-1 expression, and loss of PAX2 leads to reduced epithelial differentiation and enhanced "stemness", both characteristics that could promote tumor development.

In addition, STICs in the fallopian tubes have been identified with a "P53 signature"

(Leonhardt et al., 2011) reflecting mutation of *TP53*, and *BRCA1* mutation carriers are more likely to develop STICs in their lifetime (Easton et al., 1995), implicating both *TP53* and *BRCA1* mutations in the early stages of fallopian tube-derived ovarian cancer. Our results suggest that all three genetic alterations reported in STICs (loss of PAX2, and mutation in *TP53* and/or *BRCA1)* may contribute to STIC development by promoting an oviductal epithelial cell transition to a more mesenchymal and stem/progenitor-like state.

Fallopian tube epithelial cell morphology

Different types of cells are found in the fallopian tubes. In addition to secretory and ciliated epithelial cells, undifferentiated cells, basal cells and lymphocytes have been identified in fallopian tubes (Crow et al., 1994). In this study we initially extracted epithelial cells from mouse oviducts to generate four different OVE cell lines, each generated from a single colony. Each cell line was characterized as epithelial based on E-cadherin and cytokeratin expression. The secretory cell proteins PAX8, OVGP and the oviductal epithelial protein PAX2 were expressed in three cell lines at different levels. However, the types of epithelial cells lining the fallopian tubes, the morphology of the cells and their gene expression are not well described. Although isolation of OVE cells from 4-7 week old mice was the appropriate time to have fully differentiated oviduct, the OVE clonal cells from these mice have different cell morphology. The mice at this age would be post pubertal. The estrus cycle and presence of steroid hormones are known to have effects on oviductal cell differentiation, morphology, gene expression and the ratio of ciliated to secretory cells. In the follicular phase of the menstrual/estrus cycles, cells in

the human fallopian tube and mouse oviductal secretory cells elongate and become stratified, whereas in the luteal phase the lining cells form a simple cuboidal monolayer (Crow et al., 1994). In addition, the distribution of secretory and ciliated cells varies among the sections of the fallopian tube. For example, the fimbriae have more ciliated cells than the ampulla to help the passage of the ovulated oocyte from the ovary into the fallopian tube, whereas the ampulla has more secretory cells to facilitate fertilization (Stewart et al. 2012).

Because of the different cell types in the oviduct, it is not surprising that the isolated OVE clonal cells presented with different morphologies and gene expression. Moreover, PAX2 expression in these clonal cells was varied and associated with the cell morphology. Notably, OVE cells that have a more epithelial-like morphology expressed higher levels of PAX2. Interestingly, some clonal cells that were isolated from the fimbria were PAX2 and PAX8 null (Table 2). Immunohistochemical staining in a previous study showed that some types of epithelial cells in the fallopian tube are PAX2 negative (Ning et al., 2014). Another study has shown that PAX8 negative cells present with stem-like cell characteristics in the human tubal epithelium (Paik et al., 2012). This brought our attention to the role of PAX2 in OVE cell differentiation, and the possible consequences of its loss and the promotion of stem cell characteristics.

Stem-like cells in the OVE clonal cell lines

To determine if OVE cells include stem cell-like populations, label retention and self-renewal experiments are normally sufficient to detect quiescent cells that have low

mitotic rate (Wang et al., 2012). The *in vitro* experiments with OVE cells labeled with PKH26 identified a subpopulation of cells that have a low rate of division with PKH26 labeling retained for 30 days. In addition, growth in suspension culture demonstrated the ability of OVE clonal cells to form spheres. Interestingly, OVE cells were able to retain the PKH26 label for a long period within the spheres, indicating the existence of stem-like cells.

The capacity for sphere formation among the OVE clonal cells was varied and from assessment of multiple cell lines, we noticed that OVE cells with more epithelial-like morphology and higher levels of PAX2 have a reduced capacity for sphere formation. To further investigate the potential stem cell characteristics of these cells, the expression of the well-known stem cell markers CD44 and SCA-1 was determined. CD44 has been reported in prostate and breast cancer to be present in stem cells and to enhance formation of spheres (Korski et al, 2014; Cruz Paula et al., 2014; Chekhun et al., 2015). CD44+ cancer stem cells from ovarian cancer (Craveiro et al., 2013) and colon cancer (Du et al., 2008) have the ability to trigger tumor formation when they are injected into immune-compromised mice. However, the role of CD44 in the development of fallopian tube precursor lesions has not been investigated.

Positive and negative populations of CD44 and SCA-1 were sorted from OVE clonal cells to determine if these markers could enrich for cells with stem cell characteristics. In suspension culture with stem cell media, populations of CD44-positive cells had higher sphere-forming capacity than CD44-negative cells in two OVE lines. However, while SCA-1-positive cells were able to form spheres, the incidence was not different from the SCA-1-negative population of cells. It is worth noting that the sphere formation assay

functions very well if the stem cells are isolated from tissues with the required stem cell niche. In previous studies of fallopian tube and prostate, stem cells sorted for expression of CD44 were examined for other proteins expressed on the cell surface. The sorted cells were CD44+, EPCAM+ and integrin6 (ITGA6+), which mimic the profile for stem cells in the tissues, and they form abundant spheres compared to bulk cells (Paik et al., 2012; Guo et al., 2012).

It should be noted that the sphere formation assay has been found to have limitations in some tissues. In neural cells, neurospheres have been found to be arise from non-stem cells (Reynolds et al., 2005). Further, the stem cells sorted from normal mammary glands were not able to give consistent mammospheres using different stem cell markers (Stingl et al., 2009). Overall, the sphere formation assay is not an absolute read-out for "stemness", but it may reflect the potential of stem cell self-renewal in some tissues. Further, the incidence of sphere formation may depend on different factors such as the type of cells, cell density and the culture conditions (Pastrana et al., 2011).

We found that the spheres formed by OVE cells in response to stimuli have different characteristics compared to MOSE cells. The administration of the growth factor TGFβ to OVE cells resulted in increased sphere size compared to control, with no difference in sphere number. Since TGFβ suppresses OVE cell proliferation when the cells are cultured as a monolayer, the results suggest that TGFβ increases OVE cell proliferation when cells are in suspension and/or enhances their stem-like cell capacity for self-renewal. In contrast, the same conditions for TGFβ administration to MOSE cells resulted in an increased number of smaller spheres (Gamwell et al., 2012). In addition, in our study, SCA-1+ cells sorted from OVE clonal cells did not reveal significant sphere-

forming capacity compared to SCA-1- cells, whereas MOSE SCA-1+ cells presented higher sphere-forming capacity compared to the negative population (Gamwell et al., 2012). The results indicate that both MOSE and OVE cells contain a subpopulation of cells with stem-like characteristics, but the markers that can be used to isolate these cells may be quite different.

Follicular fluid, TGFβ and their impact on fallopian tube epithelial cells

A recent study has shown that follicular fluid induces inflammation-associated DNA damage and increased P53 accumulation in cultured fallopian tube epithelial cells, which mimic the early events found in fallopian tube neoplastic lesions (Lau et al., 2014; Bahar-Shany et al., 2014). The components in follicular fluid that are responsible for these effects are unknown, but TGFβ has been reported to be present in preovulatory follicular fluid (Gamwell et al., 2012). Since fallopian tube cells that line the fimbria are exposed to follicular fluid during ovulation (Hennessy et al., 2009), we speculated that TGFβ in follicular fluid may influence the OVE cells.

The morphology of fallopian tube epithelial cells has been reported to change during the menstrual cycle, notably to become more pseudostratified during the follicular phase, a change that may be due to the changing profile and/or abundance of hormones or cytokines released by the ovary and the tubal epithelial cells and present in the follicular fluid (Crow et al., 1994).

In our study, we provided evidence of the TGFβ contribution to initiating events in the formation of fallopian tube lesions. TGFβ treatment of OVE cells reduced PAX2

expression, which is a characteristic of STIC. In addition, the expression levels of the epithelial markers were reduced by TGFβ treatment to induce EMT, in association with a more mesenchymal morphology and enhanced cell migration. Thus, the frequent release of TGFβ during ovulation may enhance the accumulation of DNA damage which may induce STIC formation and migration of malignant cells from the tubal distal end to implant on the surface of the ovary (Figure 7-1). It has been reported that laying hens develop spontaneous epithelial ovarian cancer after 3-4 years of continuous laying (ovulation) (Johnson & Giles, 2013), suggesting that humans and mice may develop ovarian cancer as a result of repetitive exposures to the follicular fluid.

EMT has been reported to induce stemness in several tissues including breast cancer (Mallini et al., 2014) and ovarian cancer (Okamoto et al., 2009). Normal epithelial cells include quiescent stem cells attached to the extracellular matrix. When the epithelial cells undergo EMT, they lose cell polarity and the proper expression and localization of adhesion molecules such as E-cadherin, which induces cell detachment from the extracellular matrix. The cell detachment may activate stem cells to proliferate and migrate from the tissue.

TP53 mutation has been reported to induce EMT (Chang et al., 2011). STICs, which have mutations in *TP53*, do have a more mesenchymal morphology, which raised the possibility that they also acquire stem-like characteristics. The enhanced migratory ability of these cancer stem cells could increase the opportunity for them to implant on the surface of the ovary or travel to other tissues in the peritoneal cavity to develop into HGSC.

In this study, we observed higher expression of EMT markers and two known stem

cell markers, CD44 and SCA-1 after TGFβ treatment, but not any other putative stem cell markers tested. LGR5 has been proposed to mark stem cells in the ovary (Ng et al., 2014), but *Lgr5* expression increased only modestly when OVE cells were treated with TGFβ. Given the strong up-regulation of CD44 induced by TGFβ in OVE cells, this stem cell marker was selected for further study, attempting to identify stem-like cells in the OVE cell lines. OVE cells visualized by immunofluorescence microscopy after TGFβ treatment showed a higher intensity of CD44 staining, which was supported by increased expression as seen in western blots. CD44 is expressed in various isoforms, whose unique functions are not yet fully defined, but it has been frequently reported as enriching for tumor-initiating cells in ovarian cancer (Garson et al. 2015).

OVE cells highly express a variant form of CD44, which was increased further by TGFß treatment. Longer exposure to TGFβ increased the standard form of CD44, an isoform that has been associated with stem cell features in hematopoietic progenitor cells (Zoller, 2011) and in cancer cells such as HGSC (Zhang et al., 2013) and hepatocellular carcinoma (Okabe et al., 2014). It has been shown that STICs and the normal adjacent fallopian tube epithelium consist of expansion of cells expressing CD44 (Paik et al., 2012). Therefore, these results suggest that exposure to TGFβ, perhaps either from ovulatory follicular fluid and/or from tubal gene expression, can promote changes in OVE cells that are similar to those identified in STIC formation (Figure 7-2).

PAX2 maintains epithelial differentiation of OVE cells and inhibits stemness

PAX2 has a well-established role in epithelial differentiation of the embryonic

reproductive tract (Kobayashi et al., 2003), and our results suggest that PAX2 continues to promote this differentiated state in adult epithelial cells. Surprisingly, OVE cells have the ability to form efficient hollow lumen architectures that resemble the acini formed by breast epithelium (Debnath et al., 2005). While this architecture resembles the breast acini, it also resembles the normal oviduct, including the expression of PAX2, PAX8 and E-cadherin. The formation of these luminal structures was dependent on PAX2 expression. *Pax2* knockdown in OVE4 cells did not prevent the initial formation of spheres in matrigel by day 4, but these spheres were disrupted from further progression to luminal structures. A possible explanation for this disruption may be derived from a study by Torban and coworkers (Torban et al., 2000), which confirmed that PAX2 protects the renal cells from apoptosis but *Pax2* overexpression in kidney cells lacking *Pax2* does not lead to increased proliferation. Since PAX2 is the essential factor that induces epithelial differentiation of the reproductive tract (Kobayashi & Behringer, 2003), we speculate that without PAX2 function, the differentiation process of OVE cells in matrigel could not proceed. In addition, we found that OVE clonal cells that have high expression of PAX2 and weak capacity to form spheres are more able to form luminal structures, which indicates that the differentiation process may be dependent on suppressing the stem cell phenotype. Our observations from multiple clones suggest that only ciliated cells have epithelial morphology in monolayer culture, which is associated with weak sphere-forming capacity in suspension and enhanced ability to differentiate into luminal structures (Table 2). Further studies are needed to identify the specific targets of PAX2 transcriptional activity in oviductal cells to more fully understand the consequences of loss of PAX2 and the transition to STICs and SCOUTs in early ovarian cancer.

One of the most interesting observations in this study is that TGFβ significantly decreased expression of PAX2, suggesting that loss of PAX2 may mediate TGFβ action in promoting OVE stemness by shifting the phenotype away from epithelial differentiation. Since loss of PAX2 expression is a primary characteristic of STICs, there may be a possible role for TGFβ in inducing STIC formation. The mechanisms that regulate STIC formation have not yet been described; some studies suggest that these structures develop from secretory cells that have lost PAX2 expression, known as secretory cell outgrowths (SCOUT) (Chen et al., 2010). In a recent study, some types of SCOUTs were shown to acquire a stem cell phenotype by expressing ALDH1 (Ning et al., 2014), while another study has reported that STIC have an expanded number of CD44-positive cells compared to normal tubal epithelium (Paik et al., 2012). The link between PAX2 and stemness has not been studied before and the regulatory role of PAX2 is a novel investigation in this study.

To investigate whether PAX2 inhibits stemness, *Pax2* knockdown and over-expression were achieved in OVE cells and MOSE cells, respectively. Knockdown of *Pax2* using a dox-inducible shRNA (PLKO) in OVE4 and OVE16 cells resulted in reduced PAX2 and a consequent increase in expression of the stem cell markers CD44 and SCA-1. However, knockdown of PAX2 was not sufficient to increase sphere-forming capacity. Western blot confirmation of the up-regulation of CD44 showed an increase in the variant isoform but not the standard form of CD44 (associated with stemness), which may explain the lack of change in sphere-forming capacity after loss of PAX2.

As an alternative approach to studying the role of PAX2 in shifting the balance between epithelial differentiation and stemness, PAX2 was overexpressed in MOSE cells,

which do not normally express PAX2. PAX2 overexpression significantly decreased the expression of several stem cell associated genes, including *CD44*, *Sca-1* and *Lgr5*. In addition, sphere formation capacity was significantly reduced in MOSE cells with forced expression of PAX2. When PAX2 expression was ablated by treatment with AdCre, the stem cell-associated genes and sphere formation capacity were restored, suggesting that PAX2 plays an essential role to negatively regulate stemness in OVE cells and OSE cells. PAX2 therefore appears to preserve the epithelial differentiation of OVE cells, and loss of expression is associated with a transition to a more stem-like state.

Immunohistochemical studies revealed few CD44+ cells in the OSE layer, but they were abundant in the distal end of the oviduct, the site of origin of most STICs. CD44 expression was localized primarily in the basal cells and appeared to be mutually exclusive of PAX2 expression, suggesting that PAX2 may inhibit CD44 expression in oviductal cells *in vivo*. CD44+ cells sorted from breast cancer have been found to express high levels of laminin (Adamczyk et al., 2014). This co-expression may also exist in oviductal epithelium, as laminin γ1 has been detected in cells on the basement membrane of normal fallopian tube in a pattern similar to CD44, and laminin γ1 expression expands to most of the proliferative cells in the STICs (Kuhn et al., et al., 2012).

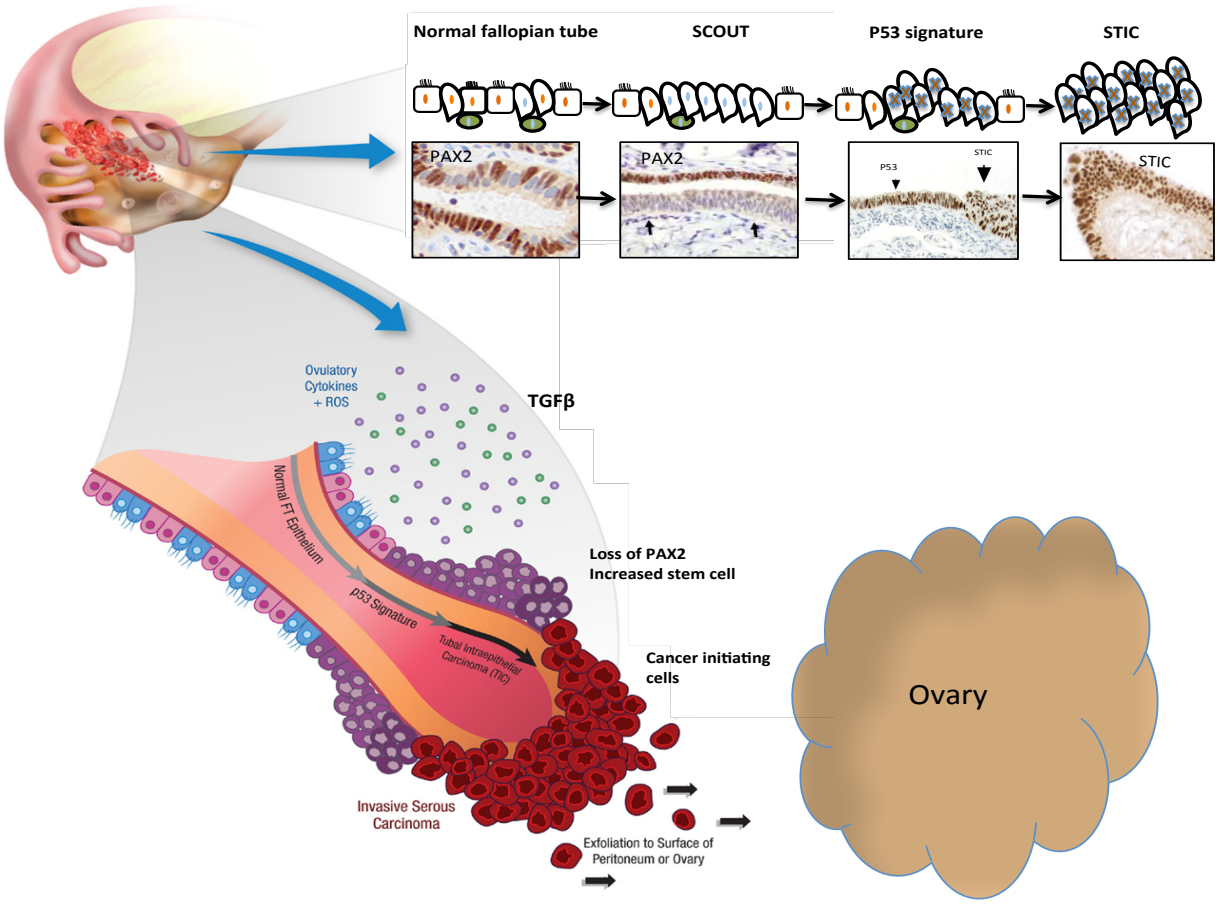

Figure 7-1: An illustration presenting the proposed events occurring in a precursor lesion within the fallopian tube.
Secretory cell outgrowth and loss of PAX2 are early events in formation of the lesion. Some of these benign-appearing SCOUTs display the P53 signature. Both loss of PAX2 and P53 mutation increase the stem cell population, and then the tumor-initiating cells exfoliate to the surface of the ovary (Adapted from Chen et al., 2010; Jarboe et al., 2008; Jones et al., 2013; Tong et al., 2007).

Effects of *Trp53* and *Brca1* mutation on OVE cell activity

To study the molecular mechanisms that might compound the effects of TGFβ during ovulation and trigger STIC formation, the consequences of mutations of *Trp53* and *Brca1* in OVE cells were investigated. We found that loss of *Trp53*, with and without loss of BRCA1, increased cell proliferation and colony formation. Similar to the effects of TGFβ, the loss of *Trp53* induced a shift to a more mesenchymal morphology in OVE cells and increased cell migration. Further, loss of *Trp53* increased OVE stemness by increasing the sphere formation capacity and expression levels of the stem cell markers CD44 and SCA-1, which indicates that *Trp53* mutation in OVE cells can promote the creation or amplification of EMT-associated stem cells.

These results are in general agreement with previous studies reporting that *Trp53* mutation is an inducer of EMT and stemness. One study showed the down-regulation of E-cadherin and up-regulation of the mammary stem cell population (CD24-/CD44+) after loss of *Trp53* (Chang et al., 2011), whereas in hematopoietic cells, loss of *Trp53* increased SCA-1 and c-Kit (TeKippe et al., 2003). In addition, loss of *Trp53* in the mammary gland increased stem cell self-renewal by increasing number and size of mammospheres, suggesting that loss of *Trp53* may increase the symmetric divisions (Tao et al., 2011).

Since we found that loss of *Trp53* increased the stem cell population and this was associated with enhanced colony formation, it may be that SCA-1+ cells with loss of *Trp53* may act as tumor-initiating cells, which could develop into the STIC precursor lesions found in fallopian tube fimbria. We have previously shown that spontaneously transformed MOSE cells with aberrant expression of P53 have a SCA-1+ population that

develops into palpable tumors faster than SCA1- cells after intrabursal injection (McCloskey et al., 2014).

BRCA1 mutation is an established risk factor for ovarian cancer and is associated with a higher incidence of STIC formation (Carlson et al., 2008). To begin to understand whether and/or how *BRCA1* mutation contributes to STIC formation, we inactivated *Brca1* with and without *Trp53* loss. We found that loss of *Brca1* alone did not alter cell proliferation, nor did it alter the cell phenotype. Not surprisingly then, loss of *Brca1* in OVE cells had no impact on any of the stemness characteristics we evaluated. This is quite different from the relationship that has been established between *BRCA1* mutation and stemness in mammary epithelial cells. BRCA1 knockout in breast epithelial cells decreased cell differentiation and increased stem/progenitor cells expressing ALDH1 (Liu et al., 2008).

Interestingly, the combination loss of *Trp53* and *Brca1* in OVE cells enhanced cell proliferation, migration and colony formation but did not alter any characteristics of stemness. Accordingly, it could be suggested that *Brca1* mutation might restrict the EMT-stem cell induction that is triggered by loss of P53. The reason for the lack of any notable neoplastic changes after *Brca1* inactivation is not clear, but several factors should be considered. Most importantly, AdCre treatment of the $Brca1^{fl/fl}$ and $Trp53^{fl/fl}Brca1^{fl/fl}$ OVE cells did not result in complete knockout of the *Brca1* gene. Multiple attempts to isolate clones with fully inactivated *Brca1* were unsuccessful and it remains unclear whether only a fraction of cells had DNA recombination or whether one allele is less amenable to Cre-mediated recombination. The latter seems unlikely since the proper *loxP*-flanked DNA sequence was confirmed by sequencing and the $Brca1^{fl/fl}$ mice have

been used successfully in previous studies (Clark-Knowles et al., 2007 and 2009). Based in Knudson's two hit hypothesis (Knudson, 2001), we speculate that loss of both *Brca1* alleles has to occur to demonstrate the biological significance of its inactivation. It may also be of significance that the *Brca1*$^{fl/fl}$ clone 2 used in this study appeared to be derived from ciliated cells, since they have high expression of the ciliated cell marker FOXJ, whereas it has been reported that secretory cells are the cell of origin of STICs and HGSC (Chen et al., 2010; Perets et al., 2013).

Tumorigenesis is a multi-step process that includes accumulation of gene mutations, and *BRCA1* mutation alone is not sufficient to initiate tumor development. *BRCA1* mutation has been linked with precursor lesion development in *BRCA1* carriers (Easton et al., 1995), and the lesions have been characterized with aberrant P53 expression or *TP53* mutations in several studies (Horn et al., 2013; Kuhn et al., 2012; Leonhardt et al., 2011). *Brca1* inactivation in mouse OSE cells *in vivo* was also not sufficient to induce tumor formation, but required additional inactivation of *Trp53* (Clark-Knowles et al., 2009). Notably, the inactivation of *Brca1* in OSE cells *in vitro* results in a modest decrease in proliferation and increased apoptosis (Clark-Knowles, et al., 2007). Cultures of mouse embryonic fibroblasts (MEFs) with a deletion of exon 11 of *Brca1* displayed a senescence-like growth defect (Cao et al., 2003), which raises the additional possibility that OVE cells with mutant *Brca1* had growth defects or increased susceptibility to apoptosis that impaired long term survival.

Unfortunately, the relationship between *Trp53* and *Brca1* mutations and PAX2 expression was not able to be investigated because some of the OVE clonal cells had low or no PAX2 expression. Additional clones will need to be generated in order for future

studies to examine the interrelationships between *Trp53* and *Brca1* mutations and PAX2 expression. Interestingly, we have recently reported the ability of PAX2 to suppress the induction of P53 expression in OSE cells after treatment with cisplatin, and the expression of P53 in a mouse model of ovarian cancer, raising the possibility that in STICs, the loss of PAX2 may be a mechanism by which P53 expression is increased (Al-Hujaily et al., 2015).

Does PAX2 play a role in vasculogenic mimicry?

Normal OSE cells do not express PAX2 (Al-Hujaily et al., 2015), whereas 61% of ovarian cancer cell lines express PAX2 (Song et al., 2013), suggesting a potential oncogenic role for PAX2 in cancers derived from the ovarian epithelium. The oncogenic role of PAX2 in ovarian cancer has recently been investigated in terms of its ability to promote cell proliferation, migration and tumor formation (Al-Hujaily et al., 2015). In our attempts to confirm the ability of PAX2 to promote epithelial differentiation of OSE cells, we found that PAX2 expression in M1102 OSE cells induced the formation of tubular-like structures in matrigel, whereas the control groups did not form these structures. The ability to form these tubular or vessel-like structures has been previously associated with aggressive tumor cell lines such as melanoma (Maniotis et al., 1999) and the phenomena is known as vasculogenic mimicry (VM). While the formation of vascular networks by normal endothelial cells is a standard measure of their organizational potential (Ponce et al., 2009), no other normal cells have been reported to have this capability. Aggressive cancer cell lines, however, can organize in a pattern to form *de novo* these webs of vessels (Maniotis et al., 1999). The tubular networks formed by

M1102-PAX2 in matrigel were morphologically similar to the vessels formed by HUVEC cells and to the VM networks formed by SKOV3 ovarian cancer cells.

The M1102-PAX2 tubular webs were supported by remodeling extracellular matrix which was positive for PAS staining and negative for CD31. However, SKOV3 VM had a few cells expressing CD31, which is consistent with previous reports suggesting that cancer cells may differentiate into endothelial cells *de novo* to induce the angiogenesis (Su et al., 2008). Thus, we hypothesized that PAX2 induces VM *in vitro* in normal OSE cells. Unfortunately, we were not able to investigate the vessel formation *in vivo* with normal OSE-PAX2, since these cells are not able to form tumors when they have been injected into mice (Al-Hujaily et al., 2015). To further investigate the possible role of PAX2 in VM during tumor progression, we used a mouse model of ovarian cancer cells (RM) created by transformation of OSE cells by *K-Ras* and *C-Myc* mutations. Forced expression of PAX2 in RM cells significantly increased tubular formation *in vitro*. RM cells are tumorigenic in mice and the forced expression of PAX2 induced tumor progression (Al-Hujaily et al., 2015). To understand if PAX2 expression enhances vasculogenesis by the cancer cells *in vivo*, tumors formed by RM and RM-PAX2 cells were analyzed for PAX2 and CD31 expression and for PAS staining. RM-PAX2 tumors showed increased angiogenesis as determined by staining with CD31. However, in the same tumor, some of the neo-vasculature was negative for CD31 and positive for PAS, which indicates that endothelial cells did not form these new vessels. Interestingly, some of the cells lining those vessels expressed PAX2 in the nucleus, which indicates that cancer cells that have high expression of PAX2 can contribute to the formation of neo-vasculature in the tumor. The molecular mechanism by which PAX2 can promote VM is

an interesting question to be addressed in future studies. Since we know that PAX2 induces COX2 in RM cells (Al-Hujaily et al., 2015) and COX2 has been reported to induce VM in breast cancer (Basu et al., 2006), we anticipate that PAX2-induced VM may be mediated by COX2 expression.

The potential role for PAX2 in VM is novel, but PAX2 has been reported to induce the tubular branching in the kidney and to induce the elongation of the inner ear precursors (Christophorou et al., 2010) and so it may play a similar role in fallopian tube morphogenesis. In established tumors, PAX2 may enhance tumor progression and metastasis by vasculogenic mimicry, which enables increased blood supply for the tumor. However, the role of PAX2 in inducing cell branching or tubular formation and the protein expression that induces VM in the ovarian cancer is certainly worth investigating.

Table 2: Summary of OVE clonal cells characteristics

	Morphology	Sphere formation capacity	OVGP1	FOXJ	PAX2	PAX8	E-cadherin	CK19	Luminal structure in 3D
OVE4	flat epithelial	Yes (weak)	Yes	Yes	Yes high	Yes	Yes	Yes (high)	Yes
OVE22	flat epithelial	Moderate	Yes	Yes (Low)	Yes	Yes	Yes	Yes	Solid sphere
OVe14A	cobblestone	Yes (High)	No	No	No	No	Yes	Yes	No (Single cells)
OVE16	fusiform	Yes	Yes	Yes	Yes	Yes (high)	Yes	Yes	Solid sphere
BRCA-1$^{fl/fl}$ clone1	flat epithelial	Yes	Yes	Yes	Yes (high)	Yes	Yes	Yes	Solid sphere
BRCA-1$^{fl/fl}$ clone2	cobblestone	No	low	Yes (high)	Yes high	Yes	Yes (high)	Yes (high)	Yes (high)
P53$^{fl/fl}$	fusiform	Yes	Yes (high)	low	low	Yes	yes	yes	Solid sphere
P53/BRCA-1$^{fl/fl}$	fusiform	Yes	Yes (high)	low	no	Yes	Yes	low	Solid sphere

OVE cells with weak or no sphere formation capacity have high ciliated cell marker, PAX2 and form luminal structures

OVE cells have high sphere formation capacity do not express PAX2 or ciliated cell marker, do not differentiate in the matrigel.

OVE cells form spheres have high secretory cell markers and low or no PAX2

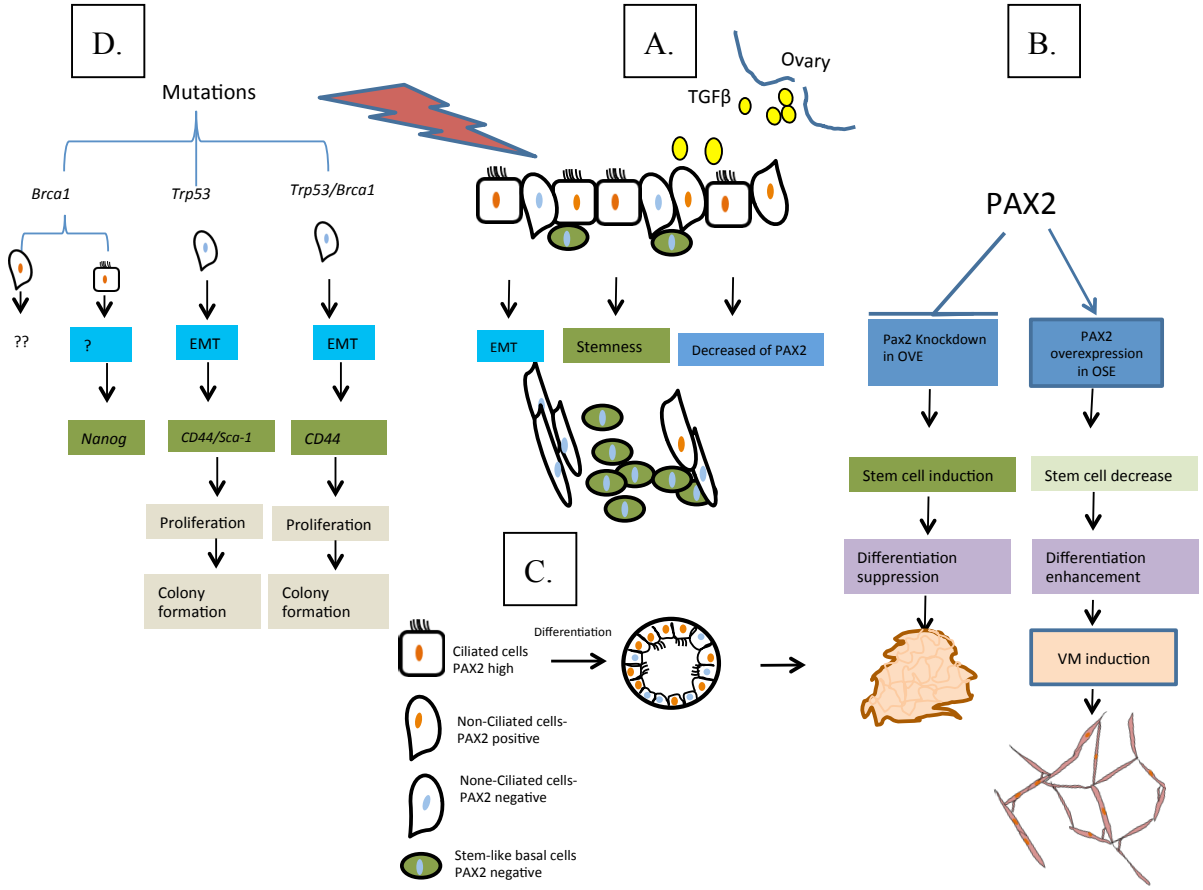

Figure 7-2: Summary of the findings in this thesis showing the effects of TGFβ, PAX2, and *Trp53* and *Brca1* mutations in OVE cells or MOSE cells.
TGFβ induces OVE cells to undergo EMT, increase stemness and repress PAX2 expression (A). PAX2 plays an important role in OVE and OSE cell differentiation (B). Loss of PAX2 in OVE increases stemness and suppresses differentiation, whereas forced expression of PAX2 in OSE cells suppresses stemness and increases differentiation and VM formation (B). Ciliated OVE cells are able to differentiate in the matrigel to form luminal structures that resemble the fallopian tube (C). *Trp*53 or *Trp*53 and *Brca1* mutations induce EMT, stemness, proliferation and colony formation (D).

Conclusions

This study provided evidence for how several features of early neoplastic lesions in fallopian tube (oviductal) epithelial cells (loss of PAX2, *Trp53* and *Brca1* mutations) may alter the balance of epithelial differentiation and stemness to increase their susceptibility to develop into ovarian carcinoma. We have determined that a subset of OVE cells show stem cell characteristics *in vitro*, including CD44 expression, and that undifferentiated stem-like cells expressing CD44 are located in the basement membrane of fallopian tubes *in vivo*.

Ovulation may have a potential involvement in inducing STIC and we provide evidence that a cytokine released at ovulation (TGFβ) suppresses PAX2 expression, induces EMT and increases stem cell characteristics in OVE cells. Expression of PAX2 in OVE cells is required to maintain their epithelial differentiation. Therefore loss of PAX2, as seen in STICs, may lead to a shift to a more mesenchymal phenotype associated with stem-like features.

Trp53 mutation also induced EMT and promoted stem cell characteristics in OVE cells that may contribute to the formation of cancer-initiating cells. Future studies are needed to determine the relationship between *Trp53* mutation and loss of PAX2, and their consequences on tumor initiation. While PAX2 expression in OVE cells maintains their epithelial differentiation and inhibits the transition to a stem cell state, its induced expression in MOSE cells results in the formation of tubular channels (vasculogenic mimicry), which may contribute to tumor progression. The contributions of PAX2 to the initiation and progression of ovarian cancer are therefore likely to be very complex.

References

Adamczyk, A., Niemiec, J.A., Ambicka, A., Mucha-Malecka, A., Mitus, J., & Rys, J. (2014). CD44/CD24 as potential prognostic markers in node-positive invasive ductal breast cancer patients treated with adjuvant chemotherapy. *J. Mol. Histol.* **45**, 35–45.

Adler, E., Mhawech-Fauceglia, P., Gayther, S.A., & Lawrenson, K. (2015). PAX8 expression in ovarian surface epithelial cells. *Hum. Pathol.* **46**, 948–956.

Afify, A., Pang, L., & Howell, L. (2007). Diagnostic utility of CD44 standard, CD44v6, and CD44v3-10 expression in adenocarcinomas presenting in serous fluids. *Appl. Immunohistochem. Mol. Morphol.* **15**, 446–450.

Ahmed, A.A., Etemadmoghadam, D., Temple, J., Lynch, A.G., Riad, M., Sharma, R., Stewart, C., Fereday, S., Caldas, C., Defazio, A., Bowtell, D., & Brenton, J.D. (2010). Driver mutations in TP53 are ubiquitous in high grade serous carcinoma of the ovary. *J. Pathol.* **221**, 49–56.

Akhurst, R.J., & Derynck, R. (2001). TGF-beta signaling in cancer--a double-edged sword. *Trends Cell Biol.* **11**, S44–S51.

Al-Hajj, M., Wicha, M.S., Benito-Hernandez, A., Morrison, S.J., & Clarke, M.F. (2003). Prospective identification of tumorigenic breast cancer cells. *Proc. Natl. Acad. Sci. U. S. A.* **100**, 3983–3988.

Al-Hujaily, E.M., Tang, Y., Yao, D.-S., Carmona, E., Garson, K., & Vanderhyden, B.C. (2015). Divergent roles of PAX2 in the etiology and progression of ovarian cancer. *Cancer Prev. Res. (Phila).* , doi: 10.1158/1940-6207.CAPR-15-0121-T.

Annes, J.P., Munger, J.S., & Rifkin, D.B. (2003). Making sense of latent TGFbeta activation. *J. Cell Sci.* **116**, 217–224.

Antoniou, A., Pharoah, P.D.P., Narod, S., et al. (2003). Average risks of breast and ovarian cancer associated with BRCA1 or BRCA2 mutations detected in case Series unselected for family history: a combined analysis of 22 studies. *Am. J. Hum. Genet.* **72**, 1117–1130.

Aprelikova, O.N., Fang, B.S., Meissner, E.G., Cotter, S., Campbell, M., Kuthiala, A., Bessho, M., Jensen, R.A., & Liu, E.T. (1999). BRCA1-associated growth arrest is RB-dependent. *Proc. Natl. Acad. Sci. U. S. A.* **96**, 11866–11871.

Asakura, A., Seale, P., Girgis-Gabardo, A., & Rudnicki, M.A. (2002). Myogenic specification of side population cells in skeletal muscle. *J. Cell Biol.* **159**, 123–134.
Auersperg, N. (2011). The origin of ovarian carcinomas: a unifying hypothesis. *Int. J. Gynecol. Pathol.* **30**, 12–21.

Auersperg, N. (2013). The stem-cell profile of ovarian surface epithelium is reproduced in the oviductal fimbriae, with increased stem-cell marker density in distal parts of the fimbriae. *Int. J. Gynecol. Pathol.* **32**, 444–453.

Auersperg, N., Wong, A.S., Choi, K.C., Kang, S.K., & Leung, P.C. (2001). Ovarian surface epithelium: biology, endocrinology, and pathology. *Endocr. Rev.* **22**, 255–288.
Auersperg, N., Woo, M.M.M., & Gilks, C.B. (2008). The origin of ovarian carcinomas: A developmental view. *Gynecol. Oncol.* **110**, 452–454.

Bahar-Shany, K., Brand, H., Sapoznik, S., Jacob-Hirsch, J., Yung, Y., Korach, J., Perri, T., Cohen, Y., Hourvitz, A., & Levanon, K. (2014). Exposure of fallopian tube epithelium to follicular fluid mimics carcinogenic changes in precursor lesions of serous papillary carcinoma. *Gynecol. Oncol.* **132**, 322–327.

Barakat, R.R., Federici, M.G., Saigo, P.E., Robson, M.E., Offit, K., & Boyd, J. (2000). Absence of premalignant histologic, molecular, or cell biologic alterations in prophylactic oophorectomy specimens from BRCA1 heterozygotes. *Cancer* **89**, 383–390.

Barbieri, F., Wurth, R., Ratto, A., Campanella, C., Vito, G., Thellung, S., Daga, A., Cilli, M., Ferrari, A., & Florio, T. (2012). Isolation of stem-like cells from spontaneous feline mammary carcinomas: phenotypic characterization and tumorigenic potential. *Exp. Cell Res.* **318**, 847–860.

Barker, N., van Es, J.H., Kuipers, J., Kujala, P., van den Born, M., Cozijnsen, M., Haegebarth, A., Korving, J., Begthel, H., Peters, P.J., & Clevers, H. (2007). Identification of stem cells in small intestine and colon by marker gene Lgr5. *Nature* **449**, 1003–1007.

Basu, G.D., Liang, W.S., Stephan, D.A., Wegener, L.T., Conley, C.R., Pockaj, B.A., & Mukherjee, P. (2006). A novel role for cyclooxygenase-2 in regulating vascular channel formation by human breast cancer cells. *Breast Cancer Res.* **8**, R69.

Basu, M., Bhattacharya, R., Ray, U., Mukhopadhyay, S., Chatterjee, U., & Roy, S.S. (2015). Invasion of ovarian cancer cells is induced byPITX2-mediated activation of TGF-beta and Activin-A. *Mol. Cancer* **14**, 162.

Berchuck, A., Rodriguez, G., Olt, G., Whitaker, R., Boente, M.P., Arrick, B.A., Clarke-Pearson, D.L., & Bast, R.C.J. (1992). Regulation of growth of normal ovarian epithelial cells and ovarian cancer cell lines by transforming growth factor-beta. *Am. J. Obstet. Gynecol.* **166**, 676–684.

Bertoncello, I., & McQualter, J. (2011). Isolation and clonal assay of adult lung epithelial stem/progenitor cells. *Curr. Protoc. Stem Cell Biol.* **Chapter 2**, Unit 2G.1.

Biddle, A., Gammon, L., Fazil, B., & Mackenzie, I.C. (2013). CD44 staining of cancer

stem-like cells is influenced by down-regulation of CD44 variant isoforms and up-regulation of the standard CD44 isoform in the population of cells that have undergone epithelial-to-mesenchymal transition. *PLoS One* **8**, e57314.

Biswas, S., Chytil, A., Washington, K., Romero-Gallo, J., Gorska, A.E., Wirth, P.S., Gautam, S., Moses, H.L., & Grady, W.M. (2004). Transforming growth factor beta receptor type II inactivation promotes the establishment and progression of colon cancer. *Cancer Res.* **64**, 4687–4692.

Blake, J.A., & Ziman, M.R. (2014). Pax genes: regulators of lineage specification and progenitor cell maintenance. *Development* **141**, 737–751.

van Bogaert, L.J., Maldague, P., & Abarca, J. (1978). Granulocytic-like cells in the human fallopian tube. *J. Reprod. Med.* **20**, 297–300.

Boland, S., Boisvieux-Ulrich, E., Houcine, O., Baeza-Squiban, A., Pouchelet, M., Schoevaert, D., & Marano, F. (1996). TGF beta 1 promotes actin cytoskeleton reorganization and migratory phenotype in epithelial tracheal cells in primary culture. *J. Cell Sci.* **109**, 2207–2219.

Bose, S.K., Gibson, W., Bullard, R.S., & Donald, C.D. (2009). PAX2 oncogene negatively regulates the expression of the host defense peptide human beta defensin-1 in prostate cancer. *Mol. Immunol.* **46**, 1140–1148.

Brussow, K.-P., Ratky, J., & Rodriguez-Martinez, H. (2008). Fertilization and early embryonic development in the porcine fallopian tube. *Reprod. Domest. Anim.* **43 Suppl 2**, 245–251.

Burdette, J.E., Kurley, S.J., Kilen, S.M., Mayo, K.E., & Woodruff, T.K. (2006). Gonadotropin-induced superovulation drives ovarian surface epithelia proliferation in CD1 mice. *Endocrinology* **147**, 2338–2345.

Burger, P.E., Xiong, X., Coetzee, S., Salm, S.N., Moscatelli, D., Goto, K., & Wilson, E.L. (2005). Sca-1 expression identifies stem cells in the proximal region of prostatic ducts with high capacity to reconstitute prostatic tissue. *Proc. Natl. Acad. Sci. U. S. A.* **102**, 7180–7185.

Burgess, M., & Puhalla, S. (2014). BRCA 1/2-Mutation Related and Sporadic Breast and Ovarian Cancers: More Alike than Different. *Front. Oncol.* **4**, 19.

Burgos-Ojeda, D., Wu, R., McLean, K., Chen, Y.-C., Talpaz, M., Yoon, E., Cho, K.R., & Buckanovich, R.J. (2015). CD24+ Ovarian Cancer Cells Are Enriched for Cancer-Initiating Cells and Dependent on JAK2 Signaling for Growth and Metastasis. *Mol. Cancer Ther.* **14**, 1717–1727.

Callahan, M.J., Crum, C.P., Medeiros, F., Kindelberger, D.W., Elvin, J. a, Garber, J.E., Feltmate, C.M., Berkowitz, R.S., & Muto, M.G. (2007). Primary fallopian tube malignancies in BRCA-positive women undergoing surgery for ovarian cancer risk reduction. *J. Clin. Oncol.* **25**, 3985–3990.

Campo, L., Zhang, C., & Breuer, E.-K. (2015). EMT-Inducing Molecular Factors in Gynecological Cancers. *Biomed Res. Int.* **2015**, 420891.

Cao, L., Li, W., Kim, S., Brodie, S.G., & Deng, C.-X. (2003). Senescence, aging, and malignant transformation mediated by p53 in mice lacking the Brca1 full-length isoform. *Genes Dev.* **17**, 201–213.

Carlson, J.W., Miron, A., Jarboe, E.A., Parast, M.M., Hirsch, M.S., Lee, Y., Muto, M.G., Kindelberger, D., & Crum, C.P. (2008). Serous tubal intraepithelial carcinoma: its potential role in primary peritoneal serous carcinoma and serous cancer prevention. *J. Clin. Oncol.* **26**, 4160–4165.

Cass, I., Walts, A.E., Barbuto, D., Lester, J., & Karlan, B. (2014a). A cautious view of putative precursors of serous carcinomas in the fallopian tubes of BRCA mutation carriers. *Gynecol. Oncol.* **134**, 492–497.

Chang, C.-J., Chao, C.-H., Xia, W., Yang, J.-Y., Xiong, Y., Li, C.-W., Yu, W.-H., Rehman, S.K., Hsu, J.L., Lee, H.-H., Liu, M., Chen, C.-T., Yu, D., & Hung, M.-C. (2011). p53 regulates epithelial-mesenchymal transition and stem cell properties through modulating miRNAs. *Nat. Cell Biol.* **13**, 317–323.

Chekhun, S. V, Zadvorny, T. V, Tymovska, Y.O., Anikusko, M.F., Novak, O.E., & Polishchuk, L.Z. (2015). capital ES, CyrillicD44+/CD24- markers of cancer stem cells in patients with breast cancer of different molecular subtypes. *Exp. Oncol.* **37**, 58–63.

Chen, E.Y., Mehra, K., Mehrad, M., Ning, G., Miron, A., Mutter, G.L., Monte, N., Quade, B.J., McKeon, F.D., Yassin, Y., Xian, W., & Crum, C.P. (2010). Secretory cell outgrowth, PAX2 and serous carcinogenesis in the Fallopian tube. *J. Pathol.* **222**, 110–116.

Chen, S., Einspanier, R., & Schoen, J. (2013). In vitro mimicking of estrous cycle stages in porcine oviduct epithelium cells: estradiol and progesterone regulate differentiation, gene expression, and cellular function. *Biol. Reprod.* **89**, 54.

Chi, N., & Epstein, J.A. (2002). Getting your Pax straight: Pax proteins in development and disease. *Trends Genet.* **18**, 41–47.

Chiche, A., Moumen, M., Petit, V., Jonkers, J., Medina, D., Deugnier, M.-A., Faraldo, M.M., & Glukhova, M.A. (2013). Somatic loss of p53 leads to stem/progenitor cell amplification in both mammary epithelial compartments, basal and luminal. *Stem Cells*

31, 1857–1867.

Christophorou, N. a D., Mende, M., Lleras-Forero, L., Grocott, T., & Streit, A. (2010). Pax2 coordinates epithelial morphogenesis and cell fate in the inner ear. *Dev. Biol.* **345**, 180–190.

Cicalese, A., Bonizzi, G., Pasi, C.E., Faretta, M., Ronzoni, S., Giulini, B., Brisken, C., Minucci, S., Di Fiore, P.P., & Pelicci, P.G. (2009). The tumor suppressor p53 regulates polarity of self-renewing divisions in mammary stem cells. *Cell* **138**, 1083–1095.

Clark, S.L., Rodriguez, A.M., Snyder, R.R., Hankins, G.D. V, & Boehning, D. (2012). Structure-function of the tumor suppressor BRCA1. *Comput. Struct. Biotechnol. J.* **1**, pii: e201204005.

Clark-Knowles, K. V, Garson, K., Jonkers, J., & Vanderhyden, B.C. (2007). Conditional inactivation of Brca1 in the mouse ovarian surface epithelium results in an increase in preneoplastic changes. *Exp. Cell Res.* **313**, 133–145.

Clark-Knowles, K. V, Senterman, M.K., Collins, O., & Vanderhyden, B.C. (2009). Conditional inactivation of Brca1, p53 and Rb in mouse ovaries results in the development of leiomyosarcomas. *PLoS One* **4**, e8534.

Comer, M.T., Leese, H.J., & Southgate, J. (1998). Induction of a differentiated ciliated cell phenotype in primary cultures of Fallopian tube epithelium. *Hum. Reprod.* **13**, 3114–3120.

Craveiro, V., Yang-Hartwich, Y., Holmberg, J.C., Sumi, N.J., Pizzonia, J., Griffin, B., Gill, S.K., Silasi, D.-A., Azodi, M., Rutherford, T., Alvero, A.B., & Mor, G. (2013). Phenotypic modifications in ovarian cancer stem cells following Paclitaxel treatment. *Cancer Med.* **2**, 751–762.

Crow, J., Amso, N.N., Lewin, J., & Shaw, R.W. (1994). Morphology and ultrastructure of fallopian tube epithelium at different stages of the menstrual cycle and menopause. *Hum. Reprod.* **9**, 2224–2233.

Crum, C.P., Drapkin, R., Miron, A., Ince, T.A., Muto, M., Kindelberger, D.W., & Lee, Y. (2007). The distal fallopian tube: a new model for pelvic serous carcinogenesis. *Curr. Opin. Obstet. Gynecol.* **19**, 3–9.

DA Cruz Paula, A., Marques, O., Rosa, A.M., DE Fatima Faria, M., Rema, A., & Lopes, C. (2014). Co-expression of stem cell markers ALDH1 and CD44 in non-malignant and neoplastic lesions of the breast. *Anticancer Res.* **34**, 1427–1434.

Dang, H., Steinway, S.N., Ding, W., & Rountree, C.B. (2015). Induction of tumor initiation is dependent on CD44s in c-Met(+) hepatocellular carcinoma. *BMC Cancer* **15**,

161.

Davidson, B., Trope, C.G., & Reich, R. (2012). Epithelial-mesenchymal transition in ovarian carcinoma. *Front. Oncol.* **2**, 33.

Debnath, J., & Brugge, J.S. (2005). Modelling glandular epithelial cancers in three-dimensional cultures. *Nat. Rev. Cancer* **5**, 675–688.

Debnath, J., Muthuswamy, S.K., & Brugge, J.S. (2003). Morphogenesis and oncogenesis of MCF-10A mammary epithelial acini grown in three-dimensional basement membrane cultures. *Methods* **30**, 256–268.

Dong, X., Sun, B., Zhao, X., Liu, Z., Gu, Q., Zhang, D., Zhao, N., Wang, J., & Chi, J. (2014). Expression of relative-protein of hypoxia-inducible factor-1alpha in vasculogenesis of mouse embryo. *J. Biol. Res. (Thessalonike, Greece)* **21**, 4.

Du, L., Wang, H., He, L., Zhang, J., Ni, B., Wang, X., Jin, H., Cahuzac, N., Mehrpour, M., Lu, Y., & Chen, Q. (2008). CD44 is of functional importance for colorectal cancer stem cells. *Clin. Cancer Res.* **14**, 6751–6760.

Dubeau, L. (1999). The cell of origin of ovarian epithelial tumors and the ovarian surface epithelium dogma: does the emperor have no clothes? *Gynecol. Oncol.* **72**, 437–442.

Duffy, M.J., Bonfrer, J.M., Kulpa, J., Rustin, G.J.S., Soletormos, G., Torre, G.C., Tuxen, M.K., & Zwirner, M. (2005). CA125 in ovarian cancer: European Group on Tumor Markers guidelines for clinical use. *Int. J. Gynecol. Cancer* **15**, 679–691.

Easton, D.F., Ford, D., & Bishop, D.T. (1995). Breast and ovarian cancer incidence in BRCA1-mutation carriers. Breast Cancer Linkage Consortium. *Am. J. Hum. Genet.* **56**, 265–271.

Eccles, M.R., He, S., Legge, M., Kumar, R., Fox, J., Zhou, C., French, M., & Tsai, R.W.S. (2002). PAX genes in development and disease: the role of PAX2 in urogenital tract development. *Int. J. Dev. Biol.* **46**, 535–544.

Eisen, A., Rebbeck, T.R., Wood, W.C., & Weber, B.L. (2000). Prophylactic surgery in women with a hereditary predisposition to breast and ovarian cancer. *J. Clin. Oncol.* **18**, 1980–1995.

Ellenbroek, S.I.J., Iden, S., & Collard, J.G. (2012). Cell polarity proteins and cancer. *Semin. Cancer Biol.* **22**, 208–215.

Elloul, S., Silins, I., Trope, C.G., Benshushan, A., Davidson, B., & Reich, R. (2006). Expression of E-cadherin transcriptional regulators in ovarian carcinoma. *Virchows Arch.* **449**, 520–528.

Endsley, M.P., Moyle-Heyrman, G., Karthikeyan, S., Lantvit, D.D., Davis, D.A., Wei, J.-J., & Burdette, J.E. (2015). Spontaneous Transformation of Murine Oviductal Epithelial Cells: A Model System to Investigate the Onset of Fallopian-Derived Tumors. *Front. Oncol.* **5**, 154.

Erickson, B.K., Conner, M.G., & Landen, C.N.J. (2013). The role of the fallopian tube in the origin of ovarian cancer. *Am. J. Obstet. Gynecol.* **209**, 409–414.

Fang, L., Chang, H.-M., Cheng, J.-C., Leung, P.C.K., & Sun, Y.-P. (2014). TGF-β1 induces COX-2 expression and PGE2 production in human granulosa cells through Smad signaling pathways. *J. Clin. Endocrinol. Metab.* **99**, jc20134100.

Fathalla, M.F. (1971). Incessant ovulation--a factor in ovarian neoplasia? *Lancet* **2**, 163.

Field, S.L., Dasgupta, T., Cummings, M., & Orsi, N.M. (2014). Cytokines in ovarian folliculogenesis, oocyte maturation and luteinisation. *Mol. Reprod. Dev.* **81**, 284–314.

Filmus, J., Zhao, J., & Buick, R.N. (1992). Overexpression of H-ras oncogene induces resistance to the growth-inhibitory action of transforming growth factor beta-1 (TGF-beta 1) and alters the number and type of TGF-beta 1 receptors in rat intestinal epithelial cell clones. *Oncogene* **7**, 521–526.

Flesken-Nikitin, A., Hwang, C.-I., Cheng, C.-Y., Michurina, T. V, Enikolopov, G., & Nikitin, A.Y. (2013). Ovarian surface epithelium at the junction area contains a cancer-prone stem cell niche. *Nature* **495**, 241–245.

Folberg, R., Hendrix, M.J., & Maniotis, A.J. (2000). Vasculogenic mimicry and tumor angiogenesis. *Am. J. Pathol.* **156**, 361–381.

Folkins, A.K., Jarboe, E.A., Saleemuddin, A., Lee, Y., Callahan, M.J., Drapkin, R., Garber, J.E., Muto, M.G., Tworoger, S., & Crum, C.P. (2008). A candidate precursor to pelvic serous cancer (p53 signature) and its prevalence in ovaries and fallopian tubes from women with BRCA mutations. *Gynecol. Oncol.* **109**, 168–173.

Fried, G., & Wramsby, H. (1998). Increase in transforming growth factor beta1 in ovarian follicular fluid following ovarian stimulation and in-vitro fertilization correlates to pregnancy. *Hum. Reprod.* **13**, 656–659.

Gamwell, L.F., Collins, O., & Vanderhyden, B.C. (2012). The mouse ovarian surface epithelium contains a population of LY6A (SCA-1) expressing progenitor cells that are regulated by ovulation-associated factors. *Biol. Reprod.* **87**, 80.

Gao, Y., Foster, R., Yang, X., Feng, Y., Shen, J.K., Mankin, H.J., Hornicek, F.J., Amiji, M.M., & Duan, Z. (2015). Up-regulation of CD44 in the development of metastasis,

recurrence and drug resistance of ovarian cancer. *Oncotarget* **6**, 9313–9326.

Garson, K., & Vanderhyden, B.C. (2015). Epithelial ovarian cancer stem cells: underlying complexity of a simple paradigm. *Reproduction* **149**, R59–R70.

George, S.H.L., Milea, A., & Shaw, P. a. (2012). Proliferation in the normal FTE is a hallmark of the follicular phase, not BRCA mutation status. *Clin. Cancer Res.* **18**, 6199–6207.

Gheldof, A., & Berx, G. (2013). Cadherins and epithelial-to-mesenchymal transition. *Prog. Mol. Biol. Transl. Sci.* **116**, 317–336.

Gudmundsdottir, K., & Ashworth, A. (2006). The roles of BRCA1 and BRCA2 and associated proteins in the maintenance of genomic stability. *Oncogene* **25**, 5864–5874.

Guo, C., Liu, H., Zhang, B.-H., Cadaneanu, R.M., Mayle, A.M., & Garraway, I.P. (2012). Epcam, CD44, and CD49f distinguish sphere-forming human prostate basal cells from a subpopulation with predominant tubule initiation capability. *PLoS One* **7**, e34219.

Hagiwara, H., Ohwada, N., Aoki, T., Suzuki, T., & Takata, K. (2008). The primary cilia of secretory cells in the human oviduct mucosa. *Med. Mol. Morphol.* **41**, 193–198.

Havrilesky, L.J., Hurteau, J.A., Whitaker, R.S., Elbendary, A., Wu, S., Rodriguez, G.C., Bast, R.C.J., & Berchuck, A. (1995). Regulation of apoptosis in normal and malignant ovarian epithelial cells by transforming growth factor beta. *Cancer Res.* **55**, 944–948.
Hay, E.D. (1995). An overview of epithelio-mesenchymal transformation. *Acta Anat. (Basel).* **154**, 8–20.

Heldin, C.H., & Moustakas, A. (2012). Role of Smads in TGF?? signaling. *Cell Tissue Res.* **347**, 21–36.

Helfrich, I., Scheffrahn, I., Bartling, S., Weis, J., von Felbert, V., Middleton, M., Kato, M., Ergun, S., Augustin, H.G., & Schadendorf, D. (2010). Resistance to antiangiogenic therapy is directed by vascular phenotype, vessel stabilization, and maturation in malignant melanoma. *J. Exp. Med.* **207**, 491–503.

Hennessy, B.T., Coleman, R.L., & Markman, M. (2009). The impact of ovulation on fallopian tube epithelial cells: evaluating three hypotheses connecting ovulation and serous ovarian cancer. *Lancet* **374**, 1371–1382.

Higashi, T., Sasagawa, T., Inoue, M., Oka, R., Shuangying, L., & Saijoh, K. (2001). Overexpression of latent transforming growth factor-beta 1 (TGF-beta 1) binding protein 1 (LTBP-1) in association with TGF-beta 1 in ovarian carcinoma. *Jpn. J. Cancer Res.* **92**, 506–515.

Hilton, J.L., Geisler, J.P., Rathe, J.A., Hattermann-Zogg, M.A., DeYoung, B., & Buller, R.E. (2002). Inactivation of BRCA1 and BRCA2 in ovarian cancer. *J. Natl. Cancer Inst.* **94**, 1396–1406.

Horn, L.-C., Kafkova, S., Leonhardt, K., Kellner, C., & Einenkel, J. (2013). Serous tubal in situ carcinoma (STIC) in primary peritoneal serous carcinomas. *Int. J. Gynecol. Pathol.* **32**, 339–344.

Huang, R., Wu, D., Yuan, Y., Li, X., Holm, R., Trope, C.G., Nesland, J.M., & Suo, Z. (2014). CD117 expression in fibroblasts-like stromal cells indicates unfavorable clinical outcomes in ovarian carcinoma patients. *PLoS One* **9**, e112209.

Hummitzsch, K., Anderson, R.A., Wilhelm, D., Wu, J., Telfer, E.E., Russell, D.L., Robertson, S.A., & Rodgers, R.J. (2015). Stem cells, progenitor cells, and lineage decisions in the ovary. *Endocr. Rev.* **36**, 65–91.

Itzhaki, O., Greenberg, E., Shalmon, B., Kubi, A., Treves, A.J., Shapira-Frommer, R., Avivi, C., Ortenberg, R., Ben-Ami, E., Schachter, J., Besser, M.J., & Markel, G. (2013). Nicotinamide inhibits vasculogenic mimicry, an alternative vascularization pathway observed in highly aggressive melanoma. *PLoS One* **8**, e57160.

Jabbour, H.N., Sales, K.J., Catalano, R.D., & Norman, J.E. (2009). Inflammatory pathways in female reproductive health and disease. *Reproduction* **138**, 903–919.

Jarboe, E., Folkins, A., Nucci, M.R., Kindelberger, D., Drapkin, R., Miron, A., Lee, Y., & Crum, C.P. (2008). Serous carcinogenesis in the fallopian tube: a descriptive classification. *Int. J. Gynecol. Pathol.* **27**, 1–9.

Jiang, H., Li, L., Yang, H., Bai, Y., Jiang, H., & Li, Y. (2014). Pax2 may play a role in kidney development by regulating the expression of TBX1. *Mol. Biol. Rep.* **41**, 7491–7498.

Johnson, P.A., & Giles, J.R. (2013). The hen as a model of ovarian cancer. *Nat. Rev. Cancer* **13**, 432–436.

Jones, P.M., & Drapkin, R. (2013). Modeling High-Grade Serous Carcinoma: How Converging Insights into Pathogenesis and Genetics are Driving Better Experimental Platforms. *Front. Oncol.* **3**, 217.

Kasuya, A., & Tokura, Y. (2014). Attempts to accelerate wound healing. *J. Dermatol. Sci.* **76**, 169–172.

Kauff, N.D., Satagopan, J.M., Robson, M.E., Scheuer, L., Hensley, M., Hudis, C.A., Ellis, N.A., Boyd, J., Borgen, P.I., Barakat, R.R., Norton, L., Castiel, M., Nafa, K., & Offit, K. (2002). Risk-reducing salpingo-oophorectomy in women with a BRCA1 or

BRCA2 mutation. *N. Engl. J. Med.* **346**, 1609–1615.

Kessler, M., Fotopoulou, C., & Meyer, T. (2013). The molecular fingerprint of high grade serous ovarian cancer reflects its fallopian tube origin. *Int. J. Mol. Sci.* **14**, 6571–6596.

Kim, J., Coffey, D.M., Creighton, C.J., Yu, Z., Hawkins, S.M., & Matzuk, M.M. (2012). High-grade serous ovarian cancer arises from fallopian tube in a mouse model. *Proc. Natl. Acad. Sci. U. S. A.* **109**, 3921–3926.

Kim, J., Coffey, D.M., Ma, L., & Matzuk, M.M. (2015). The Ovary Is an Alternative Site of Origin for High-Grade Serous Ovarian Cancer in Mice. *Endocrinology* **156**, 1975–1981.

King, S.M., Hilliard, T.S., Wu, L.Y., Jaffe, R.C., Fazleabas, A.T., & Burdette, J.E. (2011). The impact of ovulation on fallopian tube epithelial cells: evaluating three hypotheses connecting ovulation and serous ovarian cancer. *Endocr. Relat. Cancer* **18**, 627–642.

Knudson, A.G. (2001). Two genetic hits (more or less) to cancer. *Nat. Rev. Cancer* **1**, 157–162.

Ko, S.Y., Lengyel, E., & Naora, H. (2010). The Mullerian HOXA10 gene promotes growth of ovarian surface epithelial cells by stimulating epithelial-stromal interactions. *Mol. Cell. Endocrinol.* **317**, 112–119.

Kobayashi, A., & Behringer, R.R. (2003). Developmental genetics of the female reproductive tract in mammals. *Nat. Rev. Genet.* **4**, 969–980.

Koc, N., Ayas, S., & Uygur, L. (2014). The association of serous tubal intraepithelial carcinoma with gynecologic pathologies and its role in pelvic serous cancer. *Gynecol. Oncol.* **134**, 486–491.

Korski, K., Malicka-Durczak, A., & Breborowicz, J. (2014). Expression of stem cell marker CD44 in prostate cancer biopsies predicts cancer grade in radical prostatectomy specimens. *Pol. J. Pathol.* **65**, 291–295.

Kuhn, E., Meeker, A., Wang, T.-L., Sehdev, A.S., Kurman, R.J., & Shih, I.-M. (2010). Shortened telomeres in serous tubal intraepithelial carcinoma: an early event in ovarian high-grade serous carcinogenesis. *Am. J. Surg. Pathol.* **34**, 829–836.

Kuhn, E., Kurman, R.J., Vang, R., Sehdev, A.S., Han, G., Soslow, R., Wang, T.-L., & Shih, I.-M. (2012a). TP53 mutations in serous tubal intraepithelial carcinoma and concurrent pelvic high-grade serous carcinoma--evidence supporting the clonal relationship of the two lesions. *J. Pathol.* **226**, 421–426.

Kuhn, E., Kurman, R.J., Soslow, R.A., Han, G., Sehdev, A.S., Morin, P.J., Wang, T.-L., & Shih, I.-M. (2012b). The diagnostic and biological implications of laminin expression in serous tubal intraepithelial carcinoma. *Am. J. Surg. Pathol.* **36**, 1826–1834.

Kuo, S.W., Ke, F.C., Chang, G.D., Lee, M.T., & Hwang, J.J. (2011). Potential role of follicle-stimulating hormone (FSH) and transforming growth factor (TGF-beta1) in the regulation of ovarian angiogenesis. *J. Cell. Physiol.* **226**, 1608–1619.

Kurman, R.J. (2013). Origin and molecular pathogenesis of ovarian high-grade serous carcinoma. *Ann. Oncol.* **24 Suppl 1**, x16–x21.

Kurman, R.J., & Shih, I.-M. (2010). The origin and pathogenesis of epithelial ovarian cancer: a proposed unifying theory. *Am. J. Surg. Pathol.* **34**, 433–443.

Kurman Robert J., S. le-M. (2011). Molecular Pathogenesis ans extraovarian origin of epithelial Ovarian Cancer. Shiftng the paradigm. *Hum. Pathol* **42**, 918–931.

Kuroda, T., Hirohashi, Y., Torigoe, T., Yasuda, K., Takahashi, A., Asanuma, H., Morita, R., Mariya, T., Asano, T., Mizuuchi, M., Saito, T., & Sato, N. (2013). ALDH1-high ovarian cancer stem-like cells can be isolated from serous and clear cell adenocarcinoma cells, and ALDH1 high expression is associated with poor prognosis. *PLoS One* **8**, e65158.

Kutner, R.H., Zhang, X.-Y., & Reiser, J. (2009). Production, concentration and titration of pseudotyped HIV-1-based lentiviral vectors. *Nat. Protoc.* **4**, 495–505.

Lau, A., Kollara, A., St John, E., Tone, A.A., Virtanen, C., Greenblatt, E.M., King, W.A., & Brown, T.J. (2014). Altered expression of inflammation-associated genes in oviductal cells following follicular fluid exposure: implications for ovarian carcinogenesis. *Exp. Biol. Med. (Maywood).* **239**, 24–32.

Lauschová, I. (2003). Secretory Cells and Morphological Manifestation of Secretion in the Mouse Oviduct. **76**, 203–214.

Lee, M., Nam, E.J., Kim, S.W., Kim, S., Kim, J.H., & Kim, Y.T. (2012). Prognostic impact of the cancer stem cell-related marker NANOG in ovarian serous carcinoma. *Int. J. Gynecol. Cancer* **22**, 1489–1496.

Lee, Y., Miron, A., Drapkin, R., Nucci, M.R., Medeiros, F., Saleemuddin, A., Garber, J., Birch, C., Mou, H., Gordon, R.W., Cramer, D.W., McKeon, F.D., & Crum, C.P. (2007). A candidate precursor to serous carcinoma that originates in the distal fallopian tube. *J. Pathol.* **211**, 26–35.

Lengyel, E. (2010). Ovarian cancer development and metastasis. *Am. J. Pathol.* **177**, 1053–1064.

Leonhardt, K., Einenkel, J., Sohr, S., Engeland, K., & Horn, L.-C. (2011). p53 signature and serous tubal in-situ carcinoma in cases of primary tubal and peritoneal carcinomas and serous borderline tumors of the ovary. *Int. J. Gynecol. Pathol.* **30**, 417–424.

Li, H.X., Lu, Z.H., Shen, K., Cheng, W.J., Malpica, A., Zhang, J., Wei, J.J., Zhang, Z.H., & Liu, J. (2014). Advances in serous tubal intraepithelial carcinoma: Correlation with high grade serous carcinoma and ovarian carcinogenesis. *Int. J. Clin. Exp. Pathol.* **7**, 848–857.

Li, J., Abushahin, N., Pang, S., Xiang, L., Chambers, S.K., Fadare, O., Kong, B., & Zheng, W. (2011). Tubal origin of "ovarian" low-grade serous carcinoma. *Mod. Pathol.* **24**, 1488–1499.

Li, J., Ning, Y., Abushahin, N., Yuan, Z., Wang, Y., Wang, Y., Yuan, B., Cragun, J.M., Chambers, S.K., Hatch, K., Kong, B., & Zheng, W. (2013). Secretory cell expansion with aging: Risk for pelvic serous carcinogenesis. *Gynecol. Oncol.* **131**, 555–560.

Lim, H., Paria, B.C., Das, S.K., Dinchuk, J.E., Langenbach, R., Trzaskos, J.M., & Dey, S.K. (1997). Multiple female reproductive failures in cyclooxygenase 2-deficient mice. *Cell* **91**, 197–208.

Lin, J., Liu, X., & Ding, D. (2015). Evidence for epithelial-mesenchymal transition in cancer stem-like cells derived from carcinoma cell lines of the cervix uteri. *Int. J. Clin. Exp. Pathol.* **8**, 847–855.

Liu, S., Ginestier, C., Charafe-Jauffret, E., Foco, H., Kleer, C.G., Merajver, S.D., Dontu, G., & Wicha, M.S. (2008). BRCA1 regulates human mammary stem/progenitor cell fate. *Proc. Natl. Acad. Sci. U. S. A.* **105**, 1680–1685.

Luo, F., Yang, K., Liu, R.-L., Meng, C., Dang, R.-F., & Xu, Y. (2014). Formation of vasculogenic mimicry in bone metastasis of prostate cancer: correlation with cell apoptosis and senescence regulation pathways. *Pathol. Res. Pract.* **210**, 291–295.

Mallini, P., Lennard, T., Kirby, J., & Meeson, A. (2014). Epithelial-to-mesenchymal transition: what is the impact on breast cancer stem cells and drug resistance. *Cancer Treat. Rev.* **40**, 341–348.

Maniotis, A.J., Folberg, R., Hess, A., Seftor, E.A., Gardner, L.M., Pe'er, J., Trent, J.M., Meltzer, P.S., & Hendrix, M.J. (1999). Vascular channel formation by human melanoma cells in vivo and in vitro: vasculogenic mimicry. *Am. J. Pathol.* **155**, 739–752.

Mansouri, A, Hallonet, M., & Gruss, P. (1996). Pax genes and their roles in cell differentiation and development. *Curr. Opin. Cell Biol.* **8**, 851–857.

Matsuura, K., Nagai, T., Nishigaki, N., Oyama, T., Nishi, J., Wada, H., Sano, M., Toko, H., Akazawa, H., Sato, T., Nakaya, H., Kasanuki, H., & Komuro, I. (2004). Adult cardiac Sca-1-positive cells differentiate into beating cardiomyocytes. *J. Biol. Chem.* **279**, 11384–11391.

McCloskey, C.W., Goldberg, R.L., Carter, L.E., Gamwell, L.F., Al-Hujaily, E.M., Collins, O., Macdonald, E.A., Garson, K., Daneshmand, M., Carmona, E., & Vanderhyden, B.C. (2014). A new spontaneously transformed syngeneic model of high-grade serous ovarian cancer with a tumor-initiating cell population. *Front. Oncol.* **4**, 53.

McCluggage, W.G. (2011). Morphological subtypes of ovarian carcinoma: a review with emphasis on new developments and pathogenesis. *Pathology* **43**, 420–432.

Medeiros, F., Muto, M.G., Lee, Y., Elvin, J. a, Callahan, M.J., Feltmate, C., Garber, J.E., Cramer, D.W., & Crum, C.P. (2006). The tubal fimbria is a preferred site for early adenocarcinoma in women with familial ovarian cancer syndrome. *Am. J. Surg. Pathol.* **30**, 230–236.

Mehra, K., Mehrad, M., Ning, G., Drapkin, R., McKeon, F.D., Xian, W., & Crum, C.P. (2011). STICS, SCOUTs and p53 signatures; a new language for pelvic serous carcinogenesis. *Front. Biosci. (Elite Ed).* **3**, 625–634.

Meng, E., Long, B., Sullivan, P., McClellan, S., Finan, M.A., Reed, E., Shevde, L., & Rocconi, R.P. (2012). CD44+/CD24- ovarian cancer cells demonstrate cancer stem cell properties and correlate to survival. *Clin. Exp. Metastasis* **29**, 939–948.

Millimaggi, D., Mari, M., D'Ascenzo, S., Giusti, I., Pavan, A., & Dolo, V. (2009). Vasculogenic mimicry of human ovarian cancer cells: role of CD147. *Int. J. Oncol.* **35**, 1423–1428.

Mirantes, C., Espinosa, I., Ferrer, I., Dolcet, X., Prat, J., & Matias-Guiu, X. (2013). Epithelial-to-mesenchymal transition and stem cells in endometrial cancer. *Hum. Pathol.* **44**, 1973–1981.

Miyazono, K., Olofsson, A., Colosetti, P., & Heldin, C.H. (1991). A role of the latent TGF-beta 1-binding protein in the assembly and secretion of TGF-beta 1. *EMBO J.* **10**, 1091–1101.

Munakata, S., & Yamamoto, T. (2015). Incidence of serous tubal intraepithelial carcinoma (STIC) by algorithm classification in serous ovarian tumor associated with PAX8 expression in tubal epithelia: a study of single institution in Japan. *Int. J. Gynecol. Pathol.* **34**, 9–18.

Murdoch, W.J., Townsend, R.S., & McDonnel, A.C. (2001). Ovulation-induced DNA damage in ovarian surface epithelial cells of ewes: prospective regulatory mechanisms of

repair/survival and apoptosis. *Biol. Reprod.* **65**, 1417–1424.

Naor, D., Sionov, R. V, & Ish-Shalom, D. (1997). CD44: structure, function, and association with the malignant process. *Adv. Cancer Res.* **71**, 241–319.

Narlis, M., Grote, D., Gaitan, Y., Boualia, S.K., & Bouchard, M. (2007). Pax2 and pax8 regulate branching morphogenesis and nephron differentiation in the developing kidney. *J. Am. Soc. Nephrol.* **18**, 1121–1129.

Negi, L.M., Talegaonkar, S., Jaggi, M., Ahmad, F.J., Iqbal, Z., & Khar, R.K. (2012). Role of CD44 in tumour progression and strategies for targeting. *J. Drug Target.* **20**, 561–573.

Ng, A., Tan, S., Singh, G., Rizk, P., Swathi, Y., Tan, T.Z., Huang, R.Y.-J., Leushacke, M., & Barker, N. (2014). Lgr5 marks stem/progenitor cells in ovary and tubal epithelia. *Nat. Cell Biol.* **16**, 745–757.

Nilsson, E.E., & Skinner, M.K. (2002). Role of transforming growth factor β in ovarian surface epithelium biology and ovarian cancer. *Reprod. Biomed. Online* **5**, 254–258.
Nilsson, E., Doraiswamy, V., Parrott, J.A., & Skinner, M.K. (2001). Expression and action of transforming growth factor beta (TGFbeta1, TGFbeta2, TGFbeta3) in normal bovine ovarian surface epithelium and implications for human ovarian cancer. *Mol. Cell. Endocrinol.* **182**, 145–155.

Ning, G., Bijron, J.G., Yamamoto, Y., Wang, X., Howitt, B.E., Herfs, M., Yang, E., Hong, Y., Cornille, M., Wu, L., Hanamornroongruang, S., McKeon, F.D., Crum, C.P., & Xian, W. (2014). The PAX2-null immunophenotype defines multiple lineages with common expression signatures in benign and neoplastic oviductal epithelium. *J. Pathol.* **234**, 478–487.

Okabe, H., Ishimoto, T., Mima, K., et al. (2014). CD44s signals the acquisition of the mesenchymal phenotype required for anchorage-independent cell survival in hepatocellular carcinoma. *Br. J. Cancer* **110**, 958–966.

Okada, A., Ohta, Y., Brody, S.L., Watanabe, H., Krust, A., Chambon, P., & Iguchi, T. (2004). Role of foxj1 and estrogen receptor alpha in ciliated epithelial cell differentiation of the neonatal oviduct. *J. Mol. Endocrinol.* **32**, 615–625.

Okamoto, S., Okamoto, A., Nikaido, T., Saito, M., Takao, M., Yanaihara, N., Takakura, S., Ochiai, K., & Tanaka, T. (2009). Mesenchymal to epithelial transition in the human ovarian surface epithelium focusing on inclusion cysts. *Oncol. Rep.* **21**, 1209–1214.

Olsson, E., Honeth, G., Bendahl, P.-O., Saal, L.H., Gruvberger-Saal, S., Ringner, M., Vallon-Christersson, J., Jonsson, G., Holm, K., Lovgren, K., Ferno, M., Grabau, D., Borg, A., & Hegardt, C. (2011). CD44 isoforms are heterogeneously expressed in breast

cancer and correlate with tumor subtypes and cancer stem cell markers. *BMC Cancer* **11**, 418.

Ouellette, Y., Price, C. a., & Carrière, P.D. (2005). Follicular fluid concentration of transforming growth factor-β1 is negatively correlated with estradiol and follicle size at the early stage of development of the first-wave cohort of bovine ovarian follicles. *Domest. Anim. Endocrinol.* **29**, 623–633.

Paik, D.Y., Janzen, D.M., Schafenacker, A.M., Velasco, V.S., Shung, M.S., Cheng, D., Huang, J., Witte, O.N., & Memarzadeh, S. (2012). Stem-like epithelial cells are concentrated in the distal end of the fallopian tube: a site for injury and serous cancer initiation. *Stem Cells* **30**, 2487–2497.

Pangas, S.A., Li, X., Robertson, E.J., & Matzuk, M.M. (2006). Premature luteinization and cumulus cell defects in ovarian-specific Smad4 knockout mice. *Mol. Endocrinol.* **20**, 1406–1422.

Pardal, R., Molofsky, A.V, & He, S. (2005). Stem cell self-renewal and cancer cell proliferation are regulated by common networks that balance the activation of proto-oncogenes and tumor suppressors. *Cold Spring Harb. Symp. Quant. Biol.* **70**, 177-185.

Pastrana, E., Silva-Vargas, V., & Doetsch, F. (2011). Eyes wide open: A critical review of sphere-formation as an assay for stem cells. *Cell Stem Cell* **8**, 486–498.

Perets, R., Wyant, G., Muto, K., et al. (2013). Transformation of the Fallopian Tube Secretory Epithelium Leads to High-Grade Serous Ovarian Cancer in Brca;Tp53;Pten Models. *Cancer Cell* **24**, 751–765.

Piao, Y., Liang, J., Holmes, L., Henry, V., Sulman, E., & de Groot, J.F. (2013). Acquired resistance to anti-VEGF therapy in glioblastoma is associated with a mesenchymal transition. *Clin. Cancer Res.* **19**, 4392–4403.

Piek, J.M., van Diest, P.J., Zweemer, R.P., Jansen, J.W., Poort-Keesom, R.J., Menko, F.H., Gille, J.J., Jongsma, A.P., Pals, G., Kenemans, P., & Verheijen, R.H. (2001). Dysplastic changes in prophylactically removed Fallopian tubes of women predisposed to developing ovarian cancer. *J. Pathol.* **195**, 451–456.

Piek, J.M.J., Dorsman, J.C., Massuger, L.F., Ansink, A.C., Weegenaar, J., Shvarts, A., Kenemans, P., & Verheijen, R.H.M. (2006). BRCA1 and p53 protein expression in cultured ovarian surface epithelial cells derived from women with and without a BRCA1 germline mutation. *Arch. Gynecol. Obstet.* **274**, 327–331.

Ponce, M.L. (2009). Tube formation: an in vitro matrigel angiogenesis assay. *Methods Mol. Biol.* **467**, 183–188.

Qiao, L., Liang, N., Zhang, J., Xie, J., Liu, F., Xu, D., Yu, X., & Tian, Y. (2015). Advanced research on vasculogenic mimicry in cancer. *J. Cell. Mol. Med.* **19**, 315–326.

Rabban, J.T., Karnezis, A.N., & Zaloudek, C.J. (2011). Junctional epithelial zones of the fallopian tube: cancer hotspots? *Int. J. Gynecol. Pathol.* **30**, 1–3.

Reynolds, B.A., & Rietze, R.L. (2005). Neural stem cells and neurospheres--re-evaluating the relationship. *Nat. Methods* **2**, 333–336.

van de Rijn, M., Heimfeld, S., Spangrude, G.J., & Weissman, I.L. (1989). Mouse hematopoietic stem-cell antigen Sca-1 is a member of the Ly-6 antigen family. *Proc. Natl. Acad. Sci. U. S. A.* **86**, 4634–4638.

Rodriguez, C., Patel, A. V, Calle, E.E., Jacob, E.J., & Thun, M.J. (2001a). Estrogen replacement therapy and ovarian cancer mortality in a large prospective study of US women. *J. Am. Med. Assoc.* **285**, 1460–1465.

Rodriguez, G.C., Haisley, C., Hurteau, J., Moser, T.L., Whitaker, R., Bast, R.C.J., & Stack, M.S. (2001b). Regulation of invasion of epithelial ovarian cancer by transforming growth factor-beta. *Gynecol. Oncol.* **80**, 245–253.

van Roy, F., & Berx, G. (2008). The cell-cell adhesion molecule E-cadherin. *Cell. Mol. Life Sci.* **65**, 3756–3788.

Salm, S., Burger, P.E., & Wilson, E.L. (2012). TGF-beta and stem cell factor regulate cell proliferation in the proximal stem cell niche. *Prostate* **72**, 998–1005.

Scully, R.E. (1995). Pathology of ovarian cancer precursors. *J. Cell. Biochem. Suppl.* **23**, 208–218.

Seidman, J.D., Yemelyanova, A., Zaino, R.J., & Kurman, R.J. (2011). The fallopian tube-peritoneal junction: a potential site of carcinogenesis. *Int. J. Gynecol. Pathol.* **30**, 4–11.

Shao-Fang, Z., Hong-Tian, Z., Zhi-Nian, Z., & Yuan-Li, H. (2011). PKH26 as a fluorescent label for live human umbilical mesenchymal stem cells. *Vitr. Cell. Dev. Biol. - Anim.* **47**, 516–520.

Sherman-Baust, C.A., Kuhn, E., Valle, B.L., Shih, I.-M., Kurman, R.J., Wang, T.-L., Amano, T., Ko, M.S.H., Miyoshi, I., Araki, Y., Lehrmann, E., Zhang, Y., Becker, K.G., & Morin, P.J. (2014). A genetically engineered ovarian cancer mouse model based on fallopian tube transformation mimics human high-grade serous carcinoma development. *J. Pathol.* **233**, 228–237.

Shin, K., Fogg, V.C., & Margolis, B. (2006). Tight junctions and cell polarity. *Annu. Rev. Cell Dev. Biol.* **22**, 207–235.

Sillanpaa, S., Anttila, M.A., Voutilainen, K., Tammi, R.H., Tammi, M.I., Saarikoski, S. V, & Kosma, V.-M. (2003). CD44 expression indicates favorable prognosis in epithelial ovarian cancer. *Clin. Cancer Res.* **9**, 5318–5324.

Snegovskikh, V., Mutlu, L., Massasa, E., & Taylor, H.S. (2014). Identification of Putative Fallopian Tube Stem Cells. *Reprod. Sci.* **21**, 1460–1464.

So, K.A., Min, K.J., Hong, J.H., & Lee, J.-K. (2015). Interleukin-6 expression by interactions between gynecologic cancer cells and human mesenchymal stem cells promotes epithelial-mesenchymal transition. *Int. J. Oncol.* , doi: 10.3892/ijo.2015.3122.

Song, H., Kwan, S.-Y., Izaguirre, D.I., Zu, Z., Tsang, Y.T., Tung, C.S., King, E.R., Mok, S.C., Gershenson, D.M., & Wong, K.-K. (2013). PAX2 Expression in Ovarian Cancer. *Int. J. Mol. Sci.* **14**, 6090–6105.

Sood, A.K., Seftor, E.A., Fletcher, M.S., Gardner, L.M., Heidger, P.M., Buller, R.E., Seftor, R.E., & Hendrix, M.J. (2001). Molecular determinants of ovarian cancer plasticity. *Am. J. Pathol.* **158**, 1279–1288.

Srivastava, M.D., Lippes, J., & Srivastava, B.I. (1996). Cytokines of the human reproductive tract. *Am. J. Reprod. Immunol.* **36**, 157–166.

Stewart, C.A., & Behringer, R.R. (2012). Mouse oviduct development. *Results Probl. Cell Differ.* **55**, 247–262.

Stingl, J. (2009). Detection and analysis of mammary gland stem cells. *J. Pathol.* **217**, 229–241.

Su, M., Feng, Y.-J., Yao, L.-Q., Cheng, M.-J., Xu, C.-J., Huang, Y., Zhao, Y.-Q., & Jiang, H. (2008). Plasticity of ovarian cancer cell SKOV3ip and vasculogenic mimicry in vivo. *Int. J. Gynecol. Cancer* **18**, 476–486.

Tao, L., Roberts, A.L., Dunphy, K.A., Bigelow, C., Yan, H., & Jerry, D.J. (2011). Repression of mammary stem/progenitor cells by p53 is mediated by Notch and separable from apoptotic activity. *Stem Cells* **29**, 119–127.

TeKippe, M., Harrison, D.E., & Chen, J. (2003). Expansion of hematopoietic stem cell phenotype and activity in Trp53-null mice. *Exp. Hematol.* **31**, 521–527.

Tervonen, T.A., Partanen, J.I., Saarikoski, S.T., Myllynen, M., Marques, E., Paasonen, K., Moilanen, A., Wohlfahrt, G., Kovanen, P.E., & Klefstrom, J. (2011). Faulty epithelial polarity genes and cancer. *Adv. Cancer Res.* **111**, 97–161.

Tone, A. a., Virtanen, C., Shaw, P., & Brown, T.J. (2012). Prolonged postovulatory

proinflammatory signaling in the fallopian tube epithelium may be mediated through a BRCA1/DAB2 axis. *Clin. Cancer Res.* **18**, 4334–4344.

Tong, G.-X., Chiriboga, L., Hamele-Bena, D., & Borczuk, A.C. (2007). Expression of PAX2 in papillary serous carcinoma of the ovary: immunohistochemical evidence of fallopian tube or secondary Müllerian system origin? *Mod. Pathol.* **20**, 856–863.

Torban, E., Eccles, M.R., Favor, J., & Goodyer, P.R. (2000). PAX2 suppresses apoptosis in renal collecting duct cells. *Am. J. Pathol.* **157**, 833–842.

Torres, M., Gomez-Pardo, E., Dressler, G.R., & Gruss, P. (1995). Pax-2 controls multiple steps of urogenital development. *Development* **121**, 4057–4065.

Tosoni, D., Di Fiore, P.P., & Pece, S. (2012). Functional purification of human and mouse mammary stem cells. *Methods Mol. Biol.* **916**, 59–79.

Tung, C.S., Mok, S.C., Tsang, Y.T.M., Zu, Z., Song, H., Liu, J., Deavers, M.T., Malpica, A., Wolf, J.K., Lu, K.H., Gershenson, D.M., & Wong, K.-K. (2009). PAX2 expression in low malignant potential ovarian tumors and low-grade ovarian serous carcinomas. *Mod. Pathol.* **22**, 1243–1250.

Ungefroren, H., Groth, S., Sebens, S., Lehnert, H., Gieseler, F., & Fandrich, F. (2011). Differential roles of Smad2 and Smad3 in the regulation of TGF-beta1-mediated growth inhibition and cell migration in pancreatic ductal adenocarcinoma cells: control by Rac1. *Mol. Cancer* **10**, 67.

Vaidya, A., & Kale, V.P. (2015). TGF-β signaling and its role in the regulation of hematopoietic stem cells. *Syst. Synth. Biol.* **9**, 1–10.

Walsh, T., Casadei, S., Lee, M.K., et al. (2011). Mutations in 12 genes for inherited ovarian, fallopian tube, and peritoneal carcinoma identified by massively parallel sequencing. *Proc. Natl. Acad. Sci. U. S. A.* **108**, 18032–18037.

Wang, M., Ma, H., Pan, Y., Xiao, W., Li, J., Yu, J., & He, J. (2015a). PAX2 and PAX8 reliably distinguishes ovarian serous tumors from mucinous tumors. *Appl. Immunohistochem. Mol. Morphol.* **23**, 280–287.

Wang, X., Hu, Q., Nakamura, Y., Lee, J., Zhang, G., From, A.H.L., & Zhang, J. (2006). The role of the sca-1+/CD31- cardiac progenitor cell population in postinfarction left ventricular remodeling. *Stem Cells* **24**, 1779–1788.

Wang, Y., Sacchetti, A., van Dijk, M.R., van der Zee, M., van der Horst, P.H., Joosten, R., Burger, C.W., Grootegoed, J.A., Blok, L.J., & Fodde, R. (2012). Identification of quiescent, stem-like cells in the distal female reproductive tract. *PLoS One* **7**, e40691.
Wang, Y.-L., Zhao, X.-M., Shuai, Z.-F., Li, C.-Y., Bai, Q.-Y., Yu, X.-W., & Wen, Q.-T.

(2015b). Snail promotes epithelial-mesenchymal transition and invasiveness in human ovarian cancer cells. *Int. J. Clin. Exp. Med.* **8**, 7388–7393.

Weberpals, J.I., Clark-Knowles, K. V, & Vanderhyden, B.C. (2008). Sporadic epithelial ovarian cancer: clinical relevance of BRCA1 inhibition in the DNA damage and repair pathway. *J. Clin. Oncol.* **26**, 3259–3267.

Welm, B.E., Tepera, S.B., Venezia, T., Graubert, T.A., Rosen, J.M., & Goodell, M.A. (2002). Sca-1(pos) cells in the mouse mammary gland represent an enriched progenitor cell population. *Dev. Biol.* **245**, 42–56.

Wiederschain, D., Wee, S., Chen, L., Loo, A., Yang, G., Huang, A., Chen, Y., Caponigro, G., Yao, Y.-M., Lengauer, C., Sellers, W.R., & Benson, J.D. (2009). Single-vector inducible lentiviral RNAi system for oncology target validation. *Cell Cycle* **8**, 498–504.

Wu, H., Zhang, H., Hu, Y., Xia, Q., Liu, C., Li, Y., Yu, B., Gu, T., Zhang, X., Yu, X., & Kong, W. (2014). Sphere formation assay is not an effective method for cancer stem cell derivation and characterization from the Caco-2 colorectal cell line. *Curr. Stem Cell Res. Ther.* **9**, 82–88.

Xu, J., Lamouille, S., & Derynck, R. (2009). TGF-beta-induced epithelial to mesenchymal transition. *Cell Res.* **19**, 156–172.

Yamanouchi, H., Umezu, T., & Tomooka, Y. (2010). Reconstruction of oviduct and demonstration of epithelial fate determination in mice. *Biol. Reprod.* **82**, 528–533.
Yang, Z., Zhang, H., & Kumar, R. (2005). Regulation of E-cadherin. *Breast Cancer Online* **8**.

Yang-Hartwich, Y., Gurrea-Soteras, M., Sumi, N., Joo, W.D., Holmberg, J.C., Craveiro, V., Alvero, A.B., & Mor, G. (2014). Ovulation and extra-ovarian origin of ovarian cancer. *Sci. Rep.* **4**, 6116.

Yemelyanova, A., Mao, T.-L., Nakayama, N., Shih, I.M., & Kurman, R.J. (2008). Low-grade serous carcinoma of the ovary displaying a macropapillary pattern of invasion. *Am. J. Surg. Pathol.* **32**, 1800–1806.

Yu, C., Zhang, Y.-L., & Fan, H.-Y. (2013). Selective Smad4 knockout in ovarian preovulatory follicles results in multiple defects in ovulation. *Mol. Endocrinol.* **27**, 966–978.

Zeppernick, F., Meinhold-Heerlein, I., & Shih, I.-M. (2015). Precursors of ovarian cancer in the fallopian tube: serous tubal intraepithelial carcinoma--an update. *J. Obstet. Gynaecol. Res.* **41**, 6–11.

Zhang, J., & Powell, S.N. (2005). The role of the BRCA1 tumor suppressor in DNA

double-strand break repair. *Mol. Cancer Res.* **3**, 531–539.

Zhang, J., Chang, B., & Liu, J. (2013). CD44 standard form expression is correlated with high-grade and advanced-stage ovarian carcinoma but not prognosis. *Hum. Pathol.* **44**, 1882–1889.

Zhang, W., Wei, L., Li, L., Yang, B., Kong, B., Yao, G., & Zheng, W. (2015). Ovarian serous carcinogenesis from tubal secretory cells. *Histol. Histopathol.* **30**, 1295–1302.

Zhao, Y., Chegini, N., & Flanders, K.C. (1994). Human fallopian tube expresses transforming growth factor (TGF beta) isoforms, TGF beta type I-III receptor messenger ribonucleic acid and protein, and contains [125I]TGF beta-binding sites. *J. Clin. Endocrinol. Metab.* **79**, 1177–1184.

Zhou, C., Liu, J., Tang, Y., & Liang, X. (2012). Inflammation linking EMT and cancer stem cells. *Oral Oncol.* **48**, 1068–1075.

Zhu, Y., Richardson, J.A., Parada, L.F., & Graff, J.M. (1998). Smad3 mutant mice develop metastatic colorectal cancer. *Cell* **94**, 703–714.

Zhu, Y., Nilsson, M., & Sundfeldt, K. (2010). Phenotypic plasticity of the ovarian surface epithelium: TGF-beta 1 induction of epithelial to mesenchymal transition (EMT) in vitro. *Endocrinology* **151**, 5497–5505.

Zoller, M. (2011). CD44: can a cancer-initiating cell profit from an abundantly expressed molecule? *Nat. Rev. Cancer* **11**, 254–267.